AN EFFECT-DRIVEN FRACTIONATION APPROACH FOR THE ISOLATION AND CHARACTERIZATION OF CYP1A INDUCING COMPONENTS OF CRUDE OILS

by

Gurusankar Saravanabhavan

A thesis submitted to the Department of Chemistry

In conformity with the requirements for

the degree of Doctor of Philosophy

Queen's University

Kingston, Ontario, Canada

(November, 2007)

i

Abstract

Exposure to crude oils has been shown to induce CYP1A enzymes and cause chronically toxic effects in aquatic organisms. Earlier studies indicated that polycyclic aromatic hydrocarbons (PAHs) present in crude oil are primarily responsible for the chronic toxicity. Crude oil contains a variety of PAHs; the majority of them are alkyl substituted. In this work, we have used an effects-driven fractionation and analysis approach (EDFA) to isolate and characterize PAHs present in Alaskan North Slope and Scotian Light crude oils that are toxic to fish.

The crude oil components were first fractionated into four fractions using a low temperature vacuum distillation technique. Among them, the heavy gas oil fraction (boiling range 287°C – 461°C) of both oils caused highest toxicity to fish. To isolate the PAHs from waxes present in this fraction, a low temperature wax precipitation method was developed and optimized. CYP1A induction results showed that the extract contained a large number of CYP1A inducers while the residue contained none. Chemical analyses confirmed that most of the PAHs were partitioned into the extract fraction. Alkyl PAHs present in the extract were further fractionated into five fractions based on the number of aromatic rings using a normal phase HPLC method. Chemical analysis and the toxicity testing of these fractions indicated that alkyl PAHs belonging to classes such as phenanthrene, fluorene, naphthobenzothiophene, and chrysene are likely responsible for the observed toxic effects.

To aid the EDFA scheme, a new HPLC-DAD method for the analysis of alkyl PAHs was developed. The alkyl PAHs were first fractionated based on the number of aromatic rings using a normal phase column followed by their analysis using reverse phase HPLC–DAD technique. The reverse phase analysis involved classifying the alkyl PAH peaks into different PAH classes based on their DAD spectra. Then, alkyl carbon numbers for each peak were assigned based on their retention time. To analyze co-eluting alkyl PAH isomers an offline multi-dimensional HPLC method was developed. Orthogonal separation was achieved by first fractionating the alkyl PAHs on a normal phase column followed by the RP-HPLC-DAD analysis. Using these data a 2D contour plot was developed and used for the detailed analysis of alkyl PAHs isomers. Analysis results showed good agreement with a gas-chromatography-mass-spectrometric (GC-MS) analysis method, and the new method was able to distinguish some PAH types which could not be identified by GC-MS.

Co-Authorship

1. Mr. Gurusankar Saravanabhavan has written all chapters in this thesis. Dr. R. Stephen Brown edited all chapters and co-authored chapters two, three, four and five. Dr. Stephen Brown is Mr. Saravanabhavan's research supervisor and a co-investigator in the EDFA project reported in this thesis. Mr. Saravanabhavan took Dr. R. Stephen Brown's guidance throughout this thesis work.

2. Dr. P.V. Hodson co-authored and edited chapters two, three and four. Dr. Hodson is a co-investigator in the EDFA project. He is a fish toxicologist/environmental biologist at Queen's University. The biological work reported in this thesis was done in his laboratory.

3. Mr. Colin Khan co-authored the work reported in chapters two and three. He is a Master's student at Biology Department at Queen's University. His major contributions are the exposure of crude oil fractions to fish, CYP1A assay, and chronic toxicity testing.

4. Mr. Bill Shaw assisted in CYP1A induction testing of crude oil sub-fractions reported in chapter two.

5. Ms. Kyra Nabeta assisted in CYP1A induction testing of the crude oil sub-fractions reported in chapter three.

6. Ms. Anjali Helferty helped in the analysis of crude oil sub-fractions in HPLC reported in chapter four.

Acknowledgements

I would like to express my sincere gratitude to my supervisor Dr. R. Stephen Brown for his constant support throughout my PhD program. I thank you for helping me to think clearly and apply chemical principles for complex research problems. I also thank you for devoting ample time for discussions during our regular research meetings, which helped me to solidify my analytical foundation. Above all, I thank you for your friendship.

I would like to thank Dr. Peter Hodson for his help throughout my research work. I thank him for teaching me various biological aspects of the oil project. Your innovative ideas and unabated enthusiasm inspired me to work harder. I should say that I am gifted to be a part of this wonderful project.

I would also like to thank Colin Khan for his help and cooperation during my PhD work. Your nature to help others makes you an extraordinary individual. Thank you for being my friend.

I would like to extend my gratitude to Dr. Ray Bowers for teaching me different experimental techniques throughout my work. No amount of textbook reading could have given me the insight that I gained during our conversation.

It is my pleasure to thank all the Brown group members – Xiumei Han, Feng Sheng, Jun Zhang, Krista Plett, Dominique Turcotte and Eric Marcotte for your friendship and help during my stay at Queen's. It has been a wonderful experience for me to knowing each one of you individually.

Statement of Originality

All pieces of research work reported in this thesis are the original work of the author. Any published (or unpublished) ideas and/or techniques from the work of others are fully acknowledged in accordance with the standard citations given. The following are the author's original contributions to the research field:

1. Development of a novel EDFA method for the fractionation and analysis of toxic crude oil components.

2. Development and optimization of a wax precipitation method to isolate unsubstituted and alkyl substituted PAHs present in crude oils.

3. Development of a normal phase fractionation scheme for the bulk fractionation of alkyl PAHs present in crude oil.

4. Development of a new HPLC-DAD method for the identification and quantitative analysis of alkyl PAHs present in crude oils

5. Development of a new off-line multidimensional HPLC method for the detailed analysis of alkyl PAH isomers in crude oils

(Gurusankar Saravnabhavan)

(November, 2007)

Table of Contents

List of Figures

Chapter 1

Chapter 2

Chapter 3

Chapter 4

Chapter 5

Chapter 6

List of Tables

Chapter 3

Chapter 4

Chapter 5

Chapter 6

CHAPTER 1

Oil spills in aquatic environments

Crude oil remains one of the most important energy sources globally. According to the U.S Department of Energy, world oil consumption is expected to rise from 83 million barrels per day in 2004 to 97 million barrels per day by 2015 [1]. Inevitably, this will increase environmental damages associated with the crude oil production, transportation and consumption. Depending on the prevailing weather conditions, the oil spilled on the water surface can spread fairly quickly to form a thick oil slick. In due course, the spilled oil undergoes weathering processes such as evaporation, oxidation, and biodegradation by microbes. Weathering results in the evaporation of volatile components of the crude oil very quickly; however, heavier crude oil components degrade slowly and can persist in the environment for several years after the oil spill [2].

Impacts of oil spill

A substantial portion of the current knowledge on the impact of oil spills was derived from the Exxon Valdez Oil Spill (EVOS), which occurred on March 24, 1989 in Bligh Reef, Prince William Sound (PWS), Alaska. This spill resulted in the discharge of about 41 million liters of Alaskan north slope crude oil (ANSC), contaminating about 1300 miles of shorelines in a relatively pristine aquatic ecosystem with a wide variety of fauna and flora [3]. The environmental impacts due to the EVOS have been widely studied due to the ecological sensitivity of PWS as well as its impact on the commercial fisheries. Impact assessment studies carried out immediately after the spill retrieved a large number of sea

birds, bald eagles, sea otters, and other aquatic organisms coated with crude oil [3-6]. Moreover, the aggressive shoreline cleanup efforts such as the use of oil dispersant, surfactants and hot water flushing of oiled beaches has contributed significantly to the mortalities observed immediately after the spill [7].

The EVOS occurred during the spawning season of several fish species including Pacific herring and pink salmon [8]. The oil spill trajectory involved several low tide zones near small streams in which these fish lay their eggs. In these regions, the contaminated oil could not disperse effectively resulting in the exposure of eggs to high concentrations of the crude oil. This eventually resulted in high egg mortality and decreased growth of the off-spring in the years immediately after the spill [8]. One and two ring aromatic compounds present in the crude oil were predicted to be the primary causative agents for this short-term toxicity. As the oil weathers the one and two ring compounds evaporate faster and hence the observed toxic effects were expected to reduce a few years after the spill. However, studies on the pink salmon recruitment several years after the oil spill showed a continued egg and embryo mortality that indicated the long-term effects of EVOS [9, 10]. The long-term effects of the crude oil components were then attributed to two factors: (a) Just after the spill, the oil that entered the porous sediment, and the sub-surface regions covered with cobbles and boulders underwent little weathering. This sequestered oil formed "oil reservoirs" and slowly released the toxic crude oil components into the ecosystem [11-13]. (b) The weathering of the crude oil did not remove the more toxic three and four ring compounds in the crude oil and the concentration of these compounds

increased over time in the water column, contributing to much of the long-term effects [14].

What components of crude oil are toxic?

Identifying the toxic components in crude oil can be beneficial in several ways. Establishing a cause and effect relationship between specific compounds/ compound classes and the observed effects can give information about their mode of action. Better risk assessment and remediation methodologies can be developed if we know the toxic components in an oil-contaminated site. Moreover, these components can be used as chemical and biological fingerprints to identify the pollution sources in a contaminated site with an unknown pollution history.

However, crude oil is a complex mixture of several thousands of aliphatic and aromatic compounds. Therefore, it is necessary to understand the composition of crude oil to isolate and identify toxic components.,. The origin of crude oil has been debated for quite sometime; currently, there is a general consensus among the geologist that crude oil was formed from the remains of plants and animals buried millions of years ago. The organic matter underwent diagenesis, a process in which it was subjected to several redox reactions particularly governed by microbes. This resulted in the expulsion of methane, water and oxygen from the organic matter to form complex organic hydrocarbons called kerogen. Kerogen is insoluble in common petroleum solvents including carbon disulfide. It contains predominantly carbon, hydrogen, oxygen and trace levels of nitrogen and sulfur. Catagenesis of kerogen occurred in the deep subsurface in

relatively higher temperature and pressure conditions. During this phase, the kerogen underwent thermal maturation to release crude oil and gas. The rate of thermal maturation depends on several parameters; however, temperature was found to be the most crucial one. In general, the thermal maturation of kerogen between 60°C and 120°C released crude oil while between 120°C to 225°C it released natural gas. Above 225°C the kerogen did not contain any hydrocarbons [15].

The nature of organic matter and the geological conditions that were present during the formation of crude oil determined its physical and chemical properties. Bulk physical properties such as density, viscosity and boiling point have been used to compare the quality of different crude oils. These properties are very useful in determining proper conditions for drilling, transportation and refining of the crude oils.

Chemical composition crude oils

Crude oil primarily contains compounds made up of carbon and hydrogen and to a lesser extent sulfur, oxygen, and nitrogen. The presence of trace levels of metals such as vanadium, nickel, iron and copper has also been reported [16]. Broadly, crude oil components can be divided into saturates, aromatics, resins and asphaltenes (SARA). Each of these classes contains hundreds of individual compounds. Figure 1.1 shows some representative compounds from each category.
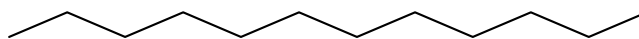
Dodecane
$C_{12}H_{26}$
Molar mass: 170
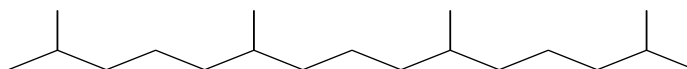
2,6,10,14-Tetramethylpentadecane (Pristane)
$C_{19}H_{40}$
Molar mass: 268
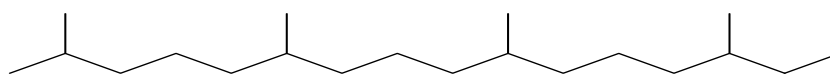
2,6,10,14-Tetramethylhexadecane (Phytane)
$C_{20}H_{42}$
Molar mass: 268
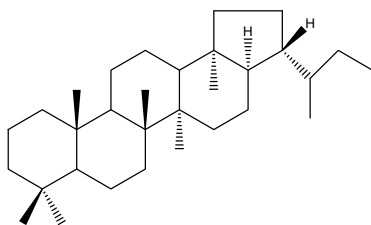
17α(H),21β(H)-Hopane
$C_{30}H_{52}$
Molar mass: 412
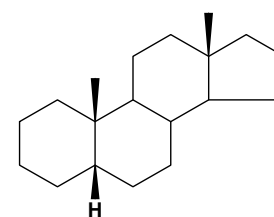
5β(H)-Androstane
C19H32
Molar mass: 260

Figure 1.1a: Structures of some of the saturated hydrocarbons commonly found in crude oils.
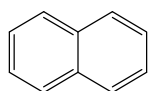
Naphthalene
$C_{10}H_8$
Molar mass: 128
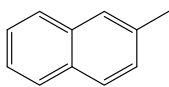
2-methyl naphthalene
$C_{11}H_{10}$
Molar mass: 142
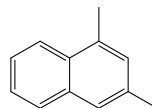
1,3-dimethyl naphthalene
$C_{12}H_{12}$
Molar mass: 156
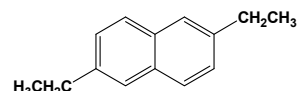
2,6-diethyl naphthalene
$C_{14}H_{16}$
Molar mass: 184
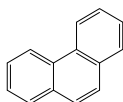
Phenanthrene
$C_{14}H_{10}$
Molar mass: 178
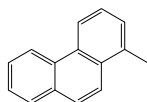
1-methyl phenanthrene
$C_{15}H_{12}$
Molar mass: 192
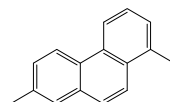
1,7-dimethyl phenanthrene
$C_{16}H_{14}$
Molar mass: 206
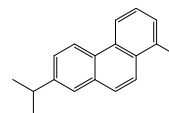
1,7-dimethyl phenanthrene
$C_{18}H_{18}$
Molar mass: 234
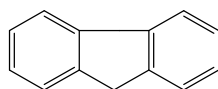
Fluorene
$C_{13}H_{10}$
Molar mass: 166
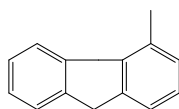
1-methyl fluorene
$C_{14}H_{12}$
Molar mass: 180
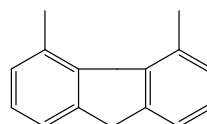
1,8-dImethyl fluorene
$C_{15}H_{14}$
Molar mass: 192
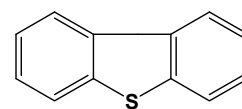
Dibenzothiophene
$C_{12}H_8S$
Molar mass: 184
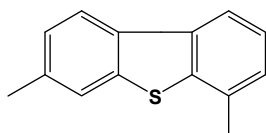
4,6-dimethyl Dibenzothiophene
$C_{14}H_{10}S$
Molar mass: 212
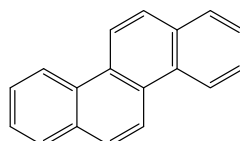
Chrysene
$C_{18}H_{12}$
Molar mass: 228
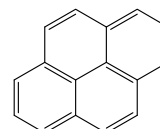
Pyrene
$C_{18}H_{12}$
Molar mass: 228
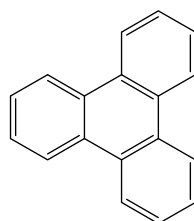
Triphenylene
$C_{18}H_{12}$
Molar mass: 228

Figure 1.1b: Structure of polycyclic aromatic compound classes that are found commonly in crude oil
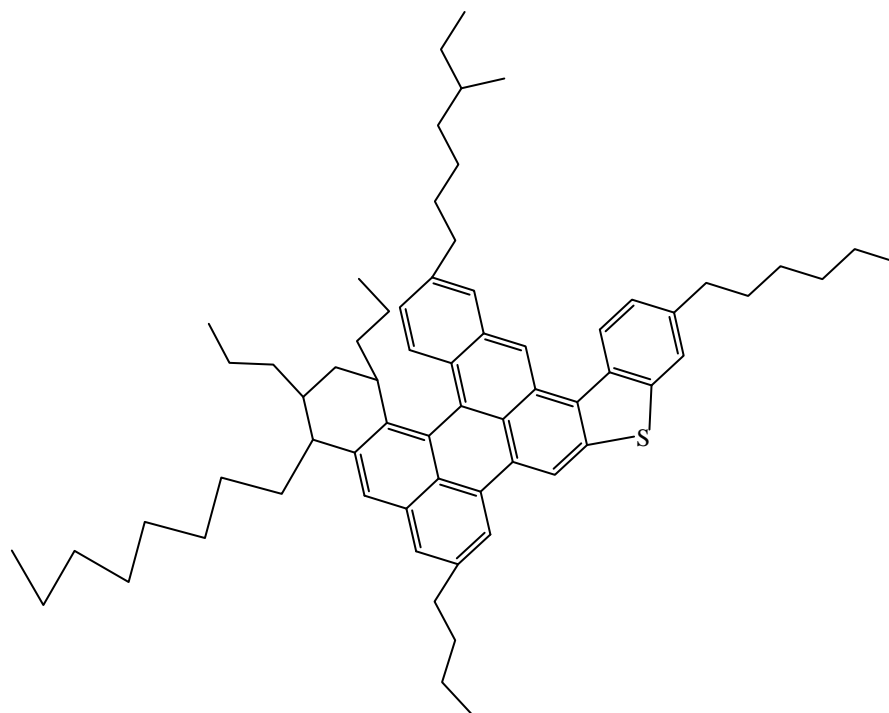
Figure 1.1c: Hypothetical structure of an asphaltene molecule. The aromatic rings are shown in solid lines while the aliphatic chains are shown in broken lines. [Source: Groenzin, H. and O.C. Mullins (2000). Energy & Fuels. 14: p. 677 - 684.]

Saturates: Saturated hydrocarbons are the predominant type of hydrocarbons in crude oils (Figure 1.1a). Saturated hydrocarbons can be grouped into the following classes:

(a). *n*-Alkanes are saturated straight chain hydrocarbons. *n*-Alkanes ranging from C5-C40 are usually detected in crude oil samples. They are present in high concentration in crude oil and are often referred to as *n*-parafins.

(b). Iso-alkanes are branched chain hydrocarbons that are found in abundance in crude oils. Iso-paraffins with branching at the 2nd and 3rd position are very common in crude oils. Some of the most commonly analyzed iso-alkanes include isoprenoid compounds such as farnesane (i-C15: 2,6,10-trimethyl-dodecane), pristane (*i*-C19: 2,6,10,14- tetramethylpentadecane) and phytane (*i*-C20: 2,6,10,14- tetramethyl hexadecane) [2, 17].

(c). Cycloalkanes (*naphthenes*) are compounds containing saturated cyclic rings (such as cyclopentane and cyclohexane) and their alkyl derivatives.

(d) Terpenes and steranes are compounds consisting of multiple condensed cyclic rings with long alkyl side chains. These compounds serve as useful biomarkers in the identification and differentiation of crude oils and their weathering status [18].

Aromatic hydrocarbons: Aromatic hydrocarbons are compounds with one or more benzene rings. Due to their toxic properties these compounds are studied widely during oil spill investigations. Crude oil contains a wide variety of aromatic hydrocarbons ranging from monaromatic hydrocarbons such as benzene to polyaromatic hydrocarbons (PAHs) with many fused aromatic rings (Figure 1.1b).

More than 85% of the aromatic hydrocarbons in crude oil contain one or more alkyl substituents on their aromatic rings [19, 20]. Aromatic compounds containing sulfur and nitrogen atoms in the rings (e.g. thiophenes) are also very common in crude oil.

Resins and asphaltenes: Polar compounds present in the crude oil can be classified into resins and asphaltenes. Elemental analysis of the polar fraction of crude oil shows the presence of high amounts of hetroatoms such as sulfur, nitrogen and metals such as vanadium, nickel, and iron. Like other crude oil component classes, they contain a variety of individual compounds with similar chemical structure. Figure 1.1c shows a hypothetical structure of an asphaltene molecule. Earlier, asphaltenes were thought to be large polar molecules with 5 to 20 aromatic rings with a molecular weight of about 2500 to 5000 amu. However, recent studies based on mass spectrometry and fluorescence polarization showed that asphaltenes have a molecular weight in the range of 500 to 1000 amu with 4 to 10 aromatic rings in their structure [21, 22]. The structure of resins is still not clearly understood. In general, it is accepted that resins are the precursors for the formation of asphalthenes. In the petroleum industry, asphaltenes are defined as the class of crude oil compounds that are not soluble in *n*-pentane or *n*-heptane [23]. The total amount of asphaltenes precipitated varies with the solvent, oil to solvent ratio, and the temperature [24]. Resins are defined as polar compounds that are soluble in n-heptane. They are usually isolated from deasphaltinized crude oil either by adsorption chromatography or by high performance liquid chromatographic (HPLC) fractionation using polar

stationary phase such as silica [25]. However, resins are considered to be less

aromatic than asphaltenes with a relatively lower proportion of hetero atoms.

Table 1.1: Effect of weathering on the overall composition of ANSC crude oil. [*Source:* Spill technology database, Environment Canada. Available online at http://www.etc-cte.ec.gc.ca/databases/spills/oil_prop_e.html. Accessed on June 12, 2007.]

Compound class	0% weathered	30.5% weathered
Saturates	75	64.8
Aromatics	15	18.5
Resins	6.1	10.3
Asphaltenes	4	6.4

Tale 1.2: Effect of weathering on the aromatic fraction of ANSC crude oil. [*Source:* Spill technology database, Environment Canada. Available online at http://www.etc-cte.ec.gc.ca/databases/spills/oil_prop_e.html. Accessed on June 12, 2007.]

Compound	0% weathering (μg/g of oil)	30.5% weathering (μg/g of oil)
Benzene	2866	0
Toluene	5928	0
Ethylbenzene	1319	0
Xylenes	6187	0
C3-benzenes	5620	30
Un-substituted PAHs	986	1182
Alkyl substituted PAHs	9711	13933

Weathering of crude oil changes its chemical composition significantly. The concentration of more volatile compounds decreases while the concentrations of semi-volatile and non-volatile compounds increases with weathering. Table 1.1 shows the SARA profiles of fresh and 30.5% weathered ANSC. In general, the saturated hydrocarbons are more easily degraded in the environment compared to their aromatic counterparts. Even in the aromatic fraction, the concentration of mono-aromatics such as BTEX (benzene, toluene, ethylbenzene, and xylene) decreases significantly due to weathering. In the case of PAHs, the concentrations of volatile PAHs such as naphthalene decreases while the concentration of 4 and higher ring PAHs increases (Table 1.2).

Origin of hydrocarbons in crude oils

Earlier geochemical studies on the formation of hydrocarbons in crude oil correlated the structural similarities between the petroleum hydrocarbons and the compounds that are commonly found in living organisms. Based on this, it was proposed that the C25 –C35 *n*-alkanes present in crude oil might have originated from natural waxes occurring in the higher plants [26]. In general, the odd numbered *n*-alkanes are abundant in living organisms. However, the significant abundance of both odd numbered and even numbered *n*-alkanes in crude oil suggests that the even numbered *n*-alkanes were formed during thermal maturation of the organic matter. Henderson *et al.* observed the formation of low molecular weight *n*-alkane and *n*-alkene mixture when *n*-octacosane ($C_{28}H_{58}$) was pyrolyzed at 375°C [27]. Moreover, when the pyrolysis was carried out in the presence of clay catalyst, these products were formed even at 200°C. Low

concentrations of n-alkenes in crude oil suggest that these compounds might have undergone further chemical reactions in the presence of natural catalysts in sediments to form branched chain, cyclic and aromatic hydrocarbons.

Likewise, the biogenic precursors for several other aliphatic hydrocarbon classes such as terpenes, isoprenoids, and hopanes present in the crude oil have also been evaluated [26]. Phytol, commonly found in plants, appears to be the major source of pristane and phytane. Similarly, hopanes and steranes present in petroleum samples are derived from hopanoids and sterols found in higher plants and microbes. These biomarker compounds are analyzed during the crude oil exploration to give vital information about the nature of the source rock as well as its thermal maturity.

The low boiling fraction (up to ~ 200°C) of crude oils contains predominantly benzene and its alkylated homologues. Alkyl benzenes with alkyl side chains as high as C40 have been identified in crude oils. Radke and other researchers suggest that the terpenoids present in the living organisms might be a major source of alkyl benzenes in crude oils [28]. Contrary to aliphatic hydrocarbons, not many PAHs are found naturally in living organisms. Tissot *et al.* analyzed the hydrocarbon content of the Toarcian shale cores in the Paris basin and found that the concentration of the total aromatic hydrocarbons were very low in cores collected up to 1.5 km deep, and increases rapidly thereafter [29]. Therefore, it is generally believed that most of the alkyl PAHs present in the crude oil were formed during the thermal maturation of kerogen. However, there are a few exceptions noted for this general trend. Wakeham *et al.* [31], based on their

study of the sediment cores from four different lakes, suggested that alkyl phenanthrenes are formed during the diagenesis phase by the dehydrogenation of steroids present in the organic matter. This hypothesis is supported by the results of Douglas and Mair who showed that a mixture of naphthalenes and phenanthrenes could be produced in the laboratory by heating cholesterol in the presence of sulfur [30]. For some alkyl phenanthrenes probable biological precursors have also been identified. For example, diterpenoid acids such as abietic acid and pimaric acid, found in conifer resins and higher plants, are suggested as precursors for the formation of retene (7-isopropyl-1-methyl phenanthrene) and 1,7-dimethyl phenanthrene [31]. In addition to alkyl phenanthrenes, other PAHs such as perylene are also studied widely in sediment cores. In the Wakeham *et al.* study [31], the concentration of perylene was found to increase with the depth of the sediment cores in all the four lakes, suggesting its formation during the diagenesis phase. However, no specific biological precursor could be identified.

Chemical analysis of crude oils

Since the beginning of the industrial revolution, a large effort has been undertaken to characterize individual classes of chemical compounds that constitute crude oil. The major impetus for this work is to correlate the chemical composition of crude oils to their behavior during the refining operations. Chemical analysis of crude oil is done at two levels of sophistication. The SARA analysis involves fractionating the crude oil components based on their polarity.

Table 1.3. List of source-specific PAHs analyzed during oil spill investigation

Name of the compound	Abbreviation	Ring number
Naphthalenes		
C0 – naphthalene	C0 NAP	2
C1 – naphthalenes	C1 NAP	2
C2 – naphthalenes	C2 NAP	2
C3 – naphthalenes	C3 NAP	2
C4 – naphthalenes	C4 NAP	2
Dibenzothiophenes		
C0 – dibenzothiophenes	C0 DBT	3
C1 – dibenzothiophenes	C1 DBT	3
C2 – dibenzothiophenes	C2 DBT	3
C3 – dibenzothiophenes	C3 DBT	3
C4 – dibenzothiophenes	C4 DBT	3
Fluorenes		
C0 – fluorene	C0 FLUOR	3
C1 – fluorenes	C1 FLUOR	3
C2 – fluorenes	C2 FLUOR	3
C3 – fluorenes	C3 FLUOR	3
C4 – fluorenes	C4 FLUOR	3
Phenanthrenes		
C0 – phenanthrenes	C0 PHEN	3
C1 – phenanthrenes	C1 PHEN	3
C2 – phenanthrenes	C2 PHEN	3
C3 – phenanthrenes	C3 PHEN	3
C4 – phenanthrenes	C4 PHEN	3
Chrysenes		
C0 – chrysene	C0 CHRY	4
C1 – chrysene	C1 CHRY	4
C2 – chrysene	C2 CHRY	4
C3 – chrysene	C3 CHRY	4
Other EPA priority pollutants		
Acenaphthylene	Acl	3
Acenaphthene	Ace	3
Anthracene	An	3
Fluoranthene	Fl	4
Pyrene	Py	4
Benz[*a*]anthracene	BaA	4
Benzo[*b*]fluoranthene	BbF	4
Benzo[*k*]fluoranthene	BkF	4
Benzo[*e*]pyrene	BeP	5
Benzo[*a*]pyrene	BaP	5
Perylene	Pe	5
Indeno[1,2,3-*cd*]pyrene	IP	6
Dibenz[*a,h*]anthrancene	DA	5
Benzo[*ghi*]perylene	BP	6

This type of analysis is very simple to perform and has found wide application in the petroleum industry [25, 32]. As the physical and chemical characteristics of crude oils and refined products (such as gasoline and lubricants) differ significantly, several methods have been developed and standardized to study their SARA composition. Several SARA analysis methods based on open column, low-pressure liquid chromatographic separation using polar stationary phases such as alumina, silica and fluorosil are reported [33]. Saturates are usually eluted with n-alkane solvents; this is followed by the elution of aromatics, resins and asphaltenes with solvents of increasing polarity. The solvent strength can be fine-tuned by mixing more than one solvent to get improved separation between compound classes. Silica gel is the preferred stationary phase for the separation due to its good stability, although alumina can better separate the aromatic fractions based on the number of aromatic rings.

In recent times, these open column methods have been substituted by normal phase HPLC methods due to the simplicity and reproducibility of the latter technique [34]. In addition to traditional polar HPLC stationary phases such as silica, different types of bonded stationary phases such as cyano, nitro and aminopropyl silica were applied to improve the separation of aromatic compounds and polar compounds [35, 36]. HPLC coupled to an ultraviolet absorbance (UV) detector is useful for the compositional analysis of aromatic compounds, while bulk property detectors such as refractive index detectors and evaporative light scattering detectors are used for the analysis of saturates [32, 34]. In addition to the HPLC methods, other chromatographic techniques such as

supercritical fluid chromatography and thin-layer chromatography have also been developed for the analysis of group composition of crude oils [37, 38].

The compositional information that can be obtained from SARA analysis is very limited. Therefore, detailed chemical analysis of saturated and aromatic hydrocarbons in crude oil is performed to understand the biogeochemistry of the crude oil formation and its thermal maturation. Moreover, the concentration of individual hydrocarbons constitute a "chemical fingerprint" that is unique for a given oil. Hence, detailed chemical analysis also finds widespread application in oil spill identification [2, 39].

Before any detailed hydrocarbon analysis, it is necessary to remove the polar and interfering substances present in the crude oil. Asphaltenes present in the crude oil are precipitated with 1:40 (w/v) pentane. The resulting maltene fraction is subjected to column chromatographic separation to isolate saturated hydrocarbons from aromatics. This step also serves to isolate resins that might interfere in further instrumental analysis.

Analysis of saturated hydrocarbons: Gas chromatography-flame ionization detection (GC-FID) and gas chromatography-mass spectrometric detection (GC-MS) are the prominent instrumental methods used in the analysis of saturated hydrocarbons [19, 20]. A variety of saturated hydrocarbons ranging from n-alkanes (C8 to C40), hopanes and steranes are routinely analyzed during an oil spill investigation [2, 39]. Distribution of *n*-alkanes has been used to differentiate the petrogenic and biogenic contribution in complex environmental samples. Usually the *n*-alkanes with an odd number of carbon atoms are found in higher

concentrations if it is derived from a biogenic source. On the other hand, the concentration of n-alkanes decreases with an increase in the carbon number if it is derived from a petrogenic source. A carbon performance index (CPI), defined as the ratio of the sum of the concentrations of odd numbered n-alkanes (n-C21 + n-C23 + n-C25 + n-C27 + n-C29 + n-C31 + n-C33) to that of even numbered n-alkanes (n-C22 + n-C24 + n-C26 + n-C28 + n-C30 + n-C32), has been used as a quantitative indicator for this purpose. A CPI value of ~1 indicates a petrogenic source while a value of >2 indicate biogenic contributions [39]. In addition, the biomarker pristane is derived predominantly from plant sources; hence the ratio of pristane to phytane will have a very high value if there is a high hydrocarbon input from biogenic sources.

Analysis of aromatic hydrocarbons: Analysis of aromatic hydrocarbons has attracted the attention of the scientific community for several decades. These are common environmental pollutants that are abundant in crude oil. The concentration of PAHs in various crude oils differs widely and therefore PAH analysis during an oil spill investigation can give important clues to identify the source of the pollution. As shown in Table 1.3, the concentrations of one to six ring un-substituted PAHs, alkyl isomers of these PAHs (up to 4 alkyl carbons; C0 – C4), and 16 PAHs from the United States Environmental Protection Agency's (US EPA) list of priority pollutants, are routinely analyzed during oil spill studies. The PAH profile of the crude oil exhibits the following general trends; (a) In most of the crude oils, the concentration of PAHs decreases with an increase in the number of aromatic rings; (b) The concentrations of alkyl PAHs are much higher

17

compared with un-substituted PAHs; (c) The alkyl PAH concentration forms a bell-shaped profile within a given PAH homologous series (e.g. C0-C4 naphthalenes); the concentration of C0 and C4 isomers are generally low compared with isomers of intermediate number of alkyl carbons.

On the other hand, the PAHs derived from combustion sources show a different profile – the concentrations of un-substituted PAHs are much higher than alkyl substituted PAHs. Moreover, the concentrations of 4-6 ring PAHs are found in high abundance compared to 2 and 3 ring PAHs. Hence the PAH profile in a contaminated site can be used to ascertain the relative contribution of PAHs from petrogenic and pyrogenic sources. For this purpose several quantitative diagnostic ratios have been developed over the years. Benlahcen *et al.* [40] assigned a concentration ratio of phenanthrene/anthracene <10 and fluoranthene/pyrene >1 to pyrogenic sources.

The PAH profile from an oil-contaminated site can also give valuable information about the weathering status of the crude oil. In general, the rate of decrease in the concentration of alkyl PAHs due to weathering show a C0 > C1 > C2 > C3 > C4 trend. Source specific diagnostic ratios based on "double plots" such as C2 C/C2 DBT vs. C3 C/C3 DBT (please refer to Table 1.3 for abbreviations) have been used to determine the source of weathered crude oils [41].

Due to their good volatility and thermal stability, most of the environmentally relevant PAHs are amenable to gas chromatographic analysis. GC columns based on methyl and phenyl substituted polysiloxane stationary phases are generally applied for the PAH analysis [42]. Liquid crystalline stationary phases

have also been used, particularly due to their improved shape selectivity over the conventional polysiloxane based columns [43, 44].

Although GC-FID and GC-MS techniques can offer equivalent sensitivity, the co-eluting peaks in a complex environmental sample could compromise the selectivity of the GC-FID technique. Therefore, GC-MS methods usually operating in selective ion monitoring (SIM) mode are preferred for the analysis of PAHs from complex samples including crude oils. Several researchers have emphasized the need for the use of per-deuterated PAHs as internal standards to develop reliable GC-MS methods. Deuterated PAHs have similar physico-chemical properties to the target PAHs and hence behave similarly during the sample preparation and analysis steps. This helps to calculate recovery estimates more reliably [42].

PAH analysis using HPLC methods offer several unique advantages. LC techniques can be used to isolate specific PAH fractions from a complex environmental sample for further analysis by HPLC – fluorescence, HPLC-UV or GC-MS techniques. Repeated fractionation of a complex sample can also be done to enrich the contaminants present in trace levels for better quantification. Secondly, due to their limited thermal stability and non-volatility, high molecular weight PAHs (> 6 aromatic rings) and those with more polar residues are generally analyzed using the HPLC techniques [45]. Moreover, in the absence of authentic standards, several alkyl PAHs (such as C3 phenanthrene and C3 anthracene) are difficult to distinguish using a MS detector due to their identical molecular weight and similar fragmentation patterns. Therefore, the standard

GC-MS methods often report combined concentrations of these structurally different PAHs [2, 39].
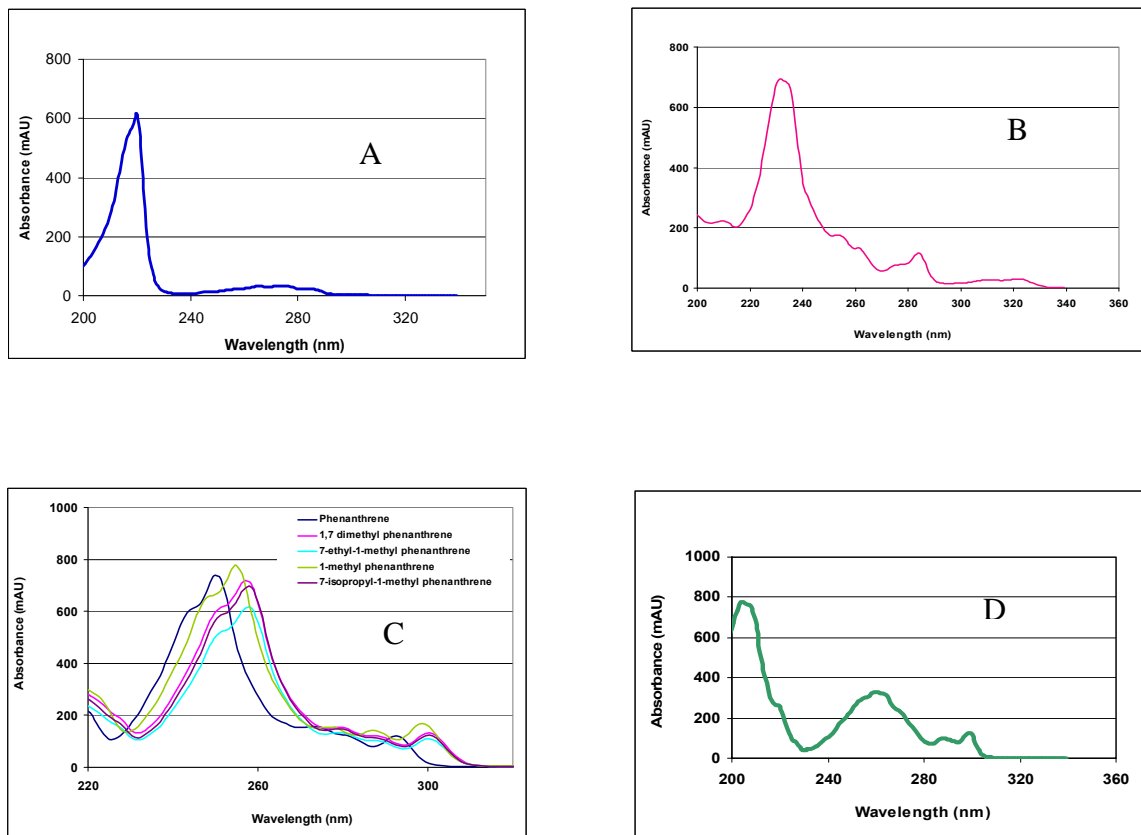
Figure 1.2: Ultraviolet absorption spectra of PAHs with different numbers aromatic rings. A: Naphthalene; B: Dibenzothiophene; C: Phenanthrene; D: Fluorene. The alkyl substitution on the aromatic ring does not change the UV spectra significantly. This is illustrated for a series of phenanthrenes (C).

On the other hand, as shown in Figure 1.2, the UV spectra of different PAHs differ significantly. In addition, the UV spectral profiles of the alkyl PAHs isomers resemble closely those of the corresponding un-substituted PAHs. Thus, using UV spectra one can easily distinguish different PAH classes (e.g. alkyl phenanthrenes and alkyl anthracenes). Previously several attempts have been made to develop gas chromatography-diode array detection (GC-DAD) methods, but the overall resolving power of such instruments is much lower than HPLC. Thus, standardized HPLC-DAD technique has been used to provide complementary information to GC-MS during oil spill research.

Many HPLC methods have been developed and validated for the analysis of PAHs from crude oils, petroleum products, petroleum contaminated water, soil, sediment, and biota [46]. Normal-phase HPLC methods have been traditionally used to separate the PAHs based on the number of aromatic rings. This is followed by the detailed analysis of individual PAH sub-fractions using reverse-phase HPLC techniques. Separation of PAHs in reverse-phase chromatography depends both on the physico-chemical properties of the PAHs and the nature of the stationary phase. Therefore, many reverse-phase HPLC columns have been evaluated for their suitability for PAH analysis [47, 48]. The column selectivity for PAHs was found to vary with stationary phase parameters such as carbon loading, length of alkyl chain, and pore size [49-51]. Even the PAH selectivity among similar octadecyl (C18) stationary phases obtained from different manufacturers showed marked differences. These selectivity differences are attributed to the differences in the silica substrate as well as the manufacturing

process used to produce the stationary phases. Generally, C18 bonded phases are synthesized using one of two different routes. The reaction of monofunctional silane (e.g. monochloro trimethylsilane) with silica produces monomeric C18 phases. On the other hand, when a trifunctional silane (such as trifluoro methylsilane) is reacted with silica in the presence of water, a polymeric stationary phase is produced. In a comparative study, Wise *et al.* showed that polymeric C18 phases can separate the 16 US EPA priority PAHs better than the monomeric C18 phase [52]. Based on the analysis of benzo[*a*]pyrene (BaP), dibenzo[*g,p*]chrysene (TBN), and phenanthro[3,4-*c*]phenanthrene (Ph-Ph), a phase selectivity index was developed to aid the classification of C18 columns into polymeric or monomeric. The elution order of these three compounds in monomeric and polymeric C18 phases are BaP < PhPh < TBN and PhPh < TBN < BaP respectively. Quantitative measures of phase selectivity can be calculated by evaluating the capacity factors (k') of these compounds in a given column. The capacity factor ratio, $k'_{TBN}/k'_{BaP,}$ for polymeric and monomeric phases are ≤ 1 and ≥ 1.7 respectively [52].

It was recognized that shape of the PAH molecule has a significant effect on its chromatographic retention. Wise *et al.* [49] pointed out that the chromatographic retention of a series of isomeric PAHs increases with an increase in its length-to-breath (L/B) ratio. The planarity of the PAHs is also found to affect their chromatographic retention - for example, on polymeric phases, among the four ring PAHs, the non-planar isomer triphenylene elutes earlier than the planar isomer chrysene [47]. Moreover, the column temperature, at which the

separation is carried out, is found to influence the PAH selectivity considerably. For both polymeric and monomeric columns, the column selectivity was found to increase with a decrease in column temperature [53].

To correlate the retention of PAHs on the reverse phase column, Wise and Sanders proposed a retention model referred to as the "slot model" [50, 53]. This model visualizes the ordering of the bonded phase molecules in the stationary phase material as "slots", and the penetration of the PAHs into these slots is responsible for their chromatographic retention. This model predicts that the long and narrow solutes (i.e. PAHs with large L/B) are able to penetrate deep into the slot and hence are retained longer. Similarly, non-planar PAH isomers are constrained from entering the slot and hence elute earlier than the planar PAH isomers. At lower column temperatures, the mobility of the bonded phase is reduced which increases rigidity and phase order, thereby improving the PAH selectivity.

HPLC techniques utilizing UV and fluorescence detectors are most commonly employed for detecting PAHs. Although UV detectors can be used to analyze a variety of compounds, their lack of sensitivity and selectivity limits their application in quantitative analysis [54]. On the other hand, the fluorescence characteristics of PAHs vary considerably and hence it is a selective detector for HPLC. Often, HPLC- combined with fluorescence wavelength programming is used to selectively quantify the PAHs in complex samples [55]. Generally speaking, the quantitative ability of HPLC-fluorescence techniques is on par with

that of GC-MS. Therefore, HPLC has been used as an alternative technique for quantifying PAHs in complex samples [56-59].

Multi-dimensional chromatographic approaches

Multi-dimensionality, in its broadest definition, includes standard analysis of complex samples using GC-MS or HPLC-DAD technique. Here the compounds are separated chromatographically in the first dimension while either their mass spectrum or DAD spectrum can be used to further differentiate co-eluting chromatographic peaks in the second dimension. Although such systems are highly useful for crude oil analysis, due to the presence of a myriad of co-eluting chromatographic peaks, extensive fractionation is required prior to the analysis. Hence, systems with multi-dimensional chromatographic capability such as GC-GC/MS, LC-GC/MS, LC-LC-DAD and SFC-GC-FID have been increasingly used for the analysis of complex samples [60-62].

The primary aim of any multi-dimensional chromatographic approach is to improve the overall separating power of the chromatographic system. The separating power is often defined in terms of peak capacity to indicate the number of solutes that can be separated at unit resolution. Mathematically, peak capacity is defined by the following Equation [63]:

$$PeakCapacity(PC) = 1 + \left(\frac{\sqrt{N}}{4}\right)\ln\left(\frac{t_1}{t_2}\right)$$

where, N represents the number of theoretical plates of the column and t_1 and t_2 represent the retention times of the first and the last eluting solutes. For a two-dimensional (2D) system, in which the solutes are separated by two different mechanisms in the first and the second dimension (orthogonal separation), the

overall peak capacity is given by the product of peak capacities in each dimension. In general, for a 2D system peak capacities as high as 1000 per hour could be achieved [63, 64]. Moreover, increased resolving power and improved detectors in the 2D systems make them more attractive for the analysis of trace components in complex samples. [65].

Several reviews have been published on online 2D chromatography, detailing its concept, instrumentation, and applications [62, 66, 67]. In an ideal 2D system, the peaks eluting in the first dimension are sampled several times and injected onto the column in the second dimension. Conventional chromatographic systems can be altered to carry out such separations with an appropriate interface to transfer the eluent of the first dimension to the second dimension. In the case of a 2D HPLC (LC - LC) system, this can be achieved in many ways. In the simplest approach, the eluent from the first dimension is stored in a sample loop that is subsequently analyzed in the second dimension. Alternatively, interfaces that contain more than one sample loop or more than one column with a "column switching" valve can be employed in the second dimension to compensate for the lag-time between the elution. In any case, a rapid separation in the second dimension is a pre-requisite for a meaningful 2D chromatographic system [63, 68, 69].

As shown in Figure 1.3, in a 3D chromatographic plot each peak is characterized by two retention indices. Intuitively, as each peak eluting from the first dimension is analyzed multiple times in the second dimension, the chromatographic peaks are arranged in a structured manner in the 2D chromatographic plane. When

crude oils are analyzed by this technique, a unique hydrocarbon pattern for different crude oils emerges. Such chromatographic plots find wide application in oil spill identification - the matching between the hydrocarbon patterns from the oil spill site and the suspected source gives a definitive clue about the nature of the spilled oil [62, 70, 71].
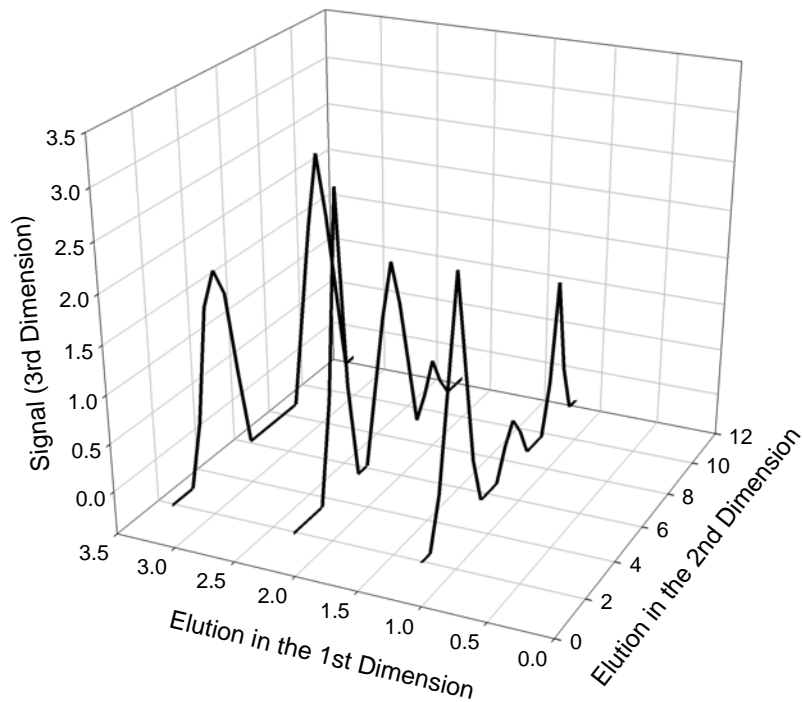
Figure 1.3: Representation of a 3D chromatogram.

For example, Frysinger and Gaines [65] developed a GC-GC-MS method for the analysis of hydrocarbons present in a diesel fuel sample. Their method could resolve over 750 peaks and helped in identification of several new compounds that were present in low concentration. They further developed this method to identify the source of a diesel spill in a marine environment [70].

Quantification of individual components in crude oil samples using 2D systems has also been carried out. A quantitative method for the analysis of BTEX and aromatic compounds present in a gasoline sample using a GC-GC-FID system is reported [71]. In this approach, the hydrocarbons were separated based on their volatility in the first dimension on a dimethylpolysiloxane column. The eluent from the second column was separated using a more polar cyanopropyl methylsiloxane column in the second dimension. This gave a clear separation of volatile compounds from polyaromatic species. A similar GC-GC-FID based system was also reported to be useful for the analysis of PAHs, alkyl PAHs and biomarker compounds present in Alaskan north slope crude oil [72]. By comparing the retention indices of the chromatographic peaks in the 2D plot with that of GC-MS, the authors could identify several individual isomers of dimethyl naphthalenes, trimethyl naphthalenes, methyl dibenzothiophenes, dimethyl dibenzothiophenes and methyl phenanthrenes.

Although 2D HPLC systems find wide applications in peptide analysis [69], their potential for the analysis of PAHs in the environmental samples is not yet fully explored. To achieve maximum orthogonality, it is desirable to combine normal phase and reverse phase separation modes (NPLC-RPLC) in an online 2D

HPLC system. A major problem in constructing such an online 2D system is the incompatibility of solvents that are used in the normal phase and the reverse phase chromatography. Secondly, the solvents usually used in the normal phase separations are relatively strong solvents in the reverse phase mode. Hence, introducing larger volume of normal phase solvents would disperse the solute band on top of the reverse phase column, resulting in severe band broadening. Sonnerfeld *et al.* [73] attempted to overcome these difficulties by coupling a semi-preparative aminosilane column with a C18 column via a diamine concentrator column. The oil sample was applied onto the aminosillane column and the PAH fraction was eluted with 1.3% (v/v) methylene chloride/n-pentane in isocratic mode. The PAH fraction was then transferred to the diamine column and the solvent was evaporated by purging with nitrogen gas. At the end of the purge period, the analytes were desorbed from the concentrator column using 40% water/acetonitrile mobile phase and re-focused onto the C18 reverse-phase column. Such approaches, although useful to analyze selected PAHs in a complex sample, could not be used to develop a comprehensive separation scheme. Recently Dugo *et al.* developed a novel approach for the online NPLC - RPLC separation of oxygen hetrocylics present in lemon oil [74]. Their experimental setup consists of a microbore column (SupelcoSil LC-SI column) in the first dimension with a monolith column (Merck Chromolith Flash) in the second dimension coupled through an interface containing a 10-port-2-position valve. Two identical sample loops (20 μL capacity) connected to the interface valve was used to transfer the sample from the first dimension to the second

dimension. The lemon oil sample applied onto the microbore column was eluted with n-hexane/acetonitrile mobile phase at a flow rate of 20 μL/minute. The normal phase eluent filled the sample loop alternatively that was injected on the monolith column. A fast gradient elution with acetonitrile/water mobile phase at a flow rate of 4 mL/minute was employed in the second dimension. Injection of a small volume of normal phase solvent (20 μL) reduced the solvent immiscibility problem considerably. Moreover, as higher flow rate was employed in the second dimension, the dilution of the strong normal phase solvent could be achieved, quickly resulting in minimum band broadening. Combination of these two effects improved the 2D separation considerably. To overcome the solvent incompatibility issue, several researchers have preferred the use of two reverse phase columns (RPLC - RPLC) for the comprehensive HPLC separation. Murahashi [75] analyzed the PAH extract from a gasoline sample with an online RPLC-RPLC system consisting of a pentabromobenzyl column in the first dimension and two short monolithic C18 columns in the second dimension. The eluent from the first dimension was delivered onto the two monolith columns alternatively using a 10-port-2-position switching valve. To achieve orthogonal separation, the capacity factors of a variety of alkanes and aromatic compounds were evaluated on 12 different stationary phases. Based on these data, it was concluded that the primary separation mechanism operating in the pentabromobenzyl column and C18 reverse-phase columns are quite different. Although this method could not resolve several cluster peaks, it could identify several priority pollutants present in the gasoline extract. Similar methods were

also developed by others for the analysis of brominated biphenyls, dioxins, alkyl benzenes, PAHs, and alkyl phenyl ketones from environmental samples [76]. Alternatively, normal phase LC column coupled to a GC-time-of-flight (ToF) MS system (LC-GC) system has been used to analyze hydrocarbons in a diesel sample [77]. Although this method was found to be suitable to identify major compound classes present in diesel, individual compound analysis could not be achieved.

Assessment of exposure: Biomarkers

One of the major goals of the risk assessment techniques is to relate the presence of toxic components in the environment to observed biological effects. Although the presence of toxic PAHs in the aquatic environment could be established by chemical analysis, toxic response might not be observed unless these PAHs are bio-available. In vertebrates, the PAHs are metabolized by cytochrome P450 (CYP-450) enzyme system. The CYP-450 enzymes represent a "superfamily" and consist of several enzymes that are structurally and functionally similar. They are found in the endoplasmic reticulum or mitochondria of the liver, kidney and other organs [78]. PAH metabolism proceeds through a multi-step metabolic pathway initiated by the binding of the PAHs to the aryl hydrocarbon receptor (AhR). The binding triggers a sequence of molecular events resulting in the increased production of CYP1A enzymes. The CYP1A enzymes in turn metabolize PAHs by catalyzing different types of reactions such as hydroxylation, oxidation, and deethylation. The CYP1A induction is very sensitive and requires exposure to only a small amount of the pollutant. In

addition to PAHs, several other xenobiotics are also known to induce CYP1A expression [79].

CYP1A induction in fish can be measured at different stages of transcription – among them measuring the catalytic activity of ethoxyresourufin-O-deethylase (EROD) is the simplest and hence widely followed [80]. The baseline natural EROD induction in fish is negligible and found to vary with fish species, age, sex and several environmental factors such as temperature. However all these external parameters can be controlled through proper experimental design. In 1975, Payne *et al.* noted that when fish were exposed to petroleum hydrocarbons the activity of the CYP1A enzymes increased significantly. Hence they suggested that CYP1A activity in fish could be used as a biomarker of exposure to petroleum hydrocarbons [81, 82]. Subsequently, several researchers have validated the use of CYP1A induction as a reliable biomarker during field studies conducted at oil-contaminated sites around the world [80, 83, 84].

The link between CYP1A induction and crude oil toxicity is still controversial. Usually elevated levels of CYP1A in fish exposed to crude oil returns to baseline values within a few days after the fish is removed from the contaminated sites [85]. On the other hand, CYP1A metabolites of some of the PAHs present in crude oil are found to be more toxic than the parent compounds [86]. Moreover, prolonged exposure to CYP1A inducing compounds, particularly during early life-stages of fish, has been associated with the development of blue sac disease [87, 88]. Carls *et al.* studied the relation between the prolonged CYP1A induction in pink salmon embryos exposed to crude oil from the fertilization up to six

months until the fry emergence. They observed a good correlation between the elevated levels of CYP1A in the embryonic stage with the reduced survival potential of these embryos after emergence [88]. Based on these observations, they suggested that the long-term effects of crude oil observed in pink salmon during the field studies might be related to the exposure to CYP1A inducers in the embryonic stage.

CYP1A inducers: Structure activity relationship

Figure 1.4 shows some of the environmental pollutants that are known to induce CYP1A enzymes in vertebrates. One of the main characteristics of these compounds is their ability to bind to the AhR receptor. In general, there is a good correlation between the ability of the chemicals to bind to AhR receptor and their CYP1A induction [80, 89]. Hence, several quantitative structure-activity relationship (QSAR) models have been developed to deduce the AhR binding affinities of several classes of compounds such as polychlorinated biphenyls (PCBs), polychlorinated dibenzo dioxins (PCDD), and dibenzofurans [90-93]Based on these studies some general conclusions about the molecular structure of CYP1A inducers can be drawn:

- Aromatic hydrocarbons with planar or nearly planar structure are found to be potential AhR ligands. For example, chrysene, a planar PAH is a relatively strong inducer of CYP1A compared to triphenylene [94]

- The ligands whose molecular dimensions not exceed 14 A° (lengh) X 12 A° (width) X 5 A° (depth), such as benzo[k]fluoranthene, show high binding affinity.

- Physicochemical properties of ligands such as lipophilicity and polarisability are found to play an important role in the ligand-AhR binding [95].
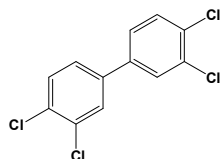
3,3',4,4'-tetrachlorobiphenyl
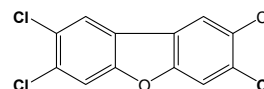
2,3,7,8-tetrachlorodibenzofuran
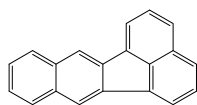
Benzo[k]fluoranthene
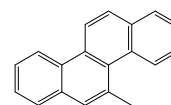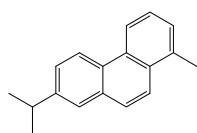
5-methyl chrysene
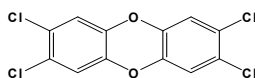
2,3,7,8-tetrachlorodibenzo-p-dioxin

Benzo[a]pyrene

Retene
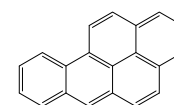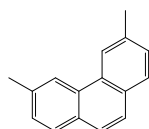
3,6-dimethyl phenanthrene
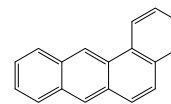
Benz[a]anthracene

Figure 1.4: Molecular structure of some of the environmental pollutants that are known to induce CYP1A enzymes in vertebrates

However, Kafafi *et al.* noted that a non-linear relationship exists between the binding of PCDDs to the AhR receptor and their ability to induce CYP1A enzymes [90]. They found this non-linearity could be accounted for only when one considers the electronic properties of the ligands such as low energy gap (Eg = Ionization potential − Electron affinity) in addition to AhR binding affinity. Thus, one can conclude that although the AhR binding affinity of a chemical is a necessary condition, other molecular parameters have to be favorable for inducing CYP1A enzymes.

Similar to the PCDD isomers, PAH isomers show marked differences in their CYP1A induction potency. Low molecular weight un-substituted PAH such as naphthalene do not induce CYP1A enzymes. On the other hand, PAHs with a higher number of aromatic rings such as benzo[a]pyrene were strong inducers of CYP1A [94]. Despite the fact that alkyl PAHs constitute more than 90% of total PAHs (by weight) in crude oils, only a little information is available on their CYP1A potency. For example, although phenanthrene is a non- inducer of CYP1A, experimental evidences show that retene is a moderate CYP1A inducer [96]. Other alkyl PAHs like 3,6-dimethyl phenanthrene and 3,9-dimethyl benzo[a]anthracene have also been shown to induce CYP1A in *in-vitro* assays using PLHC-1 fish hepatoma cell lines [97]. Thus the contribution of alkyl substituted PAHs to the observed crude oil CYP1A induction and toxicity is still not completely understood.

Screening for CYP1A inducers: Effects-driven fractionation and analysis

Currently only a handful of compounds, dominated by the 16 PAHs in the US EPA's priority pollutants list, is routinely monitored during the risk assessment of oil-contaminated sites. However, recent toxicity studies conducted at contaminated sites showed that the concentration of these priority pollutants only account for a part of the total observed toxicity [98, 99]. For example, Engwall *et al.* fractionated the lipophilic extract of sediment, suspended particulate matter, and blue mussels from a contaminated site in the coastal area of Sweden bordering the Baltic Sea [100]. They observed that the PAH fraction induced high CYP1A activity in most of the samples analyzed. They also analyzed the concentration of the priority PAHs in the PAH fraction and used it to derive the theoretical toxic equivalent quantities (TEQs) with respect to 2,3,7,8-tetrachlorodibenzo-*p*-dioxin (TCDD). They found that the total priority PAH TEQ could account for only a fraction of the observed TEQ obtained experimentally, suggesting that the non-priority pollutants could be the major contributors for observed CYP1A activity.

Crude oil contains a variety of compounds whose toxicity and ability to induce CYP1A in fish vary considerably. In spite of an exponential growth in the development of sensitive analytical techniques it is still not possible to identify many compounds present in crude oil. Moreover, stand-alone biological testing of crude oils, although useful to rank them based on their biological potency, does not necessarily identify the causative agents. Therefore, we have used an effect-driven fractionation and analysis (EDFA) approach for the isolation and

identification of toxic components present in the crude oil samples. Previously, EDFA methodologies have been successfully used to identify toxicants present in complex environmental samples such as sediments and waste water effluents [101].

```
┌─────────────────┐      ┌─────────────────┐      ┌─────────────────┐
│  Environmental  │─────▶│    Chemical     │◀────▶│   Instrument    │
│     sample      │      │                 │      │   al analysis   │
│                 │      │  fractionation  │      │                 │
└─────────────────┘      └─────────────────┘      └─────────────────┘
                                 │                          │
                                 │      ┌──────────┐        │
                                 └─────▶│ Bio-assay│◀───────┘
                                        └──────────┘
                                             │
                                             ▼
                                     ┌─────────────────┐
                                     │    Toxicant     │
                                     │  identification │
                                     └─────────────────┘
```
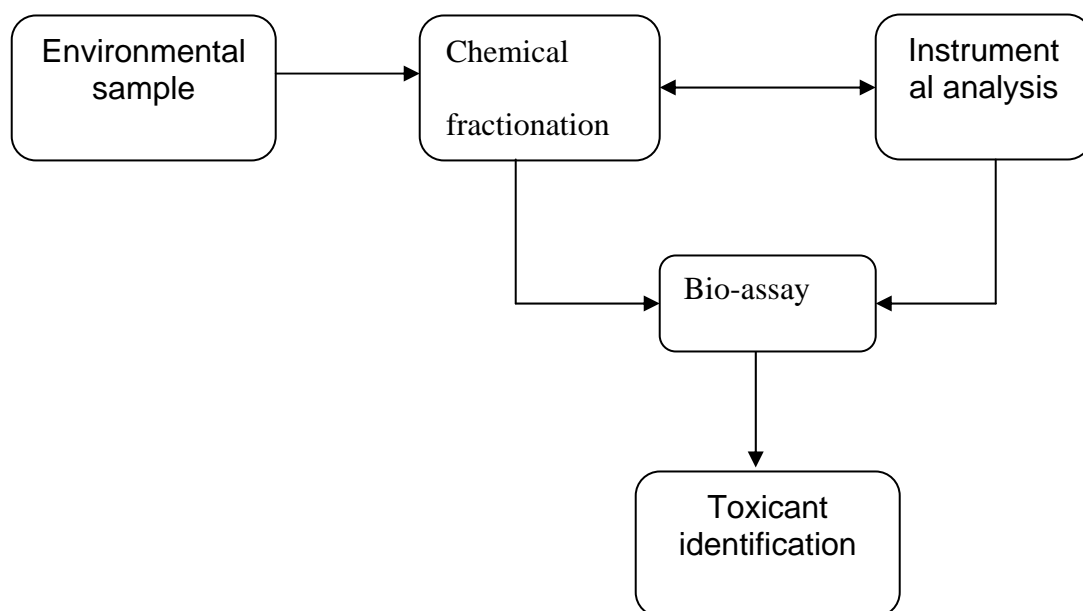
Figure 1.5: Schematics of effect-driven fractionation approach

EDFA methodology: The EDFA approach is very similar to that of toxicity identification and evaluation (TIE) approach as reviewed in a recent report [102]. The schematic of the EDFA methodology is depicted in Figure 1.5. It involves the fractionation of a complex sample into several sub-fractions using chemical methods and testing the resulting sub-fractions for their biological activity. Only fractions that are found to be biologically active are further fractionated and the toxicity test repeated. This iterative process enriches the toxicity of the sub-fractions progressively while reducing its chemical complexity during each fractionation stage. Finally, the toxic sub-fractions are analyzed by standard instrumental methods to identify individual toxicants.

Some of the advantages of EDFA methodology are as follows:

- It is a good screening technique to identify toxic sub-fraction(s) of a complex environmental sample.

- It can be used to identify toxicants in the environmental matrices whose pollution history is not known.

- It is an unbiased approach for toxicity identification and has been useful to identify previously unknown toxicants.

- Moreover, as a biological end point is used as the "detector", the toxicant identification becomes less ambiguous.

On the other hand, high sample specificity of this approach indicates a need to optimize the method for different samples, which is time consuming and expensive. Secondly, this approach works well in the contaminated sites in a highly polluted area. Analyzing toxicants from sites that are far away from the

pollution sources is problematic as a large amount of sample need to be processed during the initial stages of EDFA.

General fractionation approaches: The primary aim of the chemical fractionation is to reduce the chemical complexity of the environmental sample. To aid the fractionation, chemical analysis of the toxic fractions is done at each fractionation stage. Initial fractionation is often done on a bulk scale so as to produce enough materials for the toxicity testing as well as for further fractionation. Both chromatographic and non-chromatographic methods could be used for fractionation, although during the latter stages chromatographic methods are exclusively used. Open column chromatography, using polar stationary phases such as alumina, is widely used to separate the toxicants into non-polar, mid-polar and polar fractions [103, 104]. To further separate aromatic compounds based on the number of aromatic rings, normal phase HPLC techniques employing silica or aminopropylsililated silica columns have been used [100, 103]. Sub-fractionation of the aromatic fraction can be carried out based on other phisico-chemical properties such as size, shape and hydrophobicity to improve the selectivity [104]. Analysis of the toxic fractions is invariably done using GC-MS techniques. Relative retention time values and mass fragmentation pattern of the chromatographic peaks have been used to identify unknown toxicants in the environmental samples.

Identification of CYP1A inducers: The EDFA approach has been successfully applied not only to determine the relative contributions of different classes of toxicants to the observed CYP1A induction but also to identify unknown CYP1A

inducers. A Czech Republic study, directed to identify CYP1A inducers in contaminated sediments in the Morava river basin found that among the known toxicants present in that site, the contribution of PAH fraction to the final CYP1A induction was the highest [105]. Sundburg *et al.* studied the CYP1A induction in sediments that were known to contain high concentrations of PCBs, PCDDs and PAHs. The toxicants were solvent extracted and fractionated using HPLC into mono-aromatic, diaromatic and polyaromatic fractions. Using the retention time of the standard compounds it was found that contaminants such as PCBs, PCDDs eluted in the diaromatic fraction while PAHs dominated the polyaromatic fraction. The CYP1A induction of the sub-fractions showed that the PAHs are the major contributor to the observed CYP1A induction, although the contaminated site received high PCB inputs from past industrial activities [106]. In a separate study, Sundberg *et al.* further fractionated the PAH fraction on a aminopropylsililated silica column and determined that the sub-fractions containing 3 to 5 ring PAHs and their alkyl homologues were the major CYP1A inducers [107].

EDFA studies have also been used to identify several new EROD inducers in contaminated sediments and industrial effluents [99, 108, 109]. For example, Martel *et al.* in 1997 studied the EROD induction in effluents released during different stages of paper making processes from a thermomechanical pulp (TMP) mill. Among the process effluents analyzed, the TMP steam condensate was found to be a major source of EROD activity. Further fractionation and analysis of the condensate components revealed that the compounds that naturally occur in

wood such as juvabione, dehydrojuvabione and manool are the primary inducers [108]. Similarly, Brack *et al.* fractionated the solvent extract of a sediment sample from a highly polluted site in Germany to identify the primary EROD inducers. The non-polar polyaromatic fraction that showed high EROD activity was further fractionated in a multi-step EDFA protocol resulting in the identification of alkyl PAHs such as methyl chrysenes and methyl benz[a]anthracenes and hetrocyclic compounds such as dinaphthofurans 2-(2-naphthalenyl)benzothiophene as the major CYP1A inducers [99].

Preliminary studies

The primary aim of this thesis is to identify the CYP1A inducers and toxicants present in Alaskan north slope crude (ANSC) and Scotian light (SCOT) crude oil. Table 1.4 shows chemical composition of these crude oils. CYP1A induction studies confirmed that both crude oils exhibit dose-dependent EROD activity in rainbow trout. Moreover, the CYP1A induction and toxicity of ANSC oil was found to be much higher than that of SCOT oil. This result correlated well with the PAH content of the crude oils [110]. The first stage of fractionation of these crude oils was carried out by Dr. Zhendi Wang's group at Environment Canada, Ottawa. The crude oils were subjected to a low-temperature vacuum distillation technique to separate its constituents into four fractions based on their boiling points [111]. Table 1.5 shows the nomenclature, boiling range and chemical composition of the sub-fractions of ANSC and SCOT crude oils. For SCOT crude oil the low boiling components present in SCOT 1 and SCOT 2 fractions constitutes about 80% of the total oil mass. Moreover, the high boiling components are virtually

absent in this crude oil. On the other hand, the total oil mass was evenly distributed among the sub-fractions of ANSC oil (Table 1.5). Subsequently, the CYP1A induction and toxicity studies on these sub-fractions were carried out. For both oils, the sub-fraction 3 (ANSC 3 and SCOT 3) showed the highest EROD induction and toxicity. Sub-fractions 1 and 2 neither induced CYP1A nor caused chronic toxicity [110, 112]. The ANSC 4 sub-fraction showed only a mild CYP1A induction while SCOT 4 showed high CYP1A induction and toxicity. As only a very small amount of SCOT 4 fraction was available, further fractionation of SCOT 4 was not considered in this work. Therefore in this work, the EDFA approach is applied to identify the CYP1A inducers and toxicants present in ANSC 3 and SCOT 3 sub-fractions.

Table 1.4: Chemical composition of Alaskan North Slope Crude (ANSC) and Scotian light crude (SCOT) oils. [*Source:* Spill technology database, Environmental Technology Center, Environment Canada. Available online at http://www.etc-cte.ec.gc.ca/databases/spills/oil_prop_e.html. Accessed on June 12, 2007.]

Compound class	ANSC Mass %	SCOT Mass %
Saturates	75	92
Aromatics	15	8
Resins	6.1	1
Asphaltenes	4	0

Table 1.5. Nomenclature and mass percent of ANSC sub-fractions (with respect to whole oil) obtained using low temperature vacuum distillation

Boiling range	ANSC		SCOT	
	Nomenclature	Mass (%)	Nomenclature	Mass (%)
IBP – 180	ANSC 1	20.6	SCOT 1	46.6
180 – 287	ANSC 2	15.5	SCOT 2	32.5
287 – 481	ANSC 3	31.3	SCOT 3	16.2
>481	ANSC 4	29.5	SCOT 4	0.4

Organization of the thesis

The thesis is organized in six chapters including this introduction to illustrate the step-by step fractionation approach applied. Chapter 2 describes a novel wax precipitation method to isolate PAHs from the waxes in the ANSC 3 and SCOT 3 oil fractions. Chapter 3 describes the fractionation of the PAHs present in the extract fraction obtained in the previous step into five fractions based on the number of aromatic rings. For this purpose a semi-preparative normal phase HPLC fractionation scheme was developed and optimized. The last two core chapters (Chapter 4 and 5) focus on the development of a multi-dimensional HPLC method for the analysis un-substituted and alkyl substituted PAHs in crude oil fractions. Finally, the advantages and the limitations of the developed EDFA protocol for the identification of toxicants in the crude oil samples and its application in environmental monitoring are discussed in Chapter 6.

References

1.   Staub, J., *International Energy Outlook 2007.* 2007, Department of Energy: Washington DC. p. 29-38.

2.   Wang, Z., M. Fingas and D.S. Page, *Oil spill identification.* Journal of Chromatography A, 1999. **843**(1-2): p. 369-411.

3.   Paine, R.T., J.L. Ruesink, A. Sun, E.L. Soulanille, M.J. Wonham, C.D.G. Harley, D.R. Brumbaugh and D.L. Secord, *Trouble on oiled waters: Lessons from the Exxon Valdez Oil Spill.* Annual Review of Ecology and Systematics, 1996. **27**(1): p. 197-235.

4.   Kelso, D. and M. Kendziorek, *Alaska's response to the Exxon Valdezoil spill.* Environmental Science & Technology, 1991. **25**(1): p. 16-23.

5.   Maki, A.W., *The Exxon Valdez oil spill: initial environmental impact assessment. Part 2.* Environmental Science & Technology, 1991. **25**(1): p. 24-29.

6.   Piatt, J.F., C.J. Lensink, W. Butler, M. Kendziorek and D.R. Nysewander, *Immiediate impact of the "Exxon Valdez" oil spill on marine birds.* The Auk, 1990. **107**(2): p. 387-397.

7.   Foster, M.S., Tarpley J.A. and D. S.L., *To clean or not to clean: the rationale, methods and consequences of removing oil from temperate shores.* Northwest Environmental Journal, 1990. **6**: p. 105-120.

8.   Rice, S.D., R.E. Thomas, M.G. Carls, R.A. Heintz, A.C. Wertheimer, M.L. Murphy, J.W. Short and A. Moles, *Impacts to Pink Salmon Following the Exxon Valdez Oil Spill: Persistence, Toxicity, Sensitivity, and Controversy.* Reviews in Fisheries Science, 2001. **9**(3): p. 165 - 211.

9.   Bue, B.G., S. Sharr and J.E. Seeb, *Evidence of Damage to Pink Salmon Populations Inhabiting Prince William Sound, Alaska, Two Generations after the Exxon Valdez Oil Spill.* Transactions of the American Fisheries Society, 1998. **127**(1): p. 35-43.

10.   Bue, B.G., S. Sharr, S.D. Moffitt and A.K. Craig. *Effects of the Exxon Valdez oil spill on pink salmon embryos and preemergent fry*. in *Proceedings of the Exxon Valdez Oil Spill Symposium*. 1996. Anchorage, Alaska, USA.

11.   Hayes, M.O. and J. Michel, *Factors determining the long-term persistence of Exxon Valdez oil in gravel beaches,.* Marine Pollution Bulletin, 1999. **38**(2): p. 92-101.

12. Peterson, C.H., S.D. Rice, J.W. Short, D. Esler, J.L. Bodkin, B.E. Ballachey and D.B. Irons, *Long-Term Ecosystem Response to the Exxon Valdez Oil Spill.* Science, 2003. **302**(5653): p. 2082-2086.

13. Short, J.W., M.R. Lindeberg, P.M. Harris, J.M. Maselko, J.J. Pella and S.D. Rice, *Estimate of Oil Persisting on the Beaches of Prince William Sound 12 Years after the Exxon Valdez Oil Spill.* Environmental Science & Technology, 2004. **38**(1): p. 19-25.

14. Hostettler, F.D. and K.A. Kvenvolden, *Geochemical changes in crude oil spilled from the Exxon Valdez supertanker into Prince William Sound, Alaska.* Organic Geochemistry, 1994. **21**(8-9): p. 927-936.

15. Selley, R.C., in *Elements of Petroleum Geology*, Academic Press: Toronto. p. 181-237.

16. Speight, J.G., *Handbook of Petroleum Analysis.* 2001: John Wiley & Sons. 25-57.

17. Wang, Z. and M.F. Fingas, *Development of oil hydrocarbon fingerprinting and identification techniques.* Marine Pollution Bulletin, 2003. **47**(9-12): p. 423-452.

18. Wang, Z., M. Fingas and G. Sergy, *Study of 22-Year-Old Arrow Oil Samples Using Biomarker Compounds by GC/MS.* Environmental Science & Technology, 1994. **28**(9): p. 1733-1746.

19. Wang, Z., M. Fingas and K. Li, *Fractionation of a light crude oil and identification and quantitation of aliphatic, aromatic and biomarker compounds by GC-FID and GC-MS, Part I.* Journal of Chromatographic Science, 1994. **32**: p. 361-366.

20. Wang, Z., M. Fingas and K. Li, *Fractionation of a light crude oil and identification and quantitation of aliphatic, aromatic, and biomarker compounds by GC-FID and GC-MS, Part II.* Journal of Chromatographic Science, 1994. **32**(9): p. 367-382.

21. Groenzin, H. and O.C. Mullins, *Asphaltene Molecular Size and Structure.* J. Phys. Chem. A, 1999. **103**(50): p. 11237-11245.

22. Groenzin, H. and O.C. Mullins, *Molecular Size and Structure of Asphaltenes from Various Sources.* Energy Fuels, 2000. **14**(3): p. 677-684.

23. Sheu, E.Y., *Petroleum Asphaltene-Properties, Characterization, and Issues.* Energy Fuels, 2002. **16**(1): p. 74-82.

24. Speight, J.G., R.B. Long and T.D. Trowbridge, *Factors influencing the separation of asphaltenes from heavy petroleum feedstocks.* Fuel, 1984. **63**(5): p. 616-620.

25. Carbognani, L. and A. Izquierdo, *Preparative and automated compound class separation of Venezuelan vacuum residua by high-performance liquid chromatography.* Journal of Chromatography A, 1989. **484**: p. 399-408.

26. Philp, R.P., *Fossil fuel biomarkers-applications and spectra.* Methods in geochemistry and geophysics series. Vol. 23: Elsevier. 13-56.

27. Henderson, W., G.Eglinton, P.Simmonds and J. E.Lovelock, *Thermal alteration as a contributory process to the genesis of petroleum.* Nature, 1968. **219**: p. 1012-1016.

28. Radke, M., *Organic geochemistry of aromatic hydrocarbons*, in *Advances in Petroleum geochemistry*, J.B.a.D. Welte, Editor. 1987, Academic Press: Toronto.

29. Tissot, B., Y. Califet-debser, G. Deroo and J.L. Oudin, *Origin and evolution of hydrocarbons in early Toarcian shales, Paris basin, France.* The American Association of Petroleum Geologists Bulletin, 1971. **55**: p. 2177-2193.

30. Douglas, A.G. and B.J. Mair, *Sulfur: role in genesis of petroleum.* Science, 1965. **147**: p. 499-501.

31. Wakeham, S.G., C. Schaffner and W. Giger, *Poly cyclic aromatic hydrocarbons in Recent lake sediments--II. Compounds derived from biogenic precursors during early diagenesis.* Geochimica et Cosmochimica Acta, 1980. **44**(3): p. 415-429.

32. Barman, B.N., V.L. Cebolla and L. Membrado, *Chromatographic techniques for petroleum and related products.* Critical Reviews in Analytical Chemistry, 2000. **30**(2-3): p. 75-120.

33. Elsa Lundanes, T.G., *Separation of fuels, heavy fractions, and crude oils into compound classes: A review.* Journal of High Resolution Chromatography, 1994. **17**(4): p. 197-202.

34. Kaminski, M., R. Kartanowicz, E. Gilgenast and J. Namiesnik, *High-Performance Liquid Chromatography in Group-Type Separation and Technical or Process Analytics of Petroleum Products.* Critical Reviews in Analytical Chemistry, 2005. **35**(3): p. 193-216.

35. Grizzle, P.L. and D.M. Sablotny, *Automated liquid chromatographic compound class group type separation of crude oils and bituments using*

chemically bonded aminosilane. Analytical Chemistry, 1986. **58**(12): p. 2389-2396.

36.   Matsunaga, A., *Separation of aromatic and polar compounds in fossil fuel liquids by liquid chromatography.* Analytical Chemistry, 1983. **55**(8): p. 1375-1379.

37.   Sharma, B.K., S.L.S. Sarowha, S.D. Bhagat, R.K. Tiwari, S.K. Gupta and P.S. Venkataramani, *Hydrocarbon group type analysis of petroleum heavy fractions using the TLC-FID technique.* Fresenius' Journal of Analytical Chemistry, 1998. **360**(5): p. 539-544.

38.   Norris, T.A. and M.G. Rawdon, *Determination of hydrocarbon types in petroleum liquids by supercritical fluid chromatography with flame ionization detection.* Analytical Chemistry, 1984. **56**(11): p. 1767-1769.

39.   Alimi, H., T. Ertel and B. Schug, *Fingerprinting of Hydrocarbon Fuel Contaminants: Literature Review.* Environmental Forensics, 2003. **4**(1): p. 25 - 38.

40.   Benlahcen, K.T., A. Chaoui, H. Budzinski, J. Bellocq and P. Garrigues, *Distribution and sources of polycyclic aromatic hydrocarbons in some Mediterranean coastal sediments.* Marine Pollution Bulletin, 1997. **34**(5): p. 298-305.

41.   Sauer, T.C., J.S. Brown, P.D. Boehm, D.V. Aurand, J. Michel and M.O. Hayes, *Hydrocarbon source identification and weathering characterization of intertidal and subtidal sediments along the Saudi Arabian coast after the Gulf War oil spill.* Marine Pollution Bulletin, 1993. **27**: p. 117-134.

42.   Poster, D., M. Schantz, L. Sander and S. Wise, *Analysis of polycyclic aromatic hydrocarbons (PAHs) in environmental samples: a critical review of gas chromatographic (GC) methods.* Analytical and Bioanalytical Chemistry, 2006. **386**(4): p. 859-881.

43.   Poster, D.L., L.C. Sander and S. Wise, *Chromatographic methods of analysis for the determination of PAHs in environmental samples.* Handbook of Environmental Chemistry, 1998. **3**: p. 77-135.

44.   Poster, D.L., B.A. Benner, Jr., M.M. Schantz, L.C. Sander, S.A. Wise and M.G. Vangel, *Determination of Methyl-Substituted Polycyclic Aromatic Hydrocarbons in Diesel Particulate-Related Standard Reference Materials.* Polycyclic Aromatic Compounds, 2003. **23**(2): p. 113-139.

45.   Fetzer, J.C., W.R. Biggs and K. Jinno, *HPLC analysis of the large polycyclic aromatic hydrocarbons in a diesel particulate.* Chromatographia, 1986. **21**(8): p. 439-42.

46.   Krahn, M.M., G.M. Ylitalo, J. Buzitis, S.-L. Chan and U. Varanasi, *Rapid high-performance liquid chromatographic methods that screen for aromatic compounds in environmental samples.* Journal of Chromatography A, 1993. **642**(1-2): p. 15-32.

47.   Jinno, K. and K. Kawasaki, *Correlation between the retention data of polycyclic aromatic hydrocarbons and several descriptors in reversed-phase HPLC.* Chromatographia, 1983. **17**(8): p. 445-449.

48.   Jinno, K., K. Tanabe, Y. Saito and H. Nagashima, *Separation of polycyclic aromatic hydrocarbons with various C60 fullerene bonded silica phases in microcolumn liquid chromatography.* Analyst (Cambridge, United Kingdom), 1997. **122**(8): p. 787-791.

49.   Wise, S.A. and L.C. Sander, *Factors affecting the reversed-phase liquid chromatographic separation of polycyclic aromatic hydrocarbon isomers.* Journal of High Resolution Chromatography, 1985. **8**(5): p. 248-255.

50.   Sander, L.C. and S.A. Wise, *Shape selectivity in reversed-phase liquid chromatography for the separation of planar and non-planar solutes.* Journal of Chromatography A, 1993. **656**(1-2): p. 335-351.

51.   Sander, L.C. and S.A. Wise, *Effect of phase length on column selectivity for the separation of polycyclic aromatic hydrocarbons by reversed-phase liquid chromatography.* Analytical Chemistry, 1987. **59**(18): p. 2309-2313.

52.   Wise, S.A., L.C. Sander and W.E. May, *Determination of polycyclic aromatic hydrocarbons by liquid chromatography.* Journal of Chromatography A, 1993. **642**(1-2): p. 329-349.

53.   Sander, L.C. and S.A. Wise, *Subambient temperature modification of selectivity in reversed-phase liquid chromatography.* Anal. Chem., 1989. **61**(15): p. 1749-1754.

54.   Lawrence, J.F., *Advantages and limitations of HPLC in environmental analysis.* Chromatographia, 1987. **24**: p. 45-50.

55.   Kline, W.F., S.A. Wise and W.E. May, *The Application of Perdeuterated Polycyclic Aromatic Hydrocarbons (PAH) as Internal Standards for the Liquid Chromatographic Determination of PAH in a Petroleum Crude Oil and Other Complex Mixtures.* Journal of Liquid Chromatography and Related Technologies, 1985. **8**(2): p. 223 - 237.

56.   Wise, S.A., L.R. Hilpert, G.D. Byrd and W.E. May, *Comparison of liquid chromatography with fluorescence detection and gas chromatography/mass spectrometry for the determination of polycyclic aromatic hydrocarbons in environmental samples.* Polycyclic Aromatic Compounds, 1990. **1**(1-2): p. 81-98.

57.   Wise, S.A., B.A. Benner, S.N. Chesler, L.R. Hilpert, C.R. Vogt and W.E. May, *Characterization of the polycyclic aromatic hydrocarbons from two standard reference material air particulate samples.* Anal. Chem., 1986. **58**(14): p. 3067-3077.

58.   Gratz, L.D., S.T. Bagley, D.G. Leddy, J.H. Johnson, C. Chiu and P. Stommel, *Interlaboratory comparison of HPLC-fluorescence detection and GC/MS: analysis of PAH compounds present in diesel exhaust.* Journal of Hazardous Materials, 2000. **74**(1-2): p. 37-46.

59.   Krahn, M.M., G.M. Ylitalo, J. Buzitis, S.L. Chan, U. Varanasi, T.L. Wade, T.J. Jackson, J.M. Brooks, D.A. Wolfe and C.A. Manen, *Comparison of high-performance liquid chromatography/fluorescence screening and gas chromatography/mass spectrometry analysis for aromatic compounds in sediments sampled after the Exxon Valdez oil spill.* Environmental Science & Technology, 1993. **27**(4): p. 699-708.

60.   Davies, I.L., M.W. Raynor, P.T. Williams, G.E. Andrews and K.D. Bartle, *Application of automated on-line microbore high-performance liquid chromatography/capillary gas chromatography to diesel exhaust particulates.* Anal. Chem., 1987. **59**(21): p. 2579-2583.

61.   Focant, J.-F., A. Sjodin and D.G. Patterson, *Improved separation of the 209 polychlorinated biphenyl congeners using comprehensive two-dimensional gas chromatography-time-of-flight mass spectrometry.* Journal of Chromatography A, 2004. **1040**(2): p. 227-238.

62.   Frysinger, G.S., R.B. Gaines and C.M. Reddy, *GC × GC--A New Analytical Tool For Environmental Forensics.* Environmental Forensics, 2002. **3**: p. 27-34.

63.   Ikegami, T., T. Hara, H. Kimura, H. Kobayashi, K. Hosoya, K. Cabrera and N. Tanaka, *Two-dimensional reversed-phase liquid chromatography using two monolithic silica C18 columns and different mobile phase modifiers in the two dimensions.* Journal of Chromatography A, 2006. **1106**(1-2): p. 112-117.

64.   Venkatramani, C.J. and Y. Zelechonok, *An Automated Orthogonal Two-Dimensional Liquid Chromatograph.* Anal. Chem., 2003. **75**(14): p. 3484-3494.

65.   Frysinger, G.S. and R.B. Gaines, *Comprehensive Two-Dimensional Gas Chromatography with Mass Spectrometric Detection (GC × GC/MS) Applied to the Analysis of Petroleum.* Journal of High Resolution Chromatography, 1999. **22**(5): p. 251-255.

66. Gorecki, T., O. Panic and N. Oldridge, *Recent advances in comprehensive two-dimensional gas chromatography (GC-GC).* Journal of Liquid Chromatography and Related Technologies, 2006. **29**(7): p. 1077 - 1104.

67. Liu, Z. and M.L. Lee, *Comprehensive two-dimensional separations using microcolumns.* Journal of Microcolumn Separations, 2000. **12**(4): p. 241-254.

68. Welch, K.J. and N.E. Hoffman, *Analysis of fossil-fuel fractions by on-line coupled microcolumn HPLC capillary column GC-MS.* Journal of High Resolution Chromatography, 1992. **15**(3): p. 171-175.

69. Kimura, H., T. Tanigawa, H. Morisaka, T. Ikegami, K. Hosoya, N. Ishizuka, H. Minakuchi, K. Nakanishi, M. Ueda, K. Cabrera, and N. Tanaka, *Simple 2D-HPLC using a monolithic silica column for peptide separation.* Journal of Separation Science, 2004. **27**(10-11): p. 897-904.

70. Gaines, R.B., G.S. Frysinger, M.S. Hendrick-Smith and J.D. Stuart, *Oil Spill Source Identification by Comprehensive Two-Dimensional Gas Chromatography.* Environmental Science & Technology, 1999. **33**(12): p. 2106-2112.

71. Frysinger, G.S., R.B. Gaines and E. B. Ledford Jr., *Quantitative Determination of BTEX and Total Aromatic Compounds in Gasoline by Comprehensive Two-Dimensional Gas Chromatography (GC×GC).* Journal of High Resolution Chromatography, 1999. **22**(4): p. 195-200.

72. Frysinger, G.S. and R.B. Gaines, *Separation and identification of petroleum biomarkers by comprehensive two-dimensional gas chromatography.* Journal of Separation Science, 2001. **24**(2): p. 87-96.

73. Sonnefeld, W.J., W.H. Zoller, W.E. May and S.A. Wise, *On-line multidimensional liquid chromatographic determination of polynuclear aromatic hydrocarbons in complex samples.* Anal. Chem., 1982. **54**(4): p. 723-727.

74. Dugo, P., O. Favoino, R. Luppino, G. Dugo and L. Mondello, *Comprehensive Two-Dimensional Normal-Phase (Adsorption)-Reversed-Phase Liquid Chromatography.* Anal. Chem., 2004. **76**(9): p. 2525-2530.

75. Murahashi, T., *Comprehensive two-dimensional high-performance liquid chromatography for the separation of polycyclic aromatic hydrocarbons.* Analyst (Cambridge, United Kingdom), 2003. **128**(6): p. 611-615.

76. Tanaka, N., H. Kimura, D. Tokuda, K. Hosoya, T. Ikegami, N. Ishizuka, H. Minakuchi, K. Nakanishi, Y. Shintani, M. Furuno, and K. Cabrera, *Simple and Comprehensive Two-Dimensional Reversed-Phase HPLC Using Monolithic Silica Columns.* Anal. Chem., 2004. **76**(5): p. 1273-1281.

77.   de Koning, S., H.-G. Janssen and U.A.T. Brinkman, *Group-type characterisation of mineral oil samples by two-dimensional comprehensive normal-phase liquid chromatography-gas chromatography with time-of-flight mass spectrometric detection.* Journal of Chromatography A, 2004. **1058**(1-2): p. 217-221.

78.   Buhler, D.R. and J.-L. Wang-Buhler, *Rainbow trout cytochrome P450s: purification, molecular aspects, metabolic activity, induction and role in environmental monitoring.* Comparative Biochemistry and Physiology, 1998. **Part C**(121): p. 107-137.

79.   Denison, M.S. and S. Heath-Pagliuso, *The Ah Receptor: A Regulator of the Biochemical and Toxicological Actions of Structurally Diverse Chemicals.* Bulletin of Environmental Contamination and Toxicology, 1998. **61**(5): p. 557-568.

80.   Whyte, J.J., R.E. Jung, C.J. Schmitt and D.E. Tillitt, *Ethoxyresorufin-O-deethylase (EROD) Activity in Fish as a Biomarker of Chemical Exposure.* Critical Reviews in Toxicology, 2000. **30**(4): p. 347 - 570.

81.   Payne, J.F. and W.R. Penrose, *Induction of aryl hydrocarbon (benzo[a]pyrene) hydroxylase in fish by petroleum.* Bulletin of Environmental Contamination and Toxicology, 1975. **14**(1): p. 112-116.

82.   Payne, J.F., *Field Evaluation of Benzopyrene Hydroxylase Induction as a Monitor for Marine Petroleum Pollution.* Science, 1976. **191**(4230): p. 945-946.

83.   Arinç, E., A. Sen and A. Bozcaarmutlu, *Cytochrome P4501A and associated mixedfunction oxidase induction in fish as a biomarker for toxic carcinogenic pollutants in the aquatic environment.* Pure and Applied Chemistry, 2000. **72**(6): p. 985-994.

84.   Bucheli, T.D. and K. Fent, *Induction of cytochrome P450 as a biomarker for environmental contamination in aquatic ecosystems.* Critical Reviews in Environmental Science and Technology, 1995. **25**(3): p. 201-68.

85.   Woodin, B.R., R.M. Smolowitz and J.J. Stegeman, *Induction of Cytochrome P4501A in the Intertidal Fish Anoplarchus purpurescens by Prudhoe Bay Crude Oil and Environmental Induction in Fish from Prince William Sound.* Environ. Sci. Technol., 1997. **31**(4): p. 1198-1205.

86.   Stegeman, J.J. and J.J. Lech, *Cytochrome P-450 Monooxogenase Systems in Aquatic Species: Carinogen Metabolism and Biomarkers for Carcinogen and Pollutant Exposure.* Environmental Health Perspectives, 1991. **90**: p. 101-109.

87.   Brinkworth, L.C., P.V. Hodson, S. Tabash and P. Lee, *CYP1A induction and blue sac disease in early developmental stages of rainbow trout (Oncorhynchus mykiss) exposed to retene.* Toxicology and environmental health, 2003. **66**(7): p. 526-546.

88.   Carls, M.G., R.A. Heintz, G.D. Marty and S.D. Rice, *Cytochrome P4501A induction in oil-exposed pink salmon Oncorhynchus gorbuscha embryos predicts reduced survival potential.* Marine Ecology: Progress Series, 2005. **301**: p. 253-265.

89.   Billiard, S.M., M.E. Hahn, D.G. Franks, R.E. Peterson, N.C. Bols and P.V. Hodson, *Binding of polycyclic aromatic hydrocarbons (PAHs) to teleost aryl hydrocarbon receptors (AHRs).* Comparative Biochemistry and Physiology, Part B: Biochemistry & Molecular Biology, 2002. **133B**(1): p. 55-68.

90.   Kafafi, S.A., H.Y. Afeefy, H.K. Said and A.G. Kafafi, *Relationship between aryl hydrocarbon receptor binding, induction of aryl hydrocarbon hydroxylase and 7-ethoxyresorufin O-deethylase enzymes, and toxic activities of aromatic xenobiotics in animals. A new model.* Chem. Res. Toxicol., 1993. **6**(3): p. 328-334.

91.   Tysklind, M., K. Lundgren, C. Rappe, L. Eriksson, J. Jonsson, M. Sjoestroem and U.G. Ahlborg, *Multivariate characterization and modeling of polychlorinated dibenzo-p-dioxins and dibenzofurans.* Environmental Science & Technology, 1992. **26**(5): p. 1023-1030.

92.   Waller, C.L. and J.D. McKinney, *Comparative molecular field analysis of polyhalogenated dibenzo-p-dioxins, dibenzofurans, and biphenyls.* J. Med. Chem., 1992. **35**(20): p. 3660-3666.

93.   Waller, C.L. and J.D. McKinney, *Three-Dimensional Quantitative Structure-Activity Relationships of Dioxins and Dioxin-like Compounds: Model Validation and Ah Receptor Characterization.* Chem. Res. Toxicol., 1995. **8**(6): p. 847-858.

94.   Barron, M.G., R. Heintz and S.D. Rice, *Relative potency of PAHs and heterocycles as aryl hydrocarbon receptor agonists in fish.* Marine Environmental Research, 2004. **58**(2-5): p. 95-100.

95.   Jung, D.K.J., T. Klaus and K. Fent, *Cytochrome P450 induction by nitrated polycyclic aromatic hydrocarbons, azaarenes, and binary mixtures in fish hepatoma cell line PLHC-1.* Environmental Toxicology and Chemistry, 2001. **20**(1): p. 149-159.

96.   Billiard, S.M., N.C. Bols and P.V. Hodson, *In vitro and in vivo comparisons of fish-specific CYP1A induction relative potency factors for selected*

polycyclic aromatic hydrocarbons. Ecotoxicology and Environmental Safety, 2004. **59**(3): p. 292-299.

97. Villeneuve, D.L., J.S. Khim, K. Kannan and J. P.Giesy, *Relative potencies of individual polycyclic aromatic hydrocarbons to induce dioxinlike and estrogenic responses in three cell lines.* Environmental Toxicology, 2002. **17**(2): p. 128-137.

98. Hollert, H., M. Durr, H. Olsman, K. Halldin, B. van Bavel, W. Brack, M. Tysklind, M. Engwall and T. Braunbeck, *Biological and Chemical Determination of Dioxin-like Compounds in Sediments by Means of a Sediment Triad Approach in the Catchment Area of the River Neckar.* Ecotoxicology, 2002. **11**(5): p. 323-336.

99. Brack, W. and K. Schirmer, *Effect-Directed Identification of Oxygen and Sulfur Heterocycles as Major Polycyclic Aromatic Cytochrome P4501A-Inducers in a Contaminated Sediment.* Environmental Science & Technology, 2003. **37**(14): p. 3062-3070.

100. Engwall, M., D. Broman, C. Naf, Y. Zebuhr and B. Brunstrom, *Dioxin-like compounds in HPLC-fractionated extracts of marine samples from the east and west coast of Sweden: Bioassay- and instrumentally-derived TCDD equivalents.* Marine Pollution Bulletin, 1997. **34**(12): p. 1032-1040.

101. Brack, W., *Effect-directed analysis: a promising tool for the identification of organic toxicants in complex mixtures?* Analytical and Bioanalytical Chemistry, 2003. **377**(3): p. 397-407.

102. Ho, K.T., R.M. Burgess, M.C. Pelletier, J.R. Serbst, S.A. Ryba, M.G. Cantwell, A. Kuhn and P. Raczelowski, *An overview of toxicant identification in sediments and dredged materials.* Marine Pollution Bulletin, 2002. **44**(2): p. 286–293.

103. Brack, W., R. Altenburger, U. Ensenbach, M. Moder, H. Segner and G. Schuurmann, *Bioassay-Directed Identification of Organic Toxicants in River Sediment in the Industrial Region of Bitterfeld (Germany)-A Contribution to Hazard Assessment.* Archives of Environmental Contamination and Toxicology, 1999. **37**(2): p. 164-174.

104. Brack, W., T. Kind, H. Hollert, S. Schrader and M. Moder, *Sequential fractionation procedure for the identification of potentially cytochrome P4501A-inducing compounds.* Journal of Chromatography A, 2003. **986**(1): p. 55-66.

105. Hilscherova, K., K. Kannan, Y.-S. Kang, I. Holoubek, M. Machala, S. Masunaga, J. Nakanishi and J.P. Giesy, *Characterization of dioxin-like activity of sediments from a Czech river basin.* Environmental Toxicology and Chemistry, 2001. **20**(12): p. 2768-2777.

106. Sundberg, H., U. Tjarnlund, G. Akerman, M. Blomberg, R. Ishaq, K. Grunder, T. Hammar, D. Broman and L. Balk, *The distribution and relative toxic potential of organic chemicals in a PCB contaminated bay.* Marine Pollution Bulletin, 2005. **50**(2): p. 195-207.

107. Sundberg, H., R. Ishaq, G. Akerman, U. Tjarnlund, Y. Zebuhr, M. Linderoth, D. Broman and L. Balk, *A Bio-Effect Directed Fractionation Study for Toxicological and Chemical Characterization of Organic Compounds in Bottom Sediment.* Toxicological Sciences, 2005. **84**(1): p. 63-72.

108. Martel, P.H., T.G. Kovacs, B.I. Connor and R.H. Voss, *Source and identity of compounds in a thermomechanical pulp mill effluent inducing hepatic mixed-function oxygenase activity in fish.* Environmental Toxicology and Chemistry, 1997. **16**(11): p. 2375-2383.

109. Burnison, B.K., M.E. Comba, J.H. Carey, J. Parrott and J.P. Sherry, *Isolation and tentative identification of compounds in bleached-kraft mill effluent capable of causing mixed-function oxygenaase induction in fish.* Environmental Toxicology and Chemistry, 1999. **18**(12): p. 2882-2887.

110. Khan, C.W., S.D. Ramachandran, L.M.J. Clarke and P.V. Hodson. *EROD activity (CYP1A) inducing compounds in fractionated crude oil.* in *Proceedings of the twenty-seventh Artic and Marine Oilspill Program (AMOP) technical seminar*. 2004. Edmonton, Alberta: Emergencies Science and Technology division, Environment Canada.

111. Wang, Z., B.P. Hollebone, M. Fingas, B. Fieldhouse, L. Sigouin, M. Landriault, P. Smith, J. Noonan and G. Thouin, *Development of a composition database for selected multicomponent oil.* 2002, Environment Canada: Ottawa.

112. Hodson, P.V., C.W. Khan, G. Saravanabhavan, L.M.J. Clarke and R.S. Brown. *Alkyl PAH in crude oil cause chronic toxicity to early life stages of fish.* in *Proceedings of the thirtieth Artic and Marine Oilspill Program (AMOP) technical seminar*. 2007. Edmonton, Alberta: Emergencies Science and Technology division, Environment Canada.

CHAPTER 2

Selective extraction of CYP1A inducing components present in the heavy gas oil fraction (b.p. 287°C –461°C) of Alaskan North Slope and Scotian Light crude oils

Guru Saravanabhavan[1], Colin Khan[2], Bill Shaw[2], Peter Hodson[2], and R. Stephen Brown[1]

[1]Department of Chemistry and School of Environmental Studies, Queen's University, Kingston, ON.
[2]Department of Biology and School of Environmental Studies, Queen's University, Kingston, ON.

Abstract

Exposure to crude oils has been shown to produce elevated levels of CYP1A enzymes in fish. This is correlated with the high levels of PAHs present in crude oils. In addition to PAHs, crude oil contains a variety of other compound classes. Hence, separation of PAHs from other constituents of the crude oil is necessary to identify the CYP1A inducing PAHs of the crude oil. To this end, we have developed a procedure to precipitate waxes present in the heavy gas oil fraction (boiling range 287°C - 461°C) of Alaskan North Slope and Scotian Light crude oils. Operating parameters of the method such as the choice of the solvent, oil-to-solvent ratio, and extraction temperature were optimized. Recovery studies on the extract and the wax residue showed that the extract contains > 80% of PAHs originally present in the heavy gas oil fraction. Bulk fractions of extract and residue were produced using the optimized method to test their CYP1A activity in trout (*Oncorhynchus mykiss*). The extract showed high CYP1A activity while the residue showed none. Chemical composition of the bioassay solutions as well as the extract and the residue was analyzed using GC-MS and the results were correlated with the CYP1A induction of the respective fractions. Results showed that higher amount of alkyl PAHs present in the extract are associated with its high potency for inducing CYP1A activity.

Introduction

Aquatic ecosystems are particularly vulnerable to oil pollution. The effects of oil pollution on marine life can either be due to physical contact with the oil or through exposure to toxic chemicals contained in the oil. In 1989, the Exxon Valdez oil spill discharged about 11 million gallons of Alaskan North Slope crude (ANSC) oil in Prince William Sound, Alaska. Although this is not the largest oil spill in the world, the environmental damages associated with this spill were severe and have been studied extensively [1, 2]. Several thousands of dead seabirds that were soaked in oil were retrieved immediately after the spill [3-5]. Subsequent laboratory and field studies have shown that exposure to crude oil leads to acute and chronic toxicity in fishes and other aquatic organisms [6, 7]. Hence there is an increased impetus to identify the toxicants in the crude oil that are responsible for the observed toxic effects. Moreover, chemical analysis of toxic fractions can give "chemical fingerprints" that can be used to trace the source(s) of oil pollution [8]. This information is very crucial to resolve disputes over the responsibility among the concerned parties and eventually could lead to proper remediation strategies.

Crude oil is a complex mixture of several classes of chemical compounds and hence predicting the components that are responsible for the observed toxicity is often very difficult. Crude oil contains a wide variety of unsubstituted and alkyl substituted polycyclic aromatic hydrocarbons (PAHs). As PAHs are known environmental pollutants, crude oil toxicity is often associated with its PAH content [6, 9-11]. In fish, PAHs are metabolized by the cytochrome P450 enzyme

system (CYP1A). Binding of the PAH to the aryl hydrocarbon receptor (AhR) is the first step in the multi-step metabolic pathway. The binding triggers a sequence of events resulting in the increased production of CYP1A enzymes. The CYP1A enzymes in turn metabolize the PAH by oxidation and/or hydroxylation [12]. In addition to PAHs other classes of compounds such as polychlorinated biphenyls (PCBs), dioxins and dibenzofurans induce CYP1A expression. The induction is very sensitive and requires exposure to only a small amount of the pollutant. Therefore, CYP1A induction has been used as a reliable biomarker for contaminant exposure [13].

CYP1A induction in fish can be measured by several methods. Measuring ethoxyresourfin-*O*-deethlyase (EROD) enzyme activity is very popular due to its simplicity. EROD induction has been well characterized in different fish species. The baseline EROD induction in fish is found to vary with fish species, age, sex and several environmental factors such as temperature. However all these external parameters can be controlled through proper experimental design [14]. Field studies conducted at oil-contaminated sites showed an increased EROD induction in fish and other aquatic organisms that were found to correlate well with the PAH concentrations in these sites [15-17].

As binding of the chemical to AhR receptor is a necessary step for CYP1A induction [14], many quantitative structure-activity relationship (QSAR) models have been proposed to correlate the AhR binding affinities of compounds such as PCBs, dioxins , and dibenzofurans to their molecular structure [18-20]. In general, aromatic hydrocarbons with planar or nearly planar structure are found

to be potential AhR ligands. Secondly, the ligands whose molecular dimensions do not exceed 14 Å (length) X 12 Å (width) X 5 Å (depth) show higher binding affinities. Thirdly, physicochemical properties such as lipophilicity and polarisability are found to play an important role in the ligand:AhR binding [21, 22]. As many of these parameters vary among PAH it is expected that their CYP1A induction potency would also vary considerably. Lower molecular weight unsubstituted PAHs such as naphthalene are generally regarded as non-inducers of CYP1A. On the other hand, PAHs with a higher number of aromatic rings such as benzo[a]pyrene have been found to be strong inducers of CYP1A[23]. Despite the fact that alkyl PAHs constitute more than 90% of total PAHs (by weight) in crude oils, very little information is available on their CYP1A induction potency. For example, although phenanthrene is a weak inducer of CYP1A, experimental evidence shows that alkyl phenanthrenes such as retene (7-isopropyl-1-methyl phenanthrene) are moderate CYP1A inducers. Thus the overall contribution of alkyl substituted PAHs to the observed crude oil CYP1A induction is still unknown.

Our group is interested in isolating and characterizing CYP1A inducing components present in Alaskan North Slope (ANSC) and Scotian Light (SCOT) crude oils using an effect-driven fractionation approach (EDFA). Earlier work from our group studied EROD induction in rainbow trout by ANSC and SCOT crude oils and their distillation fractions obtained by low-temperature vacuum distillation [24]. The results of this study showed that the majority of CYP1A induction seen from whole oil is present in the heavy gas oil fraction (ANSC 3

and SCOT 3; boiling point 287°C-461°C). GC-MS analysis indicated that this fraction contains a large amount of unsubstituted and alkyl substituted PAHs and saturated hydrocarbons [25]. Due to the lack of aromatic structure, saturated hydrocarbons would not interact with AhR receptor strongly and hence are not expected to induce CYP1A. Therefore, high CYP1A activity of ANSC 3 and SCOT 3 fractions likely can be attributed to its high PAH content. This led us to the conclusion that the separation of PAHs from saturated hydrocarbons is a logical first step in understanding the observed EROD activity in ANSC 3 and SCOT 3 fractions.

Petroleum waxes are saturated hydrocarbons with carbon number ranging from C20 to C70. Waxes can be separated from other crude oil constituents using chromatographic techniques; however solvent precipitation offers a simpler alternative. Burger et al. have developed a method to precipitate waxes in crude oil samples using acetone:petroleum ether (3:1 v/v) as the precipitating solvent at -20°C [26]. Modifications to this method to use other solvents or solvent combinations have also been reported [27-29]. As other crude oil components such as asphaltenes and resins can co-precipitate with waxes, the primary aim of these solvent precipitation methods has been to isolate 'pure' waxes from the crude oil so that the isolated waxes can be further analyzed using other techniques. Usually asphaltenes present in the crude oil are removed prior to wax precipitation by treatment with n-pentane [28]. Chen et al. adopted a Chinese Petroleum Test Standard (SY/T 7550-2000) to measure the wax content of 14 crude oils with varying wax content [29]. In this method, a solution of crude

oil in petroleum ether was passed through a chromatographic column packed with alumina. The column was eluted with benzene until asphaltenes started to elute. After evaporating most of the benzene, the sample was dissolved in an acetone:toluene (1:1 v/v) mixture and cooled at -20°C for 30 minutes. The wax precipitate was then filtered and weighed in a clean glass vial. Jokuty et al. precipitated waxes using methylene chloride/methylethyl ketone as the precipitating solvent at -30°C [27]. They also reported the applicability of gas chromatography with flame ionization detection (GC-FID) for measuring wax content of the crude oil samples. Good agreement between wax content obtained by GC-FID and the solvent precipitation method was observed for light and medium crude oil samples. However, for crude oils with high wax content, the GC-FID method gave more accurate results.

The main objective of this work is to isolate PAHs from waxes present in ANSC 3 and SCOT 3 oil fractions. For this purpose a solvent precipitation method was developed to remove waxes present in these fractions. Precipitation parameters such as the nature of solvent, temperature, and oil-to-solvent ratio were optimized so as to produce a large amount of wax residue with low PAH concentration. Then the CYP1A induction of the extract and residue was tested using EROD assays with rainbow trout. Finally, the CYP1A results were correlated with the detailed chemical analysis of the bioassay solutions and the original extract and residue samples obtained using gas chromatography-mass spectrometric (GC-MS) analysis.

Materials and method

Materials: All solvents used in this study were of HPLC grade and were procured from Fisher Scientific (Ottawa, ON). Table 2.1a shows the list of alkanes and PAHs analyzed in this study. A list of internal standards and surrogate standards used in the GC-MS analysis are shown in Table 2.1b. All PAH standards had a minimum purity of >95% and were obtained from Sigma Aldrich (Milwaukee, WI) and Ultra Scientific (Kingstown, RI). ANSC and SCOT crude oil samples and their corresponding heavy gas oil fractions (ANSC 3 and SCOT 3) were obtained form Dr. Zhendi Wang, Environment Canada (Ottawa, ON).

Wax precipitation procedure: Waxes were isolated using the "Burger method" [26] with a few modifications. Briefly, the oil fraction was heated to 70°C for 30 minutes in a water bath to completely dissolve the waxes. About 5 grams of the oil was weighed into a 100 mL conical flask on an analytical balance. To this, 50 mL of the solvent was added and sonicated at room temperature for 5 minutes. The mixture was cooled to the desired temperature and maintained at that temperature for at least 5 hours. Finally, the mixture was filtered through a 0.22 μm nylon filter. The precipitate was washed with 15 mL of solvent (maintained at the desired temperature) and the washing added to the extract. The residue was dissolved using 5 mL of hexane followed by 5 mL of dichloromethane in a clean vial. Solvent in both the residue and the extract solutions was evaporated under nitrogen and the final product weighed on an analytical balance. Finally, these samples were dissolved in hexane to a known volume and analyzed using HPLC.

Table 2.1a: List of alkanes and PAHs analyzed using GC-MS. The abbreviated codes for alkyl PAH analytes are given in the parenthesis.

Compound	Retention time (min.)	Quantifying Ion m/z
ALKANES		
n-decane	4.42	57
undecane	6.38	57
dodecane	8.92	57
tridecane	11.81	57
tetradecane	14.82	57
pentadecane	17.81	57
hexadecane	20.72	57
heptadecane	23.51	57
2,6,10,14-TMPdecane (pristane)	23.61	57
octadecane	26.18	57
2,6,10,14-TMHdecane (phytane)	26.33	57
nonadecane	28.72	57
eicosane	31.17	57
heneicosane	33.50	57
docosane	35.75	57
tricosane	37.90	57
tetracosane	39.97	57
pentacosane	41.95	57
hexacosane	43.86	57
heptacosane	45.71	57
octacosane	47.48	57
n-nonacosane	49.20	57
tricontane	50.87	57
n-heneicontane	52.67	57
dotriacontane	54.83	57
tritriacontane	57.44	57
tetratriacontane	60.67	57
n-pentatriacontane	64.62	57
17beta(H), 21 alpha (H)-hopane	53.75	191
PAHs		
Naphthalene (C0 NAPH)	8.64	128
Methylnaphthalene (C1 NAPH)	11.74	142
Dimethylnaphthalene (C2 NAPH)	15.36	156
Trimethylnaphthalene (C3 NAPH)	18.64	170
Tetramethylnaphthalene (C4 NAPH)	24.77	184
Acenaphthene (Ace)	17.20	154
Acenaphthalene (Acl)	16.21	152
Fluorene (C0 FLUOR)	20.10	166
Methylfluorene (C1 FLUOR)	23.44	180

Dimethylfluorene (C2 FLUOR)	26.31	194
Trimethylfluorene (C3 FLUOR)	24.37	208
Dibenzothiophenes (C0 DBT)	24.73	184
Methyldibenzothiophene (C1 DBT)	27.31	198
Dimethyldibenzothiophene (C2 DBT)	30.30	212
Trimethyldibenzothiophene (C3 DBT)	32.44	226
Tetramethyldibenzothiophene (C4 DBT)	36.26	240
Phenanthrene (C0 PHEN)	25.45	178
Anthracene (An)	25.76	178
Methylphenanthrene (C1 PHEN)	28.50	192
Dimethylphenanthrene (C2 PHEN)	31.26	206
Trimethylphenanthrene (C3 PHEN)	34.40	220
Tetramethylphenanthrene (C4 PHEN)	37.60	234
Fluoranthene (Fl)	32.31	202
Pyrene (C0 Py)	33.50	202
Methylpyrene (C1 Py)	36.17	216
Dimethylpyrene (C2 Py)	39.00	230
Trimethylpyrene (C3 Py)	41.37	244
Tetramethylpyrene (C4 Py)	43.39	258
Naphthobenzothiophene (C0 NBT)	39.17	234
Methylnaphthobenzothiophene (C1 NBT)	42.28	248
Dimethylnaphthobenzothiophene (C2 NBT)	44.23	262
Trimethylnaphthobenzothiophene (C3 NBT)	46.67	276
Tetramethylnaphthobenzothiophene (C4 NBT)	48.27	290
Benz[a]anthracene (BaA)	40.63	228
Chrysene (C0 CHRY)	40.80	228
Methylchrysene (C1 CHRY)	43.08	242
Dimethylchrysene (C2 CHRY)	45.22	256
Trimethylchrysene (C3 CHRY)	48.01	270
Tetramethylchrysene (C4 CHRY)	49.90	284
Benzo[b]fluoranthene (BbF)	46.45	252
Benzo[k]fluoranthene (BkF)	46.59	252
Benzo[e]pyrene (BeP)	47.73	252
Benzo[a]pyrene (BaP)	47.97	252
Perylene (Pe)	48.39	252
Indeno[1,2,3-cd]pyrene (IP)	53.34	276
Dibenz[a,h]anthracene (DA)	53.67	278
Benzo[ghi]perylene (BP)	54.69	276

Table 2.1b: List of internal and surrogate standards used in the GC-MS analysis

Compounds	Retention Time (min.)	Quantifying Ion m/z (a.m.u)
Internal Standards		
d22-n-decane	4.18	66
d34-n-hexadecane	20.00	66
d42-n-eicosane	30.40	66
d62-n-triacontane	50.01	66
5alpha-androstane	31.25	245
d8-naphthalene	8.56	136
d10-anthracene	25.65	188
d12-chrysene	40.66	240
d12-perylene	48.27	264
Surrogate Standards		
d26-dodecane	8.43	66
d36-n-heptadence	22.78	66
d50-n-tetracosane	39.15	66
d66-n-dotriacontane	53.54	66
5beta-cholestane	47.33	217
d10-phenanthrene	25.34	188
d10-pyrene	33.41	212
d12-benzo[b]fluoranthene	46.33	264
d12-benzo[a]pyrene	47.87	264
d14-dibenz[a,h]anthracene	53.50	292

Optimization of extraction temperature: The -20°C experiments were done in the freezer compartment of a standard refrigerator (Isotemp, Fisher Scientific). The temperature of the freezer varied less than +/- 2°C during the course of the experiment. -40°C and -80°C experiments were carried out in a low temperature bath using an acetone/dry ice mixture. The temperature of the bath was maintained at the desired temperature by adding small amounts of dry ice continuously.

HPLC analysis: The HPLC system consisted of two pump modules (Varian prostar 215) and a UV absorbance detector (Varian prostar 330) operating at 254 nm. For PAH analysis, 650 µg of the extract or residue sample in 20 µL hexane was injected onto a semi-preparative silica column (Zorbax sil, 9.4 mm i.d. x 25 cm length; particle diameter 5 micron; Agilent, Mississauga, ON). The PAHs were eluted using 98% hexane/2% methylene chloride as the mobile phase under isocratic conditions. After the PAH elution, the column was back-flushed with 100% methylene chloride to remove resins and other polar materials. A PAH standard mixture was analyzed after every sample run to verify the column regeneration, and more back-flushing done if standards did not return to original elution times. As shown in Figure 2.1, two to five ring PAH standards eluted between 20 and 80 minutes under the chromatographic conditions used in this study. It should be noted that the alkyl homologs of these PAHs elute very close to the unsubstituted PAHs on our silica column. Therefore, the area under the chromatogram between 20 and 80 minutes would give an estimation of total PAH

content of a given sample if one assumes a linear relationship between the area and the PAH concentration.
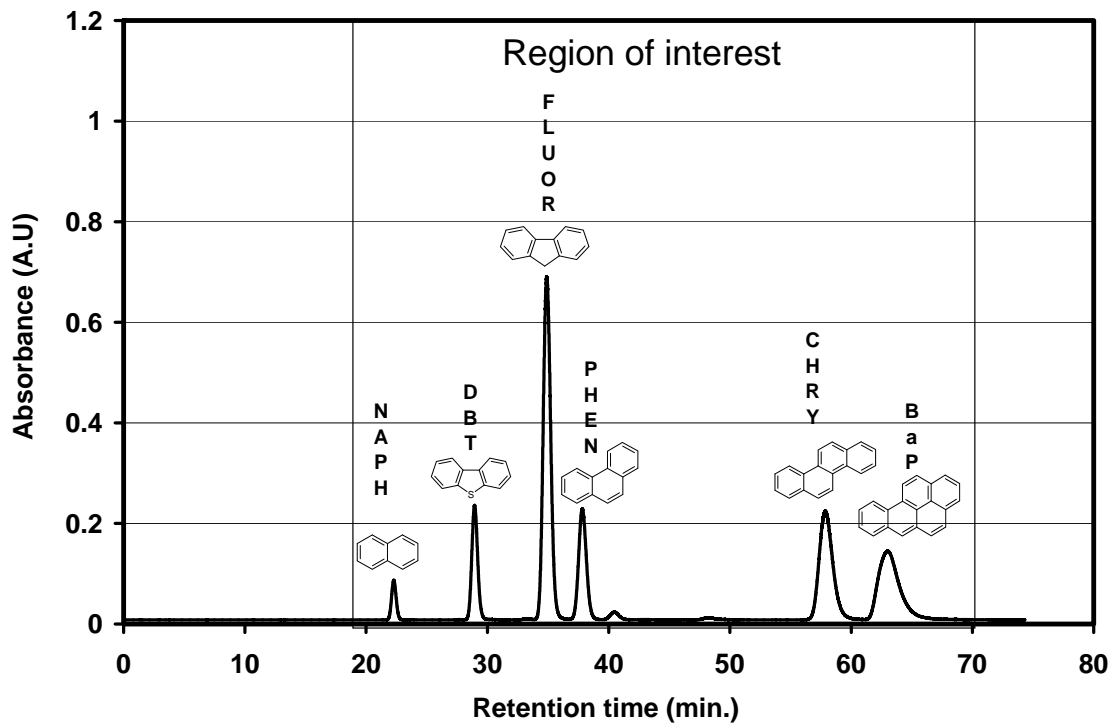
Figure 2.1: Analysis of PAH standards of varying number of aromatic ring in normal phase HPLC. PAHs are separated on a Zorbax sil column (9.4 mm i.d. x 25 cm length; particle diameter 5 micron) using 98% hexane/2% dichloromethane as a mobile phase at a flow rate of 1.5 mL/min.

Sample preparation for GC-MS analysis: A working solution of the extract and the residue sample at 1.00 mg/mL concentration was prepared in hexane. To a pre-weighed graduated centrifuge tube, a 1.0 mL aliquot of the extract or the residue sample and 5 mL of isooctane (density = 0.687g/mL) were added and evaporated under a gentle stream of nitrogen to ~ 1 mL. An aliquot of 20 μL of the internal standard stock solution containing deuterated PAHs and alkane standards (Table 2.1b) at 500 ng each was added to the sample and the final weight of the sample was recorded. From the sample weight the final volume was calculated using the density of iso-octane.

GC-MS analysis: The detailed PAH analysis was done on a high-resolution gas chromatography (Agilent 6890 GC) coupled to a mass selective detector (Agilent 5973N) (Willmington, DE) using a method developed by King et al.[30]. PAHs were separated using a MDN-5S column (30 m x 0.25mm id 0.25 µm film thickness, Supelco) with helium as the carrier gas. Cold on-column injection in oven track mode (track 3°C higher that the oven temperature program) was used to inject the sample onto the column. The temperature of the GC oven was programmed as follows: 80°C (hold 2 min) - ramp at 4°C/min to 280°C (hold 10 min). After every two samples run, a solvent run was made to check for any baseline drift. PAH quantification was done in the selective ion-monitoring mode (SIM). The list of target analytes, internal standards and their corresponding quantifying ions used are given in Table 2.1a and 2.1b. The instrument quantification limits for the target analytes were found experimentally as 100

ng/mL of the final extract. Based on this, the method detection limits were obtained for the analysis of crude oil sub-fractions and bioassay solutions.

Preparation of chemically enhanced water accommodated fraction (CEWAF): An aliquot of 200 μL of the oil fraction was mixed with 1700 μL of water and 100 μL of oil dispersant (Corexit 9500, Exxon, NJ) in a 7 mL glass vial. The contents were mixed by vortexing for 3 minutes followed by sonication for 5 minutes at room temperature. This produced a milky homogeneous suspension of the oil fraction in water. 1.0 mL of this suspension was spiked into a 10 L exposure tank.

Fish exposure: Juvenile trout (*Oncorhynchus mykiss*) were exposed for 24 h to a range of concentrations of fractionated crude oil. Five trout ranging in size from 1-3 g were placed in black buckets lined with food grade polyethylene bags containing 10L of de-chlorinated municipal water and a corresponding dose of CEWAF emulsion. Positive and negative controls β-napthoflavone (BNF, a model CYP1A inducer) and water, respectively, were included for each bioassay for quality control purposes. The fish were held at 13°C +/- 1°C with a photoperiod of 16 h light, 8 h dark. Water quality was assessed daily. Dissolved oxygen (DO) ranged from 70% to 100% saturation, pH was between 7.2 and 8.2, and conductivity ranged from 200 – 300 μS/cm. Total un-ionized ammonia and total residual chlorine were also assessed and both were always below sub-lethal concentrations. Each experiment was characterized by the nominal hydrocarbon concentration (mg/L) dispersed by Corexit 9500 and diluted in tank exposure water. Following the exposure period, the fish were anaesthetized by transferring them to a container of water having 100 mg/L of MS–222 (Ethyl-m-

aminobenzoate methanesulfonate) and killed by a blow to the head. Livers were removed, weighed, and homogenized with 500 μL of HEPES buffer (11.184 g KCl, 5.206 g HEPES sodium salt dissolved in 1 L water, pH 7.5). Samples were centrifuged at 9000 X g for 20 minutes at 2ºC and the supernatant/microsomal layers (S9 fractions) were collected. S9 fractions were snap frozen in liquid nitrogen and stored at –80ºC until further analysis.

EROD enzyme Assay: A standard EROD enzyme assay was followed throughout this work [31]. Briefly, 50 μL of each S9 fraction was added in triplicate to wells of a clear 96-well microplate. Each microplate included a concentration series of resorufin in dimethyl sulfoxide solution (DMSO). The substrate, 7-ethoxy-resorufin (7ER), was diluted to 0.22 mM in assay buffer and a volume of 50 μL dispensed into each sample well. The samples were incubated in the dark at room temperature for 10 minutes. The reaction was started with 10 μL of a 1 mg/mL solution of reduced nicotinamide adenine dinucleotide phosphate (NADPH), after which fluorescence was read once per minute for 12 minutes using a Spectromax Gemini fluorescence plate reader (Molecular Diagnostics, CA) with the excitation set at λ_{530} nm and emission set at λ_{586} nm. Total fluorescence produced per minute by each sample was calculated and expressed as crude activity (pmol/min/mL). Crude activity was normalized to protein content measured by assaying 50μL of a 21-fold dilution of each S9 sample using BioRad reagent standardized against bovine serum albumin (BSA). Protein concentrations were measured with a Spectramax Plus microplate spectrophotometer (Molecular Diagnostics) set at 600 nm. EROD values were

then divided by protein values to give specific activity (pmol/mg/min). Relative EROD induction for all treatments was calculated by dividing the treatment mean by the control mean values.

Statistical analysis: All statistical analyses were conducted with either Microsoft Excel or SigmaStat software. One-way analysis of variance (ANOVA) of EROD data was calculated using log-transformed EROD values. The log EROD values used for ANSC and SCOT failed normality tests (likely due to small sample size per treatment) but passed the equal variance test. For each ANOVA, a *post hoc* multiple comparison test (the Bonferroni *t*-test) was applied to identify treatment concentrations that were significantly different from one another [32].

Analysis of bioassay samples: A 1 L water sample from bioassay tanks of different treatment concentrations was collected at 2h and 24h dosing period. To this 1.00 mL of surrogate standard mix (Table 2.1b) having 500 ng of each compound in acetone was spiked. The sample was extracted with 3 X 20 mL of dichloromethane and the extracts were combined. About 5 mL of iso-octane was added to the extract and concentrated on a Turbo Vap Concentrator (Zymark, Hopkinton, MA) to ~1 mL. The concentrated extract was quantitatively transferred to a pre-weighed centrifuge tube and 20 μL of the internal standard solution was added. The final weight of the sample was recorded before the analysis and used to calculate the final volume of the sample. Finally, the sample was analyzed using GC-MS.

Results and Discussion

Precipitation of asphaltenes: Treatment of ANSC 3 and SCOT 3 fractions with 1:40 v/v of pentane at room temperature did not result in any asphaltene precipitation. Therefore, in the subsequent experiments this step was eliminated.
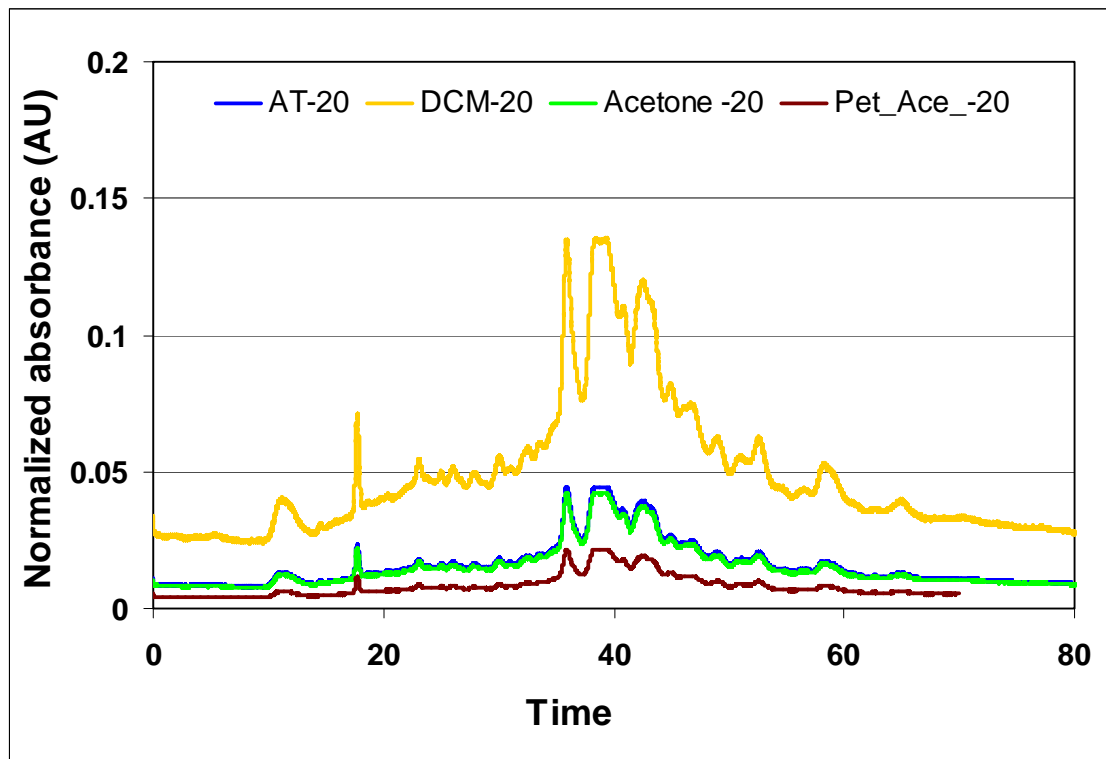
Figure 2.2: Chromatographic analysis of wax residues obtained during the precipitation of ANSC 3 with different precipitating solvents at -20°C. 650 μg of each residue sample was injected on a Zorbax sil column (9.4 mm i.d. x 25 cm length; packed with silica particles of diameter 5 micron) and eluted with 98% hexane/2% dichloromethane. The mobile phase flow rate was maintained at 1.5 mL/min. All absorbance values are normalized against the solvent blank.

Choice of solvent for wax precipitation: Several solvent or solvent combinations have been used in the literature for wax precipitation. Among them, acetone, acetone/toluene (50/50 v/v), methylene chloride, and acetone/petroleum ether (75/25 v/v) have been widely used for wax precipitation [26, 29]. We compared the suitability of these solvents for the precipitation of wax from the ANSC 3 oil fraction. Table 2.2 shows the mass percentage of wax residues obtained using the different solvent systems at -20°C. Acetone precipitated the highest amount of wax residue while dichloromethane precipitated the least. The concentrations of total PAH present in the residues obtained from different solvents were tested using normal phase HPLC. As shown in Figure 2.2, the PAH concentrations were generally very low but varied widely depending on the precipitation solvent. Among the residues tested, residue from dichloromethane precipitation showed the highest concentration of PAHs. It can also be noted that the PAH concentration in the acetone residue was relatively low. The combination of maximum wax precipitate amount and low PAH in the precipitate resulted in acetone being selected as the preferred solvent.

Optimization of extraction temperature: Although it is customary to report the wax content of crude oils at -25°C, previous studies have shown that the total wax material precipitated increases with a decrease in the precipitation temperature [33, 34]. To study the effect of temperature, wax precipitation was carried out at 20°C, 5°C, -20°C, -40°C and -80°C. Acetone was used as the precipitation solvent and the oil-to-solvent ratio was kept at 1:10. Table 2.3 shows the total amount of wax residues recovered at various temperatures for ANSC 3 and

SCOT 3 fractions. In the case of ANSC 3, the amount of wax precipitate obtained increased from <2 mass % at 20°C to about 70 mass % at -80°C. For the SCOT 3 fraction, there was no wax precipitate seen at 20°C while about 65 mass % wax residue was precipitated at -80°C. To test if there is a difference in the concentration of PAHs in residues obtained at -20°C and -80°C, the extract and the residue samples were analyzed using normal phase HPLC. As shown in Figure 2.3, the PAH profiles of the extracts -20°C and -80°C overlap with each other. The PAH content in the -80°C residue is slightly higher than in the -20°C residue, but is still a very small percentage of the total PAH in the sample. As precipitation at -80°C gave the highest yield of wax, -80°C was chosen as the optimal precipitation temperature.

Optimization of solvent volume: To study the effect of solvent volume, varying volumes of acetone were added to a fixed volume of heavy gas oil fraction and cooled at -20°C for 5 hours. Table 2.4 shows the amount of wax residue obtained at different volume ratios for ANSC 3 and SCOT 3 oil fractions. In general, the total amount of waxes precipitated increased with a decrease in the volume of precipitating solvent. On the other hand, the concentration of PAHs in the wax residue increased at lower solvent volumes. Thus, the volume of the precipitating solvent can influence both the total amount of wax residue precipitated and its PAH content. As our aim is to increase total amount of wax precipitate without having PAHs in the residue, either extreme of the oil-to-solvent ratio was unfavorable. It can be noted from Table 2.4 that the total wax precipitated at the oil-to-solvent volume ratio of 0.1 is higher (48%) than that at 0.05 (37%). At the

same time, the PAH concentration in wax residues obtained at 0.1 and 0.05

volume ratios did not differ significantly. Based on these results, an oil-to-solvent

volume ratio of 0.1 was chosen as optimum.
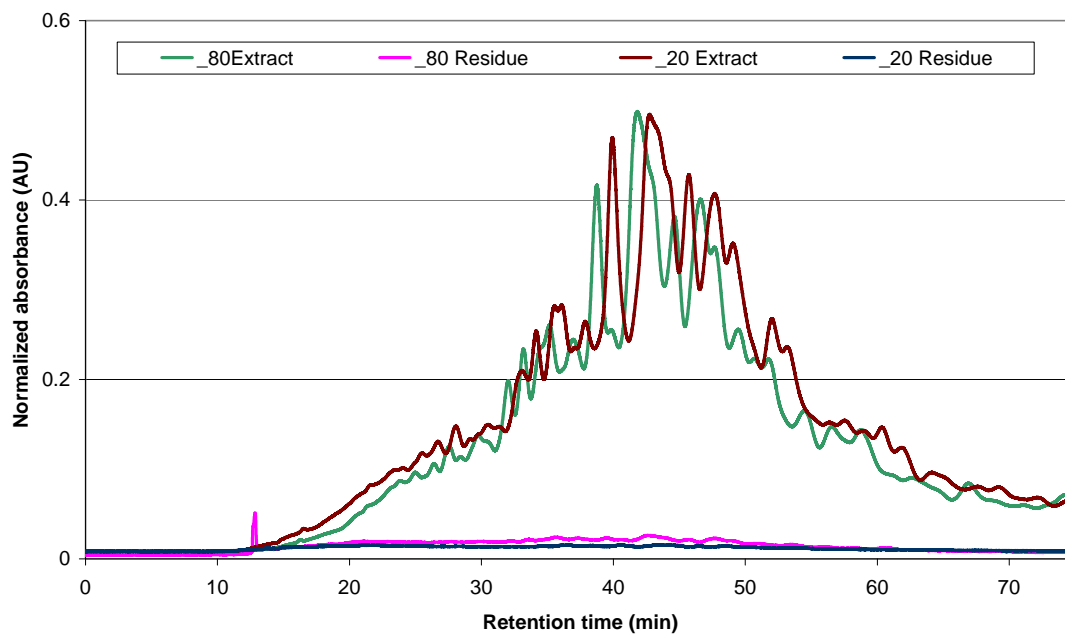
Figure 2.3: Comparison of PAH profile of extracts and wax residues obtained at -20°C and -80°C. In each case, 650 µg of the sample was injected in the normal phase HPLC system. PAHs are eluted using 98% hexane/2% dichloromethane at a flow rate of 1.5 mL/min.

Table 2.2: Total amount of residue obtained during the precipitation of ANSC 3 with different solvents. The precipitation was carried out at -20°C with 1:10 oil-to-solvent ratio (w/v) for 5 hours. The total recovery of the materials (extract+residue) was >95%.

Solvent system	Mass of ANSC 3 used (g)	Mass % of residue
Acetone	4.9155	39
Dichloromethane	0.4876	2
Acetone/toluene (1:1)	0.8638	8
Acetone/Pet. Ether (3:1)	4.3280	7

Table 2.3: Optimization of precipitation temperature for the wax precipitation protocol. A solvent-to-oil ratio of 1:10 is used. Precipitation time was maintained at 5 hours. The total recovery of the material (extract+residue) was >95%.

Extraction Temperature (°C)	ANSC 3		SCOT 3	
	Mass of oil fraction used (g)	Mass % of residue (g)	Mass of oil fraction used (g)	Mass % of residue
20	2.7810	1.6	2.008	No precipitate
5	2.0393	26	----	-----
-20	4.9155	45	1.9797	39
-40	2.2906	52	1.6967	55
-80	1.4957	71	1.9420	63

Table 2.4: Optimization of solvent volume for the wax precipitation protocol. Precipitations were carried out at -20°C and the precipitation time was kept at 5 hours. PAH content was measured using normal phase HPLC method as described in the text.

Volume of heavy oil/Volume of acetone	ANSC 3			SCOT 3	
	Mass of oil used (g)	Mass % of residue	Total PAH content (arbitary units)	Mass of oil used (g)	Mass % of residue (g)
1	3.6120	74	----	----	----
0.2	1.9047	56	409	1.8228	45
0.1	1.7927	48	292	1.7348	42
0.05	1.9949	37	267	1.7788	26
0.025	1.7460	25	206	1.7788	28

Optimization of extraction time: The time required to completely precipitate waxes from ANSC 3 was assessed at -20°C. For this, the crude oil was mixed with acetone in a 1:10 volume ratio in a centrifuge tube. The contents were cooled at -20°C for 30 minutes and centrifuged at 6000 X g for 30 minutes using a cold centrifuge (Beckman, USA). The precipitated waxes were separated and the supernatant was again cooled to -20°C. The process was repeated until no further precipitation was observed. The results showed that about 2 hours was sufficient to precipitate all the waxes and this time was used as a minimum time for wax precipitation in the subsequent trials.

Bulk fractionation heavy gas oil fractions: Large quantities of cold acetone extract and wax residue were prepared by subjecting ANSC 3 and SCOT 3 to the optimized wax precipitation method in several batches. Tables 2.5 and 2.6 show the mass % of extract and wax residue obtained at -80°C for ANSC 3 and SCOT

3 oil fractions. In all batches, the total recovery of the material was > 95%. Low variability (< 5%) of the total wax material precipitated among batches indicated good reproducibility of the overall precipitation technique. Under the precipitation conditions of the method, it is expected that the waxes, resins and other high molecular weight aromatic compounds would co-precipitate. Hence, the total amount of residue obtained would not necessarily correlate with the wax content of the oil fractions. Bulk extract and residue samples were obtained by pooling together the corresponding fractions from different batches. These composite samples were used in the CYP1A induction studies.

Table 2.5: Average mass percentage of extract and residue obtained in different batches

Trail No.	Mass of ANSC 3 (grams)	Mass % of extract	Mass % of residue
1	2.9048	35	68
2	2.9201	29	65
3	3.9941	31	63
4	4.0039	29	67
5	4.0030	31	61
6	3.9962	28	65
7	4.0057	29	69
8	4.0009	29	65
9	4.0106	28	71
	Average	**30 ± 2**	**66 ± 3**

Table 2.6: Average mass percentage of extract and residue obtained in different batches

Trail No.	Mass of SCOT 3 used (grams)	Mass % of extract	Mass % of residue
1	4.0019	41	58
2	4.0056	38	57
3	3.9991	35	63
4	3.9999	37	59
5	3.9940	31	67
6	3.9948	32	65
7	4.0045	34	64
8	3.9999	31	65
	Average	**35 ± 3**	**62 ± 4**

Table 2.7: Percentage distribution of PAHs in the extract and residue

Trial No.	ANSC 3		SCOT 3	
	Extract (%)	Residue (%)	Extract (%)	Residue (%)
1	84	13	91	9
2	79	16	94	6
3	83	15	92	8
Average	**82±2.6**	**14.6 ±1.5**	**92.3 ±1.5**	**7.6 ±1.5**

Recovery Studies: Recovery studies were performed to determine the distribution of PAHs in the extract and the residue upon the cold acetone precipitation of the original heavy gas oil samples. For this, two ANSC 3 samples of equal mass (+/- 5 mg) were weighed in an analytical balance and one of them was subjected to cold acetone extraction. The cold acetone extract, residue and the untreated

sample were then dissolved separately in hexane in a 10 mL volumetric flask.

These samples were analyzed using normal phase HPLC.
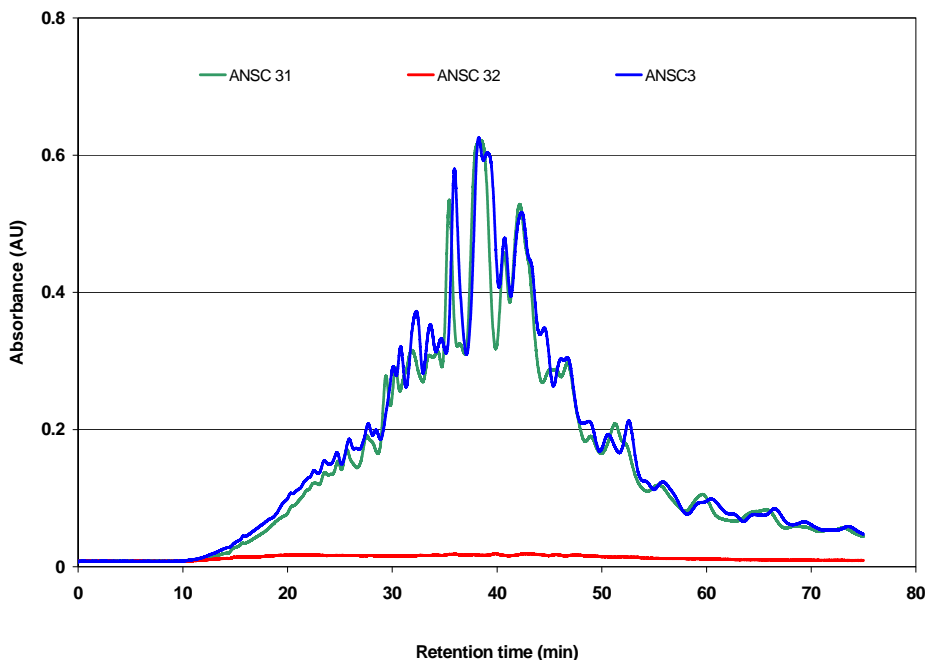
Figure 2.4: Distribution of PAHs in extract (ANSC 31) and residue (ANSC 32) samples after cold acetone extraction of ANSC 3 oil fraction. Column: ZorbaxSil 9.6 mm X 25 cm; 650 μg of each sample was injected on the column; Mobile phase: 98% hexane/2% dichloromethane.

Figure 2.4 shows the PAH profiles of the cold acetone extract (ANSC 31), the residue (ANSC 32) and the untreated ANSC 3 fraction. It can be noted from Figure 2.4 that the PAH profiles of ANSC 31 and the untreated ANSC 3 overlap with each other, indicating efficient recovery of PAHs in the extract. The profile also indicates that only trace amount of PAH was present in the residue. The recovery experiments with SCOT 3 gave similar results. Semi-quantitative estimates of PAH content present in the extract and the residue were obtained by

measuring the area under the chromatograms between 20 and 80 minutes. These results were used to calculate the percentage recovery of PAHs in these samples with respect to the unextracted heavy gas oil fraction and tabulated in Table 2.7. For ANSC 3 sub-fractions, the distribution of PAHs in ANSC 31 and ANSC 32 was about 80% and 15% respectively. In the case of SCOT 3 fraction, about 94% of the PAHs were partitioned in the extract while 6% were found in the residue.

Bioassay: To test the usefulness of the wax precipitation method for the effect-driven fractionation of crude oil samples, the dose-dependent CYP1A activity of the cold acetone extract and the wax residue sub-fractions were conducted in rainbow trout. In Figures 2.5 and 2.6 the EROD induction in fish exposed to different nominal concentrations of cold acetone extract, residue and the un-extracted ANSC 3 and SCOT 3 oil fractions are shown. Induction was calculated by normalizing the absolute activity against the water control. EROD activity of ANSC 3 and SCOT 3 sub-fractions showed some common trends:

- For both oils, the extracts caused a dose-dependent increase in CYP1A response. At the highest concentration, the induction from the extracts was equivalent to that of the BNF positive control.

- The EROD induction from residue samples at all concentrations was very low and close to that of the solvent control.

- For both oils, the overall response curves of the extracts were shifted to lower concentrations compared to that of un-extracted crude oil, indicating an enrichment of CYP1A inducers in the extract.

These results demonstrate that the majority of CYP1A inducers originally present in the heavy gas oil were extracted in the cold acetone extract after wax precipitation. It can also be noted from Figure 2.5 that the EROD induction by the ANSC 31 increased with concentration until it reached a plateau at about 0.009 mg/L hydrocarbon concentration. In contrast, the EROD induction by the SCOT 31 reached a plateau at about 1 mg/L (Figure 2.6), demonstrating that the extract from ANSC 31 is about 100 times more potent than the SCOT 31.
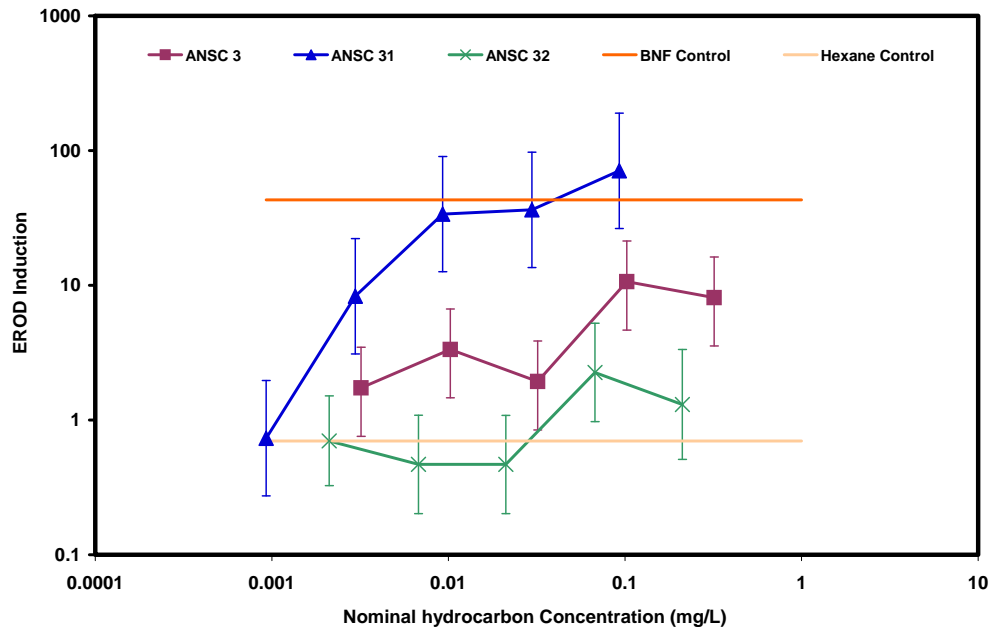
Figure 2.5: EROD induction of the ANSC3 and its sub-fractions. Error bars represent 95% confidence interval.
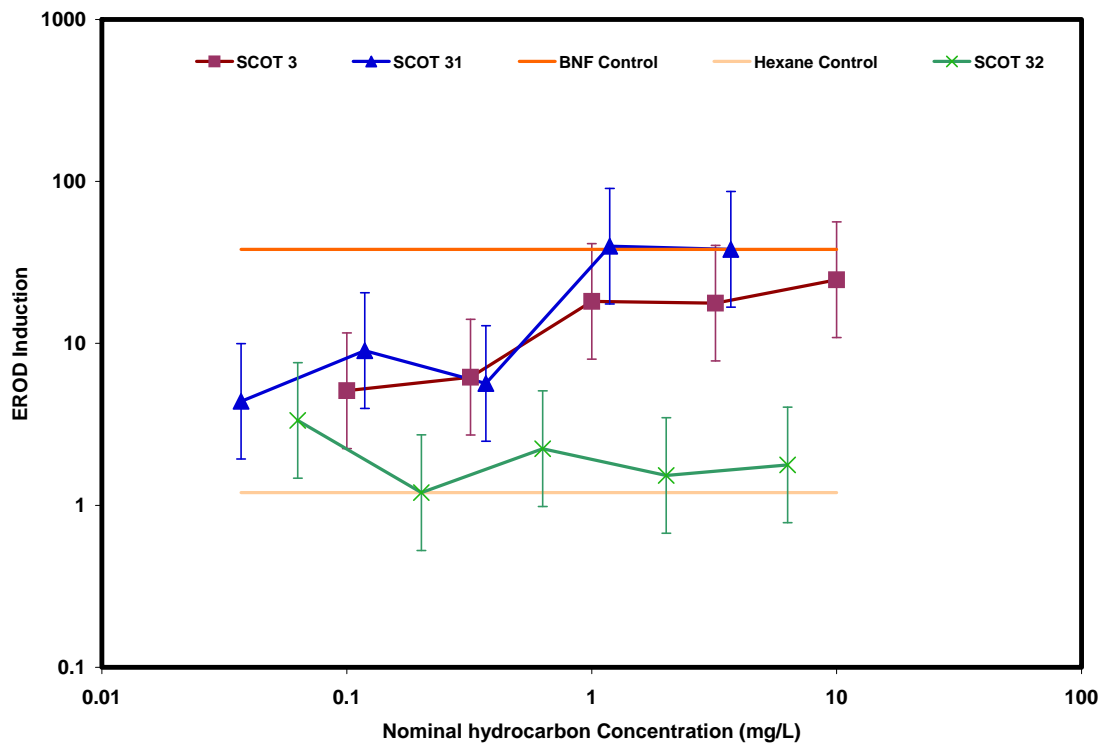
Figure 2.6: EROD induction of the SCOT 3 and its sub-fractions. Error bars represent 95% confidence interval.

Table 2.8: Concentration of alkanes and alkyl PAHs in ANSC 3 and SCOT 3 sub-fraction analyzed using GC-MS. Samples were analyzed using a MDN-5S column with helium as the carrier gas. Target analytes were quantified at SIM mode using quantification ions listed in Table 1a. Method quantification limit for all the analytes was 10 μg/g.

Compound	ANSC 31	ANSC 32	SCOT31	SCOT32
	μg/g	μg/g	μg/g	μg/g
ALKANES				
n-decane				
undecane				
dodecane			24	
tridecane	70	82	58	37
tetradecane	525	1151	2271	2505
pentadecane	732	3077	4832	11030
hexadecane	498	4383	3422	16812
heptadecane	228	5755	1627	18687
2,6,10,14-TMPdecane (pristane)	1381	2703	5406	4399
octadecane	137	5084	1191	18004
2,6,10,14-TMHdecane (phytane)	895	2865	2562	3255
nonadecane	45	4872	795	16926
eicosane	29	5135	687	15749
heneicosane	27	5259	693	14839
docosane	35	5255	507	12454
tricosane	44	5176	449	10987
tetracosane	43	5318	321	9368
pentacosane	44	5703	262	8667
hexacosane	52	8645	306	11037
heptacosane	63	8767	229	10765
octacosane	35	5016	96	4359
n-nonacosane	44	5384	63	3225
tricontane		4050	29	1542
n-heneicontane	36	4031	34	1026
dotriacontane		2153	22	312
tritriacontane		1544		154
tetratriacontane		673		51
n-pentatriacontane		380		35
17beta(H), 21 alpha (H)-hopane		24		
Total Alkanes	**4962**	**102486**	**25886**	**196225**
PAHs				
NAPHTHALENES (NAPH)				
C0-NAPH				

C1-NAPH			521	41
C2-NAPH	2370	39	1131	84
C3-NAPH	4524	134	4048	351
C4-NAPH	2045	68	2903	354
SUM	**8939**	**241**	**8604**	**830**
FLUORENES (FLUOR)				
C0-FLUOR	347		104	0
C1-FLUOR	1042	36	597	63
C2-FLUOR	2045	81	1143	110
C3-FLUOR	65		104	48
SUM	**3498**	**117**	**1947**	**222**
DIBENZOTHIOPHENE (DBT)				
C0-DBT	864			0
C1-DBT	1680	44	291	0
C2-DBT	2223	66	167	20
C3-DBT	1907	71	68	0
C4-DBT	1115	55		22
SUM	**7789**	**236**	**526**	**42**
PHENANTHRENES (PHEN)				
C0-PHEN	1256	25	312	0
C1-PHEN	3566	77	807	28
C2-PHEN	2977	70	708	21
C3-PHEN	2253	78	640	36
C4-PHEN	1332	55	521	23
SUM	**11384**	**305**	**2989**	**107**
PYRENES (Py)				
C0-Py	66		34	
C1-Py	397		262	
C2-Py	657	22	232	
C3-Py	755		152	
C4-Py	863	42	210	
SUM	**2737**	**64**	**891**	**0**
Naphthobenzothiophenes (NBT)				
C0-NBT	231			
C1-NBT	847	28	29	
C2-NBT	4415	131	46	
C3-NBT	675	30		
C4-NBT	452	34		
SUM	**6619**	**223**	**75**	**0**
CHRYSENES (CHRY)				
C0-CHRY	261		39	
C1-CHRY	462		90	

C2-CHRY	2086	47	456	
C3-CHRY	508		61	
C4-CHRY	335		33	
SUM	**3651**	**47**	679	0
Total alkyl PAHs (excluding C0)	**41593**	**1208**	**14931**	**1202**
UN-SUBSTIUTED PAHs				
acenaphthene	25			
acenaphthalene				
anthracene				
fluoranthene	26		43	
benz[a]anthracene	42		33	
benzo[b]fluoranthene	67		35	
benzo[k]fluoranthene				
benzo[e]pyrene	67		24	
benzo[a]pyrene	21			
Perylene				
indeno[1,2,3-cd]pyrene				
dibenz[a,h]anthracene				
benzo[ghi]perylene	21		23	
Total unsubstituted PAHs	**3294**	**25**	**647**	**0**

GC-MS analysis of oil fractions: A detailed GC-MS analysis of the crude oil sub-fractions was done to understand the differences in EROD induction among the different samples. Target analytes included a suite of alkanes, unsubstituted and alkyl substituted PAHs (Table 2.1a). The residue samples for both the oils showed much higher amounts of alkanes compared to the corresponding extracts (Table 2.8). Secondly, the extracts contained higher concentrations of PAHs compared to their corresponding residues. Thirdly, for both extracts, the concentrations of total alkyl substituted PAHs were much higher than that of unsubstituted PAHs. Finally, the concentrations of smaller PAHs such as

naphthalene and its alkyl homologues were higher than large PAHs such as chrysene.

Chemical analysis also showed marked differences between the concentrations of target analytes between the two different oil samples. The residue from SCOT crude oil contained twice as much alkanes as ANSC. This is consistent with fact that SCOT is a light oil. Moreover, the total PAH concentration in ANSC 31 was much higher than in SCOT 31 (Table 2.8), consistent with the higher CYP1A potency of the ANSC 31 fraction. Thus our analysis showed that the PAHs present in the crude oil samples are associated with the observed CYP1A induction in trout.

GC-MS analysis of bioassay solutions: To correlate EROD induction with the chemical constituents of extracts, the actual concentrations of PAHs and alkanes present in the bioassay solution were measured at 2- and 24-hours after the start of the assay. The concentration of target analytes in the solvent control samples was below LOQ. Tables 2.9 and 2.10 show the distributions of alkanes and PAHs for ANSC and SCOT bioassay solutions from different treatment concentrations. At any given concentration, the bioassay solutions prepared with the extract showed higher concentrations of PAH than the solution prepared with the residue. For all the extract bioassay solutions tested, the concentrations of PAH decreased with a decrease in their nominal concentration. This result, together with the CYP1A induction data presented in Figures 2.5 & 2.6, indicates that the CYP1A induction in trout follows a dose-dependent response to the PAH concentration in the bioassay solution. Moreover, the concentration of alkyl

substituted PAHs in the bioassay solutions were higher than that of unsubstituted PAHs. This indicates that, in addition to the presence of strong inducers such as chrysene, the presence of alkyl substituted PAHs plays a vital role in determining the total CYP1A induction potency of the extract samples.

Alkanes are detected in all treatment concentrations for both the oils. The concentrations of the alkanes in the residue-spiked bioassay solutions were higher than those treatments prepared from the extract. Low CYP1A induction on residue treatments indicates that waxes are not primary inducers of CYP1A in crude oils. For SCOT bioassay solutions, the alkane distribution shows a clear trend, decreasing with a decrease in the nominal hydrocarbon concentration. However, the concentration of alkanes in ANSC bioassay solutions did not show any trend with the nominal concentration. This could be due to the relatively low amounts of alkanes present in the ANSC sub-fractions compared to that of SCOT.

The concentrations of PAHs and alkanes measured after 2 hr exposure in all the treatments were higher compared to the concentrations after 24 hr. This shows the loss of chemicals during the exposure period. Other researchers have made similar observations [35, 36]. The loss of chemicals during exposure could be due to several factors including adsorption of the chemicals on the walls of the exposure vessels, uptake by fish, and adsorption on the exterior of the fish.

Table 2.9: GC-MS analysis of bioassay solutions prepared from ANSC 3 sub-fractions. PAHs and alkanes were analyzed on a MDN-5S column with helium as the carrier gas. Target analytes were quantified at SIM mode using quantification ions listed in Table 1a. Method quantification limit for all the analytes was 100 ng/L

Nominal hydrocarbon concentration (µg/L) and the sampling peroid	ANSC 31bio-assay samples				ANSC 32 bio-assay samples				
	29.7 2h	92.8 24h	29.7 24h	9.3 24h	211.2 2h	67.6 2h	21.1 2h	211.2 24h	67.6 24h
Measured concentration	ng/L	ng/L	ng/L	ng/L	ng/L	ng/L	ng/L	ng/L	ng/L
Alkanes									
undecane	295	327		205					
dodecane	488	511		325	746	313	236	361	396
tridecane	362	333		464	554	294	158	295	294
pentadecane	198	207	115	226	437			365	154
hexadecane	132	151	110		503			458	108
heptadecane	127	126	119		664			600	145
2,6,10,14-TMPdecane	128	173			458			384	
octadecane	103				675	105		690	160
2,6,10,14-TMHdecane	123	150			342			320	
nonadecane					682	104		723	163
eicosane					760	108		776	178
heneicosane	109				760	111		781	184
docosane	148	122	125		738	120		715	191
tricosane	190	148	158	116	707	129		676	192
tetracosane	308	177	215	184	691	151		652	243
pentacosane	281	214	187	209	627	137	110	573	203
hexacosane	399	246	259	239	601	137	116	563	205
heptacosane	498	212	223	227	492	111		437	153
octacosane	374	185	218	199	435	108		395	148

n-nonacosane	304	169	186	167	443	109		380	141
tricontane	266	175	197	172	218	107		217	117
n-heneicontane	417	242	160		257	142	133	299	172
dotriacontane	253			172	183	139		173	
tritriacontane	122				158			158	
tetratriacontane					131				
TOTAL ALKANES	**5625**	**3868**	**2274**	**2906**	**12261**	**2425**	**752**	**10991**	**3547**
dimethyldibenzothiophene	144								
trimethyldibenzothiophene	129	117							
tetramethyldibenzothiophene	195	105							
methylphenanthrene	171								
dimethylphenanthrene	195	109							
trimethylphenanthrene	166	155							
tetramethylphenanthrene	119	136							
dimethylpyrene									
dimethylNBenzothiophene	294	397	232						
dimethylchrysene	146	159							
TOTAL PAHS	**1700**	**1177**	**232**	**0**	**0**	**0**	**0**	**0**	**0**

Table 2.10: GC-MS analysis of bioassay solutions prepared from SCOT 3 sub-fractions. PAHs and alkanes were analyzed on a MDN-5S column with helium as the carrier gas. Target analytes were quantified at SIM mode using quantification ions listed in Table 1a. Method quantification limit for all the analytes was 100 ng/L

Nominal hydrocarbon concentration (μg/L) and the sampling peroid	SCOT 31 bio-assay samples				SCOT 32 bio-assay samples			
	3700 2h	1184 2h	3700 24h	1184 24h	6300 2h	2016 2h	6300 24h	2016 24h
Measured concentration	ng/L	ng/L	ng/L	ng/L	ng/L	ng/L	ng/L	ng/L
Alkanes								
dodecane	512	283	175		202	638	122	728
tridecane	598	302	345		179	396		509
tetradecane	3695	265	2686		2772	1418	1354	2339
pentadecane	8175	827	6346	250	17205	7578	7443	8954
hexadecane	6636	602	5149	362	34372	14465	14680	16492
heptadecane	4719	376	2382	299	42216	18882	18990	20922
2,6,10,14-TMPdecane (pristane)	10818	1220	9047	876	7658	3176	3237	3315
octadecane	3406	286	2017	228	41897	18413	18272	19339
2,6,10,14-TMHdecane (phytane)	4904	574	4093	467	6315	2287	2336	2393
nonadecane	2878	212	1463	179	39043	17508	17329	18185
eicosane	2446	202	1314	181	35933	16065	15710	16955
heneicosane	2224	183	1201	168	32753	14588	14168	15482
docosane	1618	162	874	147	25159	11126	10694	11832
tricosane	1336	146	721	137	20475	9044	8535	9600
tetracosane	987	131	495	122	16187	7059	6608	7476
pentacosane	790	132	416	117	13098	5624	5157	5936
hexacosane	586	128	336	119	9800	4082	3694	4338
heptacosane	417	111	240		7613	3039	2676	3175

octacosane	303	110	168	103	4540	1789	1597	1886
n-nonacosane	216		151		2960	1132	974	1171
tricontane	136		107		1237	405	362	409
n-heneicontane	170				836	378	326	384
dotriacontane	146				335	215	179	201
tritriacontane					232	151	137	158
TOTAL ALKANES	**57716**	**6253**	**39727**	**3754**	**363017**	**159459**	**154581**	**172177**
PAHs								
2,6-dimethlynaphthalene	124							
dimethylnaphthalene	463	138						
2,3,5-trimethylnaphthalene	1480	416						
trimethylnaphthalene	4070	1131	278		288			
tetramethylnaphthalene	5496	1310	748		513	128		
fluorene	131							
methylfluorene	881	215	143					
dimethylfluorene	1432	335	342		183			
trimethylfluorene	219		116					
methyldibenzothiophene	313		153					
dimethyldibenzothiophene	180							
tetramethyldibenzothiophene	150				106			
phenanthrene	480	121						
methylphenanthrene	1052	235	151					
2-methylphenanthrene	316							
dimethylphenanthrene	1151	242	340					
3,6-dimethylphenanthrene	115							
trimethylphenanthrene	1170	201	649					
tetramethylphenanthrene	944	154	683					
fluoranthene	78							
pyrene	61							
methylpyrene	463		168					

trimethylpyrene	253		182					
tetramethylpyrene	339		291					
dimethylpyrene	371		212					
methylchrysene	164		112					
dimethylchrysene	462		348					
TOTAL PAHS	**22357**	**4499**	**4915**	**0**	**1090**	**128**	**0**	**0**

Conclusions: The cold acetone precipitation method was found to be a good tool to isolate CYP1A inducers present in the heavy gas oil fraction. The CYP1A induction of the crude oil sub-fractions follows closely with the PAH concentration of the given sample. Our results suggest that waxes present in crude oil are not the primary CYP1A inducers. Chemical analysis of the inducing sub-fractions showed the presence of large amounts of alkyl substituted PAHs. However at this moment it is not clear which alkyl PAHs are the most important CYP1A inducers.

References

1.   Renner, R., *Long-term effects of Exxon Valdez.* Analytical Chemistry, 2006. **78**(7): p. 2091-2092.

2.   Short, J.W., *Long-Term Effects of Crude Oil on Developing Fish: Lessons from the Exxon Valdez Oil Spill.* Energy Sources, Part A: Recovery, Utilization, and Environmental Effects, 2003. **25**(6): p. 509-517.

3.   Piatt, J.F. and C.J. Lensink, *Exxon Valdez bird toll.* Nature, 1989. **342**: p. 865-866.

4.   Piatt, J.F., C.J. Lensink, W. Butler, M. Kendziorek and D.R. Nysewander, *Immiediate impact of the "Exxon Valdez" oil spill on marine birds.* The Auk, 1990. **107**(2): p. 387-397.

5.   Irons, D.B., S.J. Kendall, W.P. Erickson, L.L. McDonald and B.K. Lance, *Nine years after Exxn Valdez oil spill: Effects on marine bird populations in Prince William Sound, Alaska.* The Condor, 2000. **102**(4): p. 723-737.

6.   Carls, M.G., J.E. Hose, R.E. Thomas and S.D. Rice, *Exposure of Pacific herring to weathered crude oil: assessing effects on ova.* Environmental Toxicology and Chemistry, 2000. **19**(6): p. 1649-1659.

7.   Hose JE, M.M., Marty GD, Hinton DE, Biggs ED, Baker TT, *Sublethal effects of the Exxon Valdez oil spill on herring embryos and larvae: Morphologic, cytogenetic, and histopathological assessments, 1989–1991.* Canadian Journal of Fisheries and Aquatic Sciences, 1996. **53**: p. 2355-2365.

8.   Wang, Z. and M. Fingas, *Oil and petroleum product fingerprinting analysis by gas chromatographic techniques.* 3 ed. Chromatographic analysis of the environment, ed. L.N.L. Nollet. 2006, Boca Raton, Florida: Taylor & Francis Group.

9.   Billiard, S.M., K. Querbach and P.V. Hodson, *Toxicity of retene to early life stages of two freshwater fish species.* Environmental Toxicology and Chemistry, 1999. **18**: p. 2070-2077.

10.   Billiard, S.M., M.E. Hahn, D.G. Franks, R.E. Peterson, N.C. Bols and P.V. Hodson, *Binding of polycyclic aromatic hydrocarbons (PAHs) to teleost aryl hydrocarbon receptors (AHRs).* Comparative Biochemistry and Physiology, Part B: Biochemistry & Molecular Biology, 2002. **133B**(1): p. 55-68.

11.   Lee, R.F. and J.W. Anderson, *Significance of cytochrome P450 system responses and levels of bile fluorescent aromatic compounds in marine*

wildlife following oil spills. Marine Pollution Bulletin, 2005. **50**(7): p. 705-723.

12. Stegeman, J.J. and J.J. Lech, *Cytochrome P-450 Monooxygenase Systems in Aquatic Species: Carcinogen Metabolism and Biomarkers for Carcinogen and Pollutant Exposure.* Environmental Health Perspectives, 1991. **90**: p. 101-109.

13. Bucheli, T.D. and K. Fent, *Induction of cytochrome P450 as a biomarker for environmental contamination in aquatic ecosystems.* Critical Reviews in Environmental Science and Technology, 1995. **25**(3): p. 201-68.

14. Whyte, J.J., Jung, R.E., Schmitt, C.J., and Tillitt, D.E., *Ethoxyresorufin-O-deethylase (EROD) activity in fish as a biomarker of chemical exposure.* Critical Reviews in Toxicology, 2000. **30**(4): p. 347-570.

15. George, S.G., J. Wright and J. Conroy, *Temporal studies of the impact of the Braer oilspill on inshore feral fish from Shetland, Scotland.* Archives of Environmental Contamination and Toxicology, 1995. **29**(4): p. 530-4.

16. Marty, G.D., J.W. Short, D.M. Dambach, N.H. Willits, R.A. Heintz, S.D. Rice, J.J. Stegeman and D.E. Hinton, *Ascites, premature emergence, increased gonadal cell apoptosis, and cytochrome P4501A induction in pink salmon larvae continuously exposed to oil-contaminated gravel during development.* Canadian Journal of Zoology, 1997. **75**(6): p. 989-1007.

17. Woodin, B.R., R.M. Smolowitz and J.J. Stegeman, *Induction of Cytochrome P4501A in the Intertidal Fish Anoplarchus purpurescens by Prudhoe Bay Crude Oil and Environmental Induction in Fish from Prince William Sound.* Environmental Science and Technology, 1997. **31**(4): p. 1198-1205.

18. Kafafi, S.A., H.Y. Afeefy, H.K. Said and A.G. Kafafi, *Relationship between aryl hydrocarbon receptor binding, induction of aryl hydrocarbon hydroxylase and 7-ethoxyresorufin O-deethylase enzymes, and toxic activities of aromatic xenobiotics in animals. A new model.* Chem. Res. Toxicol., 1993. **6**(3): p. 328-334.

19. Waller, C.L. and J.D. McKinney, *Three-Dimensional Quantitative Structure-Activity Relationships of Dioxins and Dioxin-like Compounds: Model Validation and Ah Receptor Characterization.* Chem. Res. Toxicol., 1995. **8**(6): p. 847-858.

20. Tysklind, M., K. Lundgren, C. Rappe, L. Eriksson, J. Jonsson, M. Sjoestroem and U.G. Ahlborg, *Multivariate characterization and modeling of polychlorinated dibenzo-p-dioxins and dibenzofurans.* Environ. Sci. Technol., 1992. **26**(5): p. 1023-1030.

21.   Jung, D.K.J., T. Klaus and K. Fent, *Cytochrome P450 induction by nitrated polycyclic aromatic hydrocarbons, azaarenes, and binary mixtures in fish hepatoma cell line PLHC-1.* Environmental Toxicology and Chemistry, 2001. **20**(1): p. 149-159.

22.   Tysklind, M., P. Andersson, P. Haglund, B. vanBavel and C. Rappe, *Selection of Polychlorinated Biphenyls for use in Quantitative Structure-Activity Modelling.* SAR and QSAR in Environmental Research, 1995. **4**(1): p. 11 - 19.

23.   Barron, M.G., R. Heintz and S.D. Rice, *Relative potency of PAHs and heterocycles as aryl hydrocarbon receptor agonists in fish.* Marine Environmental Research, 2004. **58**(2-5): p. 95-100.

24.   Khan, C.W., S.D. Ramachandran, L.M.J. Clarke and P.V. Hodson. *EROD activity (CYP1A) inducing compounds in fractionated crude oil.* in *Proceedings of the twenty-seventh Artic and Marine Oilspill Program (AMOP) technical seminar.* 2004. Edmonton, Alberta: Emergencies Science and Technology division, Environment Canada.

25.   Wang, Z., B.P. Hollebone, M. Fingas, B. Fieldhouse, L. Sigouin, M. Landriault, P. Smith, J. Noonan and G. Thouin, *Development of a composition database for selected multicomponent oil.* 2002, Environment Canada: Ottawa.

26.   Burger, E.D., T.K. Perkins and J.H. Striegler, *Studies of wax deposition in trans Alaska pipeline.* Journal of Petroleum Technology, 1981. **33**(6): p. 1075-1086.

27.   Jokuty, P., S. Whiticar, Z. Wang, M. Landriault, L. Sigouin and J. Mullin, *A new method for the determination of wax content of crude oils.* Spill Science & Technology Bulletin, 1996. **3**(4): p. 195-198.

28.   Elsharkawy, A.M., T.A. Al-Sahhaf and M.A. Fahim, *Wax deposition from Middle East crudes.* Fuel, 2000. **79**(9): p. 1047-1055.

29.   Chen, J., J. Zhang and H. Li, *Determining the wax content of crude oils by using differential scanning calorimetry.* Thermochimica Acta, 2004. **410**(1-2): p. 23-26.

30.   King, T.L. and K. Lee. *Assessment of sediment quality based on toxic equivalent benzo[a]pyrene concentrations.* in *Artic and Marine Oilspill Program (AMOP).* 2004. Edmonton, Alberta, Canada: Environmental science and technology division, Environment Canada, Ottawa, ON, Canada.

31.   Hodson, P.V., S. Efler, J.Y. Wilson, A. El-Shaarawi, M. Maj and T.G. Williams, *Measuring the potency of pulp mill effluents for induction of*

hepatic mixed-function oxygenase activity in fish. Journal of toxicology and environmental health: Part A, 1996. **49**: p. 101-128.

32.   Ramachandran, S.D., P.V. Hodson, C.W. Khan and K. Lee, *Oil dispersant increases PAH uptake by fish exposed to crude oil.* Ecotoxicology and Environmental Safety, 2004. **59**(3): p. 300-308.

33.   Batsberg Pedersen, W., A. Baltzer Hansen, E. Larsen, A.B. Nielsen and H.P. Roenningsen, *Wax precipitation from North Sea crude oils. 2. Solid-phase content as function of temperature determined by pulsed NMR.* Energy Fuels, 1991. **5**(6): p. 908-913.

34.   Baltzer Hansen, A., E. Larsen, W. Batsberg Pedersen, A.B. Nielsen and H.P. Roenningsen, *Wax precipitation from North Sea crude oils. 3. Precipitation and dissolution of wax studied by differential scanning calorimetry.* Energy Fuels, 1991. **5**(6): p. 914-923.

35.   Billiard, S.M., N.C. Bols and P.V. Hodson, *In vitro and in vivo comparisons of fish-specific CYP1A induction relative potency factors for selected polycyclic aromatic hydrocarbons.* Ecotoxicology and Environmental Safety, 2004. **59**(3): p. 292-299.

36.   Basu, N., S. Billiard, N. Fragoso, A. Omoike, S. Tabash, S. Brown and P. Hodson, *Ethoxyresorufin O-deethylase induction in trout exposed to mixtures of polycyclic aromatic hydrocarbons.* Environmental Toxicology and Chemistry, 2001. **20**(6): p. 1244-1251.

CHAPTER 3

Identification of PAHs present in Alaskan North Slope and Scotian Light crude oils that are responsible for CYP1A induction in trout

Gurusankar Saravanabhavan[1], Kyra Nabeta[2], Colin Khan[2], Peter Hodson[2], and

R. Stephen Brown[1]

[1]Department of Chemistry and School of Environmental Studies, Queen's University, Kingston, ON.
[2]Department of Biology and School of Environmental Studies, Queen's University, Kingston, ON.

Abstract

We report an effect-driven fractionation approach for the isolation and identification of crude oil components that induce CYP1A enzymes in trout (*Oncorhynchus mykiss*). Polycyclic aromatic hydrocarbons present in crude oil have been associated with the induction of CYP1A enzymes and chronic toxicity observed in fish. In our previous work we reported a solvent extraction method to isolate the PAHs from waxes present in crude oils. Chemical analysis of the extract fraction showed the presence of a variety of alkylated PAHs while the wax residue contained only a trace level of PAHs. In this work, we report further fractionation and analysis of the PAHs present in the extract fraction. A normal phase HPLC method was developed and optimized for this purpose. The extract components were fractionated into a saturate fraction, a naphthalene fraction, a phenanthrene fraction, a chrysene fraction and a high molecular weight PAH fraction using a semi-preparative silica column. Repeated fractionation of the extract was carried out to produce enough sub-fractions for CYP1A induction assays. Only fractions that contained higher levels of PAHs with three or more aromatic rings were found to induce CYP1A enzymes in fish. Detailed GC-MS analysis of these sub-fractions showed that alkyl PAHs belonging to the PAH classes such as phenanthrene, fluorene, naphthobenzothiophene, and chrysene are associated with the observed CYP1A activity.

Introduction

Crude oil is an important energy source and its production and transportation is often associated with the spillage of oil in the open water. Exposure of aquatic organisms to crude oil causes numerous toxic effects [1-4]. Crude oil contains large amounts of unsubstituted and alkyl substituted polycyclic aromatic hydrocarbons (PAHs) that are well-known environmental pollutants. Laboratory and field studies conducted at oil-contaminated sites show a positive correlation between the PAH concentration and crude oil toxicity [5, 6]. Similarly, exposure of fish to individual or mixtures of PAHs present in crude oils in the laboratory results in a multitude of toxic effects including cardiovascular dysfunction, edema, and carcinogenecity [3, 7]. Some of these toxic effects have been associated with the induction of CYP1A enzymes [6, 8, 9].

PAHs are metabolized in vertebrates by the family of cytochrome P 450 enzymes. In fish, binding of PAHs to the aryl hydrocarbon receptor (AhR) triggers a sequence of molecular events resulting in the production of elevated levels of cytochrome P450 enzymes, specifically CYP1A protein. In turn, the CYP1A protein metabolizes the PAHs by oxidation and hydroxylation [10]. In addition to PAHs, other classes of compounds such as polychlorinated biphenyls and dibenzofurans are known to induce CYP1A enzymes. Induction is very sensitive to contaminant exposure and hence has been widely used as reliable biomarker in several field studies [10-13].

CYP1A induction in fish can be measured at different stages of transcription. Due to its simplicity and sensitivity, measuring the catalytic activity of CYP1A

enzymes, particularly ethoxyresourfin-O-deethlyase (EROD), is very popular [10]. Previous structure-activity relationship studies showed that CYP1A induction potency of a toxicant depends on several structural and physico-chemical properties [14-16]. As binding of toxicants to AhR receptor is a necessary condition for CYP1A induction, molecular properties of toxicants that affect AhR binding have been studied in great detail. Aromatic hydrocarbons that are planar or nearly planar and have dimensions that do not exceed 14 Å (length) X 12 Å (width) X 5 Å (depth) showed high AhR binding affinities [10]. The ability of different PAHs to induce CYP1A varies considerably based on their molecular structure, alkyl substitution patterns and octanol-water partition coefficient (K_{ow}) [17, 18]. Two- and three-ring unsubstituted PAHs such as naphthalene and phenanthrene are generally non-inducers of CYP1A enzymes, while four and higher ring PAHs cause high CYP1A induction. Field studies of contaminated sediment sites showed that the total concentration of unsubstituted PAHs could account for only a fraction of the total CYP1A induction caused by PAH sub-fractions of sediment extracts [19, 20]. This implies the presence of other CYP1A inducing PAHs that are previously uncharacterized. In this regard, alkyl substituted PAHs that are known to be present in the PAH sub-fractions have been scrutinized for their role in inducing CYP1A enzymes [18]. Only very limited information is available on the CYP1A induction potency of different alkyl PAHs. *In-vitro* studies showed that alkyl PAHs such as retene, 3,6-dimethylphenanthrene and 5-methyl chrysene, are weak–to-moderate CYP1A inducers [18].

More than 90% of the PAHs present in some crude oils are alkyl substituted [21]. The contribution of alkyl PAHs to the overall CYP1A induction observed from the exposure of fish to crude oil is unknown. The possible number of alkyl PAH isomers increases exponentially with the number of aromatic rings as well as the number of alkyl substitutions. Therefore, it is practically impossible to test all the individual isomers of a PAH class to identify the potential inducers. Hence we have used the effect-driven fractionation approach to screen for the CYP1A inducing alkyl PAHs in crude oil samples. Effect-driven fractionation and analysis (EDFA) approaches have been successfully used previously to screen for CYP1A inducers in complex environmental samples [19, 22]. Using this approach the relative contribution of different toxicants to the overall CYP1A induction of a complex sample has been elucidated [23, 24]. This approach has been used successfully to identify new CYP1A inducers [25].

EDFA is an iterative approach in which a complex sample is chemically fractionated into several sub-fractions and their toxicity is tested. Only fraction(s) that are found to be toxic are further fractionated and the toxicity test is repeated. This procedure is continued until simple fractions are generated and the toxic components identified with detailed chemical analysis. In our previous work, we have used the EDFA approach to identify CYP1A inducing compounds present in Alaskan North Slope (ANSC) and Scotian Light crude (SCOT) oils. During the first stage of fractionation, the oils were subjected to low temperature vacuum distillation technique (ASTM D 1160) and four distinct fractions based on the boiling point were obtained. In *in-vivo* CYP1A induction studies using rainbow

trout the heavy gas oil fraction of ANSC and SCOT crude oils (ANSC3 and SCOT 3; boiling range 287°C to 461°C) produced highest CYP1A activity [26]. Chemical analysis of ANSC 3 and SCOT 3 fractions revealed the presence of a variety of PAHs, in addition to a large amount of saturated hydrocarbons. Therefore, as discussed in Chapter 2, we have developed a cold acetone extraction technique to isolate PAHs present in ANSC 3 and SCOT 3 sub-fractions. EROD assays of these sub-fractions showed that the cold acetone extracts (ANSC 31 and SCOT 31) contained a large amount of CYP1A inducers while the residues (ANSC 32 and SCOT 32) contained none.

In this work, as the third stage of fractionation, we report the further separation of PAHs present in the ANSC 31 and SCOT 31 into five fractions, based on the number of aromatic rings. For this purpose, a normal phase HPLC method was developed and utilized for the bulk fractionation of oil fractions. The PAH sub-fractions were tested for their CYP1A activity in rainbow trout. Detailed PAH analysis of all the sub-fractions were carried out using gas chromatography-mass spectrometry (GC-MS) and used to interpret the CYP1A activities of the fractions.

Materials and Methods

Materials: All solvents used in this study were of HPLC grade and were procured from Fisher Scientific (Ottawa, ON). Table 3.1a shows the list of alkanes and PAHs analyzed in this study. A list of internal standards and surrogate standards used in the GC-MS analysis is shown in Table 3.1b. All PAH standards had a minimum purity of 95% and were obtained from Sigma Aldrich (Milwaukee, WI) and Ultra Scientific (Kingstown, RI). ANSC and SCOT crude oil samples and

103

their corresponding heavy gas oil fractions (ANSC 3 and SCOT 3) were obtained

from Dr. Zhendi Wang of Environment Canada (Ottawa, ON).

Table 3.1a: List of alkanes and PAHs analyzed using GC-MS. The abbreviated codes for alkyl PAH analytes are given in the parenthesis.

Compound	Retention time (min.)	Quantifying Ion m/z
ALKANES		
n-decane	4.42	57
undecane	6.38	57
dodecane	8.92	57
tridecane	11.81	57
tetradecane	14.82	57
pentadecane	17.81	57
hexadecane	20.72	57
heptadecane	23.51	57
2,6,10,14-TMPdecane (pristane)	23.61	57
octadecane	26.18	57
2,6,10,14-TMHdecane (phytane)	26.33	57
nonadecane	28.72	57
eicosane	31.17	57
heneicosane	33.50	57
docosane	35.75	57
tricosane	37.90	57
tetracosane	39.97	57
pentacosane	41.95	57
hexacosane	43.86	57
heptacosane	45.71	57
octacosane	47.48	57
n-nonacosane	49.20	57
tricontane	50.87	57
n-heneicontane	52.67	57
dotriacontane	54.83	57
tritriacontane	57.44	57
tetratriacontane	60.67	57
n-pentatriacontane	64.62	57
17beta(H), 21 alpha (H)-hopane	53.75	191
PAHs		
Naphthalene (C0 NAP)	8.64	128

Methylnaphthalene (C1 NAP)	11.74	142
Dimethylnaphthalene (C2 NAP)	15.36	156
Trimethylnaphthalene (C3 NAP)	18.64	170
Tetramethylnaphthalene (C4 NAP)	24.77	184
Acenaphthene (Ace)	17.20	154
Acenaphthalene (Acl)	16.21	152
Fluorene (C0 FLUOR)	20.10	166
Methylfluorene (C1 FLUOR)	23.44	180
Dimethylfluorene (C2 FLUOR)	26.31	194
Trimethylfluorene (C3 FLUOR)	24.37	208
Dibenzothiophenes (C0 DBT)	24.73	184
Methyldibenzothiophene (C1 DBT)	27.31	198
Dimethyldibenzothiophene (C2 DBT)	30.30	212
Trimethyldibenzothiophene (C3 DBT)	32.44	226
Tetramethyldibenzothiophene (C4 DBT)	36.26	240
Phenanthrene (C0 PHEN)	25.45	178
Anthracene (An)	25.76	178
Methylphenanthrene (C1 PHEN)	28.50	192
Dimethylphenanthrene (C2 PHEN)	31.26	206
Trimethylphenanthrene (C3 PHEN)	34.40	220
Tetramethylphenanthrene (C4 PHEN)	37.60	234
Fluoranthene (Fl)	32.31	202
Pyrene (C0 Py)	33.50	202
Methylpyrene (C1 Py)	36.17	216
Dimethylpyrene (C2 Py)	39.00	230
Trimethylpyrene (C3 Py)	41.37	244
Tetramethylpyrene (C4 Py)	43.39	258
Naphthobenzothiophene (C0 NBT)	39.17	234
Methylnaphthobenzothiophene (C1 NBT)	42.28	248
DimethylNBenzothiophene (C2 NBT)	44.23	262
TrimethylNbenzothiophene (C3 NBT)	46.67	276
TetramethylNbenzothiophene (C4 NBT)	48.27	290
Benz[a]anthracene (BaA)	40.63	228
Chrysene (C0 CHRY)	40.80	228
Methylchrysene (C1 CHRY)	43.08	242
Dimethylchrysene (C2 CHRY)	45.22	256
Trimethylchrysene (C3 CHRY)	48.01	270
Tetramethylchrysene (C4 CHRY)	49.90	284
Benzo[b]fluoranthene (BbF)	46.45	252
Benzo[k]fluoranthene (BkF)	46.59	252
Benzo[e]pyrene (BeP)	47.73	252
Benzo[a]pyrene (BaP)	47.97	252

	48.39	252
Perylene (Pe)	48.39	252
Indeno[1,2,3-cd]pyrene (IP)	53.34	276
Dibenz[a,h]anthracene (DA)	53.67	278
Benzo[ghi]perylene (BP)	54.69	276

Table 3.1b: List of internal and surrogate standards used in the GC-MS analysis

Compounds	Retention Time (min.)	Quantifying Ion m/z
Internal Standards		
d22-n-decane	4.18	66
d34-n-hexadecane	20.00	66
d42-n-eicosane	30.40	66
d62-n-triacontane	50.01	66
5alpha-androstane	31.25	245
d8-naphthalene	8.56	136
d10-anthracene	25.65	188
d12-chrysene	40.66	240
d12-perylene	48.27	264
Surrogate Standards		
d26-dodecane	8.43	66
d36-n-heptadence	22.78	66
d50-n-tetracosane	39.15	66
d66-n-dotriacontane	53.54	66
5beta-cholestane	47.33	217
d10-phenanthrene	25.34	188
d10-pyrene	33.41	212
d12-benzo[b]fluoranthene	46.33	264
d12-benzo[a]pyrene	47.87	264
d14-dibenz[a,h]anthracene	53.50	292

Wax precipitation procedure: The wax precipitation protocol optimized previously (Chapter 2) was used to precipitate waxes from ANSC 3 and SCOT 3 oil fractions. Briefly, the oil fraction was heated to 70°C for about 30 minutes to dissolve all the waxes. To 5 g of the oil fraction, 50 mL of acetone was added and sonicated at room temperature for five minutes. Then the mixture was cooled to -80°C for five hours. At the end of the cooling period, the wax precipitate was filtered on a 0.22 μm nylon filter paper. The precipitate was washed with 15 mL of the cold solvent (maintained at -80°C) and the washing added to the extract. The residue was dissolved using 5 mL of hexane followed by 5 mL of dichloromethane in a clean vial. Both the residue and the extract solutions were evaporated, solvent exchanged to hexane and subjected to further fractionation.

HPLC system: PAH fractionation was carried out using a Varian HPLC system (Varian, Mississauga, ON), consisting of two pump-modules (Prostar 215) and a UV absorbance detector (Prostar 330) operating at 254 nm. The fractionation was done on a semi-preparative silica column (Zorbax sil, 9.4 mm i.d. x 25 cm length; packed with silica particles of diameter 5 micron)(Agilent Technologies, Mississauga, ON).

During fractionation, 100 mg of ANSC 31 or SCOT 31 sample in 200 μL of hexane was injected onto the HPLC column. The PAHs were eluted using the mobile phase conditions given in Table 3.2. Five fractions were collected using a fraction collector (Dynamax model FC-4, Varian). The fractionation windows were determined by analyzing a suite of unsubstituted and alkyl PAH standards. The column was regenerated by back-flushing with 100% methylene chloride to

remove resins and other polar materials as indicated in Table 3.2. After every two sample runs, the PAH standard mixture was injected to confirm the column regeneration. Finally, similar fractions from each batch were pooled together and evaporated in a rotary evaporator to ~10 mL. The sample was exchanged into dichloromethane in a 10.00 mL volumetric flask. The sample concentration was measured gravimetrically by evaporating 0.50 mL of each sample to dryness under N_2 in a pre-weighed glass vial. The samples were diluted in dichloromethane to a concentration between 1.0 mg/mL and 0.05 mg/mL and analyzed using GC-MS to obtain detailed the PAH composition. The GC-MS analysis was done at Dr. Kenneth Lee's lab at the Bedford Institute of Oceanography, Dartmouth, NS.

Table 3.2: Mobile phase conditions used for the normal phase fractionation of ANSC 31 and SCOT 31 oil fractions. The fractionation was carried out using a semi-preparative silica column (Zorbax sil, 9.4 mm i.d. x 25 cm length; packed with silica particles of diameter 5 micron)(Agilent Technologies, Mississauga, ON)

Time (min)	Operation mode	Mobile phase composition	Flow rate (mL/min)
PAH elution			
0	Normal	98% hexane/2% methylene chloride	1.5
86	Normal	98% hexane/2% methylene chloride	1.5
Column regeneration			
86	Backflush mode	100% methylene chloride	7
125	Backflush mode	100% methylene chloride	7
130	Backflush mode	98% hexane/2% methylene chloride	7
160	Backflush mode	98% hexane/2% methylene chloride	7
165	Equlibrate	98% hexane/2% methylene chloride	1.5

Sample preparation for GC-MS analysis: To a pre-weighed graduated centrifuge tube, a 1.0 mL aliquot of the sample and 5 mL of isooctane (density = 0.687g/mL) were added and evaporated under a gentle stream of nitrogen to ~ 1 mL. An aliquot of 20 μl of the internal standard stock solution containing 500 ng of each deuterated PAHs and alkane standards (3.1b) was added to the sample and the final weight of the sample was recorded. From the sample weight the final volume was calculated using the density of isooctane.

GC-MS analysis: The detailed PAH analysis was done on a high-resolution gas chromatography (Agilent 6890 GC) coupled to a mass selective detector (Agilent 5973N) (Willmington, DE) using a method developed by King *et al.* [27, 28]. PAHs were separated using a MDN-5S column (30 m x 0.25mm id 0.25 µm film thickness, Supelco) with helium as the carrier gas. The sample was injected onto the column using a cold on-column injector in oven track mode (track 3°C higher that the oven temperature program). The temperature of the GC oven was programmed as follows: 80°C (hold 2 min) - ramp at 4°C/min to 280°C (hold 10 min). After every two sample runs, a solvent run was made to check for any baseline drift. PAH quantification was done in the selective ion monitoring mode (SIM). The list of target analytes, internal standards and their corresponding quantifying ions used is given in 3.1a and 3.1b. The limit of quantification (LOQ) measured at 10 X S/N (signal to noise ratio) for the target analytes was 25 ng/mL.

Preparation of chemically enhanced water accommodated fraction (CEWAF): The CEWAF preparation procedure was slightly modified from the procedure

described in Chapter 2. An aliquot of 100 μL of the oil fraction in dichloromethane was mixed with 850 μL of water and 50 μL of oil dispersant (Corexit 9500, Exxon, NJ) in a 1 mL glass vial. The contents were mixed by vortexing for 3 minutes followed by sonication for 5 minutes at room temperature. This produced a milky homogeneous suspension of the oil fraction in water. The entire suspension was added to 11 L water in the exposure tank and mixed well.

Fish exposure and EROD assay: Details on fish exposure and EROD assay protocols were published elsewhere [29]. Briefly, five Juvenile trout (*Oncorhynchus mykiss;* 1-3 g each) were added to 11 L of de-chlorinated water spiked with a dose of CEWAF suspension. At 2h- and 24h exposure periods a 1L water sample was collected for GC-MS analysis. Water quality parameters such as temperature, dissolved oxygen, pH, and conductivity were measured daily. β-naphthoflavone (positive control) and water (negative control) were included for each bioassay. Following the exposure period, the fish were anaesthetized by transferring them to a container of water having 100 mg/L of MS–222 (Ethyl-m-aminobenzoate methanesulfonate) and killed by a blow to the head. Livers were removed, weighed, and homogenized with 500 μL of HEPES buffer (11.184 g KCl, 5.206 g HEPES sodium salt dissolved in 1 L water, pH 7.5). Samples were centrifuged at 9000 X g for 20 minutes at 2ºC and the supernatant/microsomal layers (S9 fractions) were collected.

The EROD assay was done using S9 fraction of each sample in triplicate in a 96-well microplate reader coupled to a Spectromax Gemini spectrofluorimeter (Molecular Diagnostics, CA). Briefly, 50 μL of each S9 fraction was mixed with a

50 μL aliquot of 7-ethoxy-resorufin (7ER) dissolved in 0.22 M assay buffer and incubated in the dark for 10 minutes. Then the deethylation reaction was started by adding 10 μL of a 1 mg/mL solution of reduced nicotinamine adenosine diphosphate (NADPH), after which fluorescence was read once per minute for 12 minutes with the excitation set at λ_{530} nm and emission set at λ_{586} nm. Total fluorescence produced per minute by each sample was normalized to protein content to give specific activity (pmol/mg/min). Relative EROD induction for all treatments was calculated by dividing the treatment mean by the control mean values.

Statistical analysis: All statistical analyses were conducted with either Microsoft Excel or SigmaStat software. One-way analysis of variance (ANOVA) of EROD data was calculated using log-transformed EROD values. The log EROD values used for ANSC and SCOT failed normality tests (likely due to small sample size per treatment) but passed the equal variance test. For each ANOVA, a *post hoc* multiple comparison test (the Bonferroni *t*-test) was applied to identify treatment concentrations that were significantly different from one another [4].

Analysis of bioassay samples: To a 1 L water sample collected at 2h- and 24h dosing period 1.00 mL of surrogate standard mix (Table 3.1b) having 500 ng of each compound in acetone was added. The sample was extracted with 3 X 20 mL of dichloromethane and the extracts were combined. About 5 mL of isooctane was added to the extract and concentrated on a Turbo Vap Concentrator (Zymark Hopkinton, Massachusetts, USA,) to 1 mL. The concentrated extract was quantitatively transferred to a pre-weighed centrifuge tube, 20 μL of the

internal standard solution was added, and the sample was analyzed using GC-MS. The final weight of the sample was recorded before the analysis and used to calculate the final volume of the sample.

Results and discussion

HPLC method development: The primary aim of the HPLC fractionation was to isolate alkyl and unsubstituted PAHs based on the number of aromatic rings. Figure 3.1 shows the elution of PAH standard mix and the ANSC 31 fraction using the mobile phase condition given in Table 3.2.
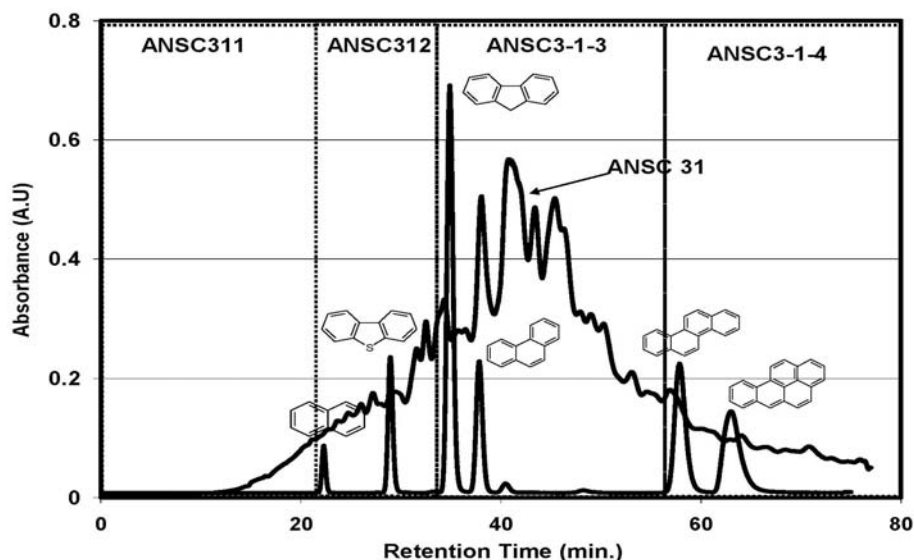
Figure 3.1: Elution profile of PAH standard mix and ANSC 31 sub-fraction on a semi-preparative silica column (Zorbax sil, 9.4 mm i.d. x 25 cm length; packed with silica particles of diameter 5 micron) using the mobile phase program in Table 3.2. The retention time windows for the normal phase sub-fractions are indicated. ANSC 315 fraction was collected after 80 minutes in the back-flush mode.

Table 3.3: Nomenclature, retention time window and the expected composition of PAH sub-fractions

Fraction No.	Time window (min.)	Major constituents
ANSC 311	0-20	Saturated hydrocarbons
ANSC 312	20-36	Naphthalene, Dibenzothiophene, and their alkyl isomers
ANSC 313	36-66	Phenanthrene, fluorenes and their alkyl isomers
ANSC 314	66-86	Chrysene, pyrene and their alkyl isomers
ANSC 315	86-165	> 5 ring PAH, resins

Table 3.4: Percentage composition of PAH sub-fractions of ANSC 31 and SCOT 31 crude oils.

ANSC 31		SCOT 31	
Fraction No.	Mass % of ANSC 31	Fraction No.	Mass % of SCOT 31
ANSC 311	47	SCOT 311	54
ANSC 312	25	SCOT 312	30
ANSC 313	15	SCOT 313	10
ANSC 314	4	SOCT 314	8
ANSC 315	13	SCOT 315	4

The analyzed mixture of PAHs consisted of 50 μg each of naphthalene, dibenzothiophene, phenanthrene, fluorene, chrysene and benzo[a]pyrene in 200 μl n-hexanes. As the alkyl PAHs (C1 to C4) co-eluted with their corresponding unsubstituted PAHs, the retention time of the unsubstituted PAHs was used to ascertain the fractionation window (Figure 3.1). Table 3.3 shows the nomenclature, expected PAH composition, time windows of each PAH sub-fractions. ANSC 31 fraction did not contain mono-aromatic hydrocarbons such as benzene, toluene, ethyl benzene and xylene, and hence the first sub-fraction (ANSC 311) is expected to contain mainly saturated hydrocarbons. To elute high molecular weight PAHs and resins that were bound to the silica column strongly,

the last fraction (ANSC 315) was collected in the back-flush mode using 100% dichloromethane. Fractionation of SCOT 31 sample was carried out in a similar fashion to produce sub-fractions SCOT 311 to SCOT 315.

To study the mass balance of oil fractions before and after normal phase fractionation, the mass percentage of each sub-fraction was estimated gravimetrically. Table 3.4 shows the mass percentages of normal phase sub-fractions of ANSC 31 and SCOT 31 oil fractions. A slight increase in the sum of the sub-fractions observed might be due to the carry-over of strongly bound compounds between different batches of fractionation experiments. Although ANSC and SCOT crude oil vary widely in their chemical composition, the mass percentages of their normal phase sub-fractions were similar. This is due to the fact that during the primary fractionation of crude oils using low temperature vacuum distillation, the compounds with similar boiling point from both oils were fractionated into their respective heavy gas oil fraction (ANSC 3 and SCOT 3). Therefore further fractionation of the heavy gas oil fractions resulted in sub-fractions with similar percentage compositions. However, the concentration of individual compounds measured using GC-MS (see below) present in these sub-fractions showed significant differences consistent with the original characteristics of crude oils.

Table 3.5: Concentrations of saturated hydrocarbons and PAHs in different fractions of ANSC crude oil determined by GC/MS.

Compound	ANSC 31	ANSC 311	ANSC 312	ANSC 313	ANSC 314	ANSC 315
	µg/g	µg/g	µg/g	µg/g	µ/g	µg/g
Alaknes						
n-decane						
Undecane			232	292		
Dodecane						
Tridecane		203				
tetradecane	525	1796				
Pentadecane	732	2873	120			
Hexadecane	498	2673	245	162		
Heptadecane	228	2262	329	235		105
2,6,10,14-TMPdecane (pristane)	1381	5390				177
Octadecane	137	1643	345	244		167
2,6,10,14-TMHdecane (phytane)	895	3484				124
Nonadecane		1198	326	234		181
Eicosane		980	292	213		168
Heneicosane		907	255	196		145
Docosane		651	211	167		128
Tricosane		537	189	157		112
Tetracosane		400	151	132		
Pentacosane		358	137	117		
Hexacosane		229	132	120		
Heptacosane		195	105			
Octacosane		129	101			
n-nonacosane		112	118			
Tricontane			125			
n-heneicontane		122	128			
Dotriacontane						
Tritriacontane						
Tetratriacontane						
n-pentatriacontane						
17beta(H), 21 alpha (H)-hopane						
Total Alkanes	**4962**	**26141**	**3541**	**2267**	**0**	**1306**
PAHs						
Naphthalenes (NAPH)						
C0-NAPH						
C1-NAPH			898			
C2-NAPH	2370		12958			202
C3-NAPH	4524	304	25499			538
C4-NAPH	2045	635	12283	157		369
SUM	**8939**	**939**	**51637**	**157**	**0**	**1109**

Fluorenes (FLUOR)						
C0-FLUOR	347			3037		
C1-FLUOR	1042		411	9434		121
C2-FLUOR	2045	134	558	14515		195
C3-FLUOR	65			435		
SUM	**3498**	**134**	**969**	**27421**	**0**	**316**
Dibenzothiophenes (DBT)						
C0-DBT	864		4013			
C1-DBT	1680		8058	749		193
C2-DBT	2223		11428	1248		298
C3-DBT	1907		7476	5835		275
C4-DBT	1115		4203	4090		170
SUM	**7789**	**0**	**35179**	**11922**	**0**	**936**
Phenanthrenes (PHEN)						
C0-PHEN	1256		4631	3043		143
C1-PHEN	3566		1105	30793		451
C2-PHEN	2977		546	28593		419
C3-PHEN	2253		773	21336	1328	689
C4-PHEN	1332		913	11022	3133	770
SUM	**11384**	**0**	**7968**	**94787**	**4461**	**2473**
Pyrenes (Py)						
C0-Py				578		
C1-Py	397			2837	3600	207
C2-Py	657			3043	13778	376
C3-Py	755			2624	11710	1346
C4-Py	863			2956	7998	4113
SUM	**2737**	**0**	**0**	**12039**	**37086**	**6042**
Naphthobenzothiophene (NBT)						
C0-NBT	231			2207		
C1-NBT	847		132	8138	1514	342
C2-NBT	4415		113	43150	1628	778
C3-NBT	675					149
C4-NBT	452					
SUM	**6619**	**0**	**245**	**53495**	**3142**	**1268**
Chrysenes (CHRY)						
C0-CHRY	261			1623	4013	
C1-CHRY	462			376	16521	536
C2-CHRY	2086			1904	48944	4418
C3-CHRY	508			582	6715	1978
C4-CHRY	335			492	3406	1217
SUM	**3651**	**0**	**0**	**4977**	**79598**	**8149**
Total alkyl PAHs (excluding C0)	**41593**	**1072**	**87354**	**194310**	**120274**	**20150**

Unsubstituted PAHs						
Acenaphthene			106			
Acenaphthalene						
Anthracene				326		
Fluoranthene				248		
Benz[a]anthracene				173		
Benzo[b]fluoranthene					1229	108
Benzo[k]fluoranthene						
Benzo[e]pyrene					2315	
Benzo[a]pyrene						
Perylene						
Indeno[1,2,3-cd]pyrene						
Dibenz[a,h]anthracene						
Benzo[ghi]perylene						
Total unsubstituted PAHs	**3294**	**0**	**8750**	**11234**	**7556**	**251**
Mass % of analytes in the fractions	**4.9**	**2.7**	**10.0**	**21.0**	**12.7**	**2.2**

Table 3.6: Concentration of alkanes and PAHs present in SCOT 31 and its normal phase sub-fractions analyzed using GC-MS. The concentration of alkanes and PAHs in SCOT 314, and 315 sub-fractions were below quantification limit (10 µg/g).

Compound	SCOT31	SCOT311	SCOT312	SCOT313
	µg/g	µg/g	µg/g	µg/g
Alakanes				
n-decane				
Undecane				
Dodecane	24			
Tridecane	58			
tetradecane	2271	3313		
Pentadecane	4832	8278		
Hexadecane	3422	6183		
Heptadecane	1627	3363		
2,6,10,14-TMPdecane (pristane)	5406	10493		
Octadecane	1191	2212		
2,6,10,14-TMHdecane (phytane)	2562	4618		
Nonadecane	795	1541		
Eicosane	687	1335		234
Heneicosane	693	1187		
Docosane	507	871		323
Tricosane	449	685		0
Tetracosane	321	553	120	416
Pentacosane	262	386		251
Hexacosane	306	364	181	652
Heptacosane	229	205		249
Octacosane	96	238	207	835
n-nonacosane	63	116	0	239
Tricontane	29	204	223	927
n-heneicontane	34	130	128	291
Dotriacontane	22	206	244	861
Tritriacontane		0	129	311
Tetratriacontane		177	218	858
n-pentatriacontane		0		312
5beta-cholestane		0		
17beta(H), 21 alpha (H)-hopane				
Total alkanes	**25886**	**46655**	**1451**	**6757**
PAHs				
Naphthalenes (NAPH)				
C0-NAPH				

C1-NAPH	521		1415	
C2-NAPH	1131		3236	692
C3-NAPH	4048		12919	2129
C4-NAPH	2903	156	10553	4541
SUM	**8604**	**156**	**28123**	**7362**
Fluorenes (FLUOR)				
C0-FLUOR	104			766
C1-FLUOR	597		359	4758
C2-FLUOR	1143	110	343	8134
C3-FLUOR	104	117		735
SUM	**1947**	**227**	**703**	**14393**
Dibenzothiophenes (DBT)				
C0-DBT				
C1-DBT	291		296	1911
C2-DBT	167		197	612
C3-DBT	68		125	336
C4-DBT			187	
SUM	**526**	**0**	**805**	**2859**
Phenanthrenes (PHEN)				
C0-PHEN	312			2967
C1-PHEN	807			8267
C2-PHEN	708			7715
C3-PHEN	640			6787
C4-PHEN	521			4982
SUM	**2989**	**0**	**0**	**30718**
Pyrenes (Py)				
C0-Py	34			411
C1-Py	262			1504
C2-Py	232			895
C3-Py	152			449
C4-Py	210			457
SUM	**891**	**0**	**0**	**3715**
Naphthobenzothiophenes (NBT)				
C0-NBT				
C1-NBT	29			
C2-NBT	46			
C3-NBT				
C4-NBT				
SUM	**75**	**0**	**0**	**0**
Chrysenes (CHRY)				
C0-CHRY	39			
C1-CHRY	90			226
C2-CHRY	456			428

C3-CHRY	61			
C4-CHRY	33			
SUM	**679**	**0**	**0**	**654**
Total alkyl PAHs (excluding C0)	**14931**	**383**	**29335**	**53646**
Unsubstituted PAHs				
Acenaphthene				
Acenaphthalene				
Anthracene				216
Fluoranthene	43			453
benz[a]anthracene	33			
benzo[b]fluoranthene	35			
benzo[k]fluoranthene				
benzo[e]pyrene	24			
benzo[a]pyrene				
Perylene				
indeno[1,2,3-cd]pyrene				
dibenz[a,h]anthracene				
benzo[ghi]perylene	23			
Total unsubstituted PAHs	**158**	**0**	**0**	**669**
Mass % of analytes in the fractions	**4.0**	**4.7**	**3.1**	**6.1**

Table 3.7: Actual concentration of alkanes and PAHs in bioassay test solution prepared using PAH sub-fractions of ANSC crude oil. Analysis was carried out using GC-MS with the condition described in the experimental section.

	ANSC 311 (ng/L)		ANSC 312 (ng/L)		ANSC 313 (ng/L)				ANSC 314 (ng/L)		ANSC 315 (ng/L)	
Nominal hydrocarbon concentration	0.043 mg/L 2h	0.043 mg/L 24h	0.023 mg/L 2h	0.023 mg/L 24h	0.014 mg/L 2h	0.0044 mg/L 2h	0.014 mg/L 24h	0.0044 mg/L 24h	0.0037 mg/L 2h	0.0037 mg/L 24h	0.012 mg/L 2h	0.012 mg/L 24h
Alkanes												
undecane	201.75	235.31	151.75	189.74	182.08	159.68	259.66	200.71	191.32		183.85	230.14
dodecane	312.01	416.8	224.41	161.16	271.46	229.14	219.9	361.18	283.11		274.5	391.56
tridecane	108.24	230.54		139.63	127.16	156.13	198.33	303				208.69
pentadecane	137.25	167.84				106.38	149.55	189.85				143.39
hexadecane	125.65	141.06					114.96	112.68				105.44
heptadecane	130.06	129.9					121.02	117.9			102.15	109.79
2,6,10,14-TMPdecane (pristane)	137.75	126.14										
octadecane	102.52	103.77										
2,6,10,14-TMHdecane (phytane)	119.94	119.07										
eicosane									56.12			
heneicosane	108.62	106.08										
docosane	129.6	130.3	120.49	118.72	119.6	132.2	124.77	125.51			117.72	123.16
tricosane	154.98	173.09	167.88	146.83	151.11	171.26	157.47	165.48	114.4		147.41	155.91
tetracosane	220.63	227.85	243.61	214.7	217.08	277.11	214.98	236.47	127.59	200.95	205.31	226.73
pentacosane	219.31	221.78	243.96	206.92	203.95	308.52	223.68	207.18	154.14	230.29	181.81	208.68
hexacosane	224.92	203.9	253.75	185.92	209.43	389.82	217.76	246.27	179.25	253.04	170.3	224.29
heptacosane	267.18	238.73	323.98	227.48	197.59	485.61	239.09	269.72	169.98	226.55	162.24	227.31
octacosane	137.23	163.61	181.67	116.6	143.3	261.59	151.65	187.3	156.28	214.98	105.98	143.62
n-nonacosane	175.83	183.58	200.15	172.61	168.85	261.01	190.31	202.53	121.68	208.94	168.17	187.33
tricontane	123.25	138.04	152.66	122.41	141.77	247.75	147.72	152.26	137.51	213.68	124.45	146.94

n-heneicontane	224.15		224.38	230.32		351.46	1699.65	2432.36	183.3	246.19	174.04	
dotriacontane	132.8		135.05			233.56						157.48
5alpha-androstane	500.37	501.15	498.18	512.68	498.08	506.2	495.77	496.81	499.12	502.07	500.35	499.99
Total alkanes	**3994.04**	**3958.54**	**3121.92**	**2745.72**	**2631.46**	**4277.42**	**4926.27**	**6007.21**	**2373.8**	**2296.69**	**2618.28**	**3490.45**
PAHs												
C3 NAPH			129.47									
C1 PHEN					187.18	101.82						
C2 PHEN					191.22	106.93						
C3 PHEN					144.73							
C2 NBT					282.25	166.46	196.17	139.79				
Total PAHs	**0**	**0**	**129.47**	**0**	**805.38**	**375.21**	**196.17**	**139.79**	**0**	**0**	**0**	**0**

GC-MS analysis: Tables 3.5 and 3.6 shows the GC-MS characterization of the normal phase sub-fractions of ANSC 31 and SCOT 31 oil samples respectively. In general, the chemical composition of the sub-fractions followed the expected trend shown in Table 3.3.

ANSC 311 and SCOT 311 fractions contained predominantly alkanes; only a small amount of alkyl naphthalene was detected. The concentration of individual alkanes in SCOT 311 was higher than that of ANSC 311 consistent with the fact that SCOT is a lighter crude oil. ANSC 312 and SCOT 312 fractions contained large amounts of alkyl naphthalenes while higher ring PAHs were present only at trace levels. Similarly, ANSC 313 and SCOT 313 fraction contained predominantly fluorene, pheanthrene, pyrene, napthobenzothiophene and their alkyl isomers. Alkyl naphthalenes were virtually absent in this fraction and 4 ring PAHs such as chrysenes were present only in trace levels. Most of the alkyl chrysenes and 5-ring PAHs such as benzo[e]pyrene and benzo[b]fluoranthene were present in ANSC 314 fraction. Alkyl phenanthrenes and other low molecular weight PAHs were detected in this fraction only at low concentration. ANSC 315 fraction, collected in back-flush mode using 100% dichloromethane, contained small amounts of compounds from different PAH classes. This indicates that dichloromethane, being a strong solvent, has removed residual amounts of PAHs and other components that were strongly adsorbed to the column, thereby minimizing the carry-over effects. The concentrations of PAHs were below the detection limit in SCOT 314 and 315 sub-fractions. However a semi-quantitative

analysis of these fractions showed the presence of similar classes of compounds as in the ANSC sub-fractions.

GC-MS analysis of bioassay solution: To correlate EROD induction with the chemical constituents of different normal phase sub-fractions, the actual concentrations of PAHs and alkanes present in the bioassay solutions were measured at 2- and 24h after the start of the assay. The concentration of target analytes in the solvent control samples was below the LOQ. Table 3.7 show the distributions of alkanes and PAHs in bioassay solutions prepared using ANSC normal phase sub-fractions at different treatment concentrations. In general, alkanes are detected in all bioassay samples while the concentration of PAHs were above the detection limit in only a few bioassay samples. Among PAHs, methyl, dimethyl, and trimethyl phenanthrenes, and dimethyl naphthobenzothiophenes were detected in ANSC 313 treatments. The total concentration of these PAHs sampled after a 2-hour exposure period decreased with nominal concentration from 805 ng/L at 0.014 mg/L to 375 ng/L at 0.0044 mg/L. This indicates that PAH concentration in the exposure solution decreases with a decrease of nominal concentration; however concentrations of alkanes did not show any trend. Moreover, at a nominal concentration of 0.014 mg/L, the total concentration of PAHs were found to decrease with exposure time from 805 ng/L in the 2-hour sample to 196 ng/L in the 24-hour sample. This shows the loss of chemicals during the exposure period. Other researchers have made a similar observations [18, 30]. The loss of chemicals during the exposure could be due to several factors including the adsorption of the chemicals on the walls of the

exposure vessels, uptake by fish, and adsorption of the chemicals on the exterior of the fish.

Figure 3.2: *In-vivo* EROD induction assay of normal phase sub-fractions of ANSC 31 fraction in rainbow trout. The error bars indicate the 95% confidence interval on the variation in the EROD data. To improve clarity, the error bars are indicated on selected points. The error bars on other points are similar in magnitude.
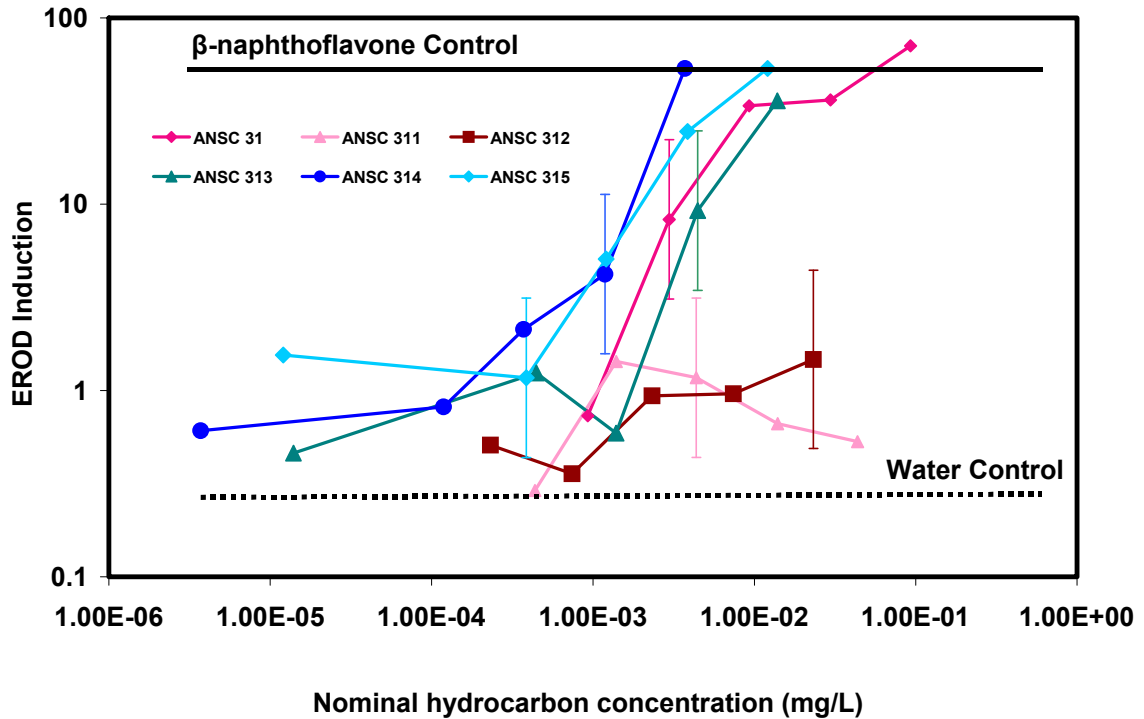
Figure 3.3: *In-vivo* EROD induction assay of normal phase sub-fractions of SCOT 31 fraction in rainbow trout. The error bars indicate the 95% confidence interval on the variation in the EROD data. To improve clarity, the error bars are indicated on selected points. The error bars on other points are similar in magnitude.
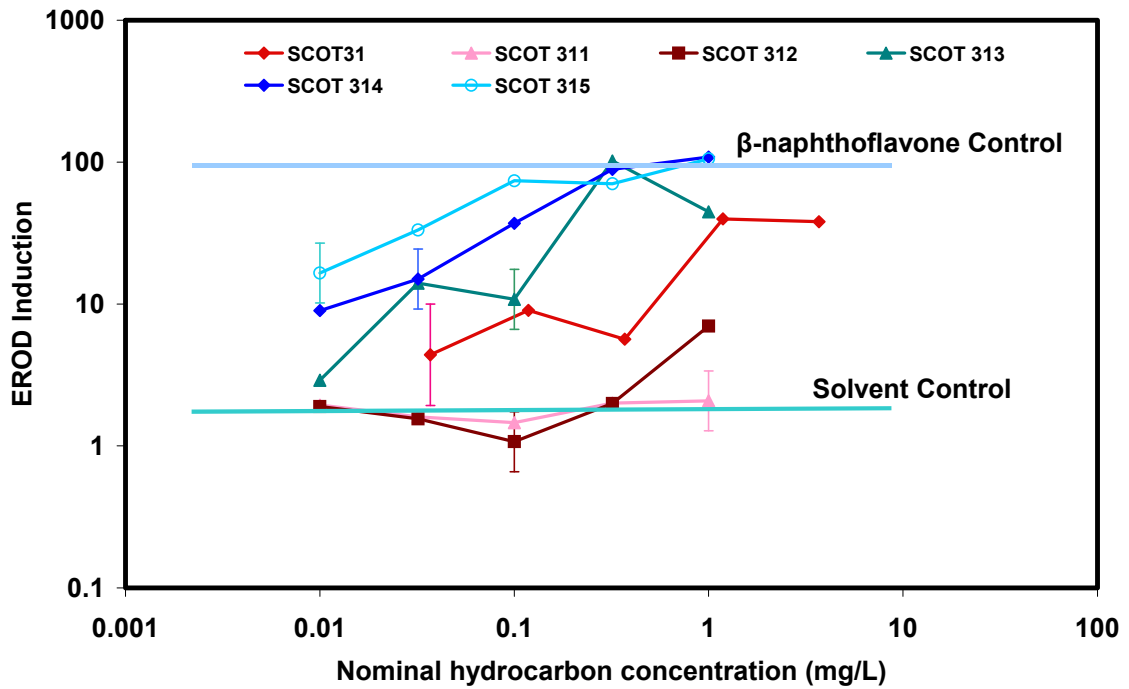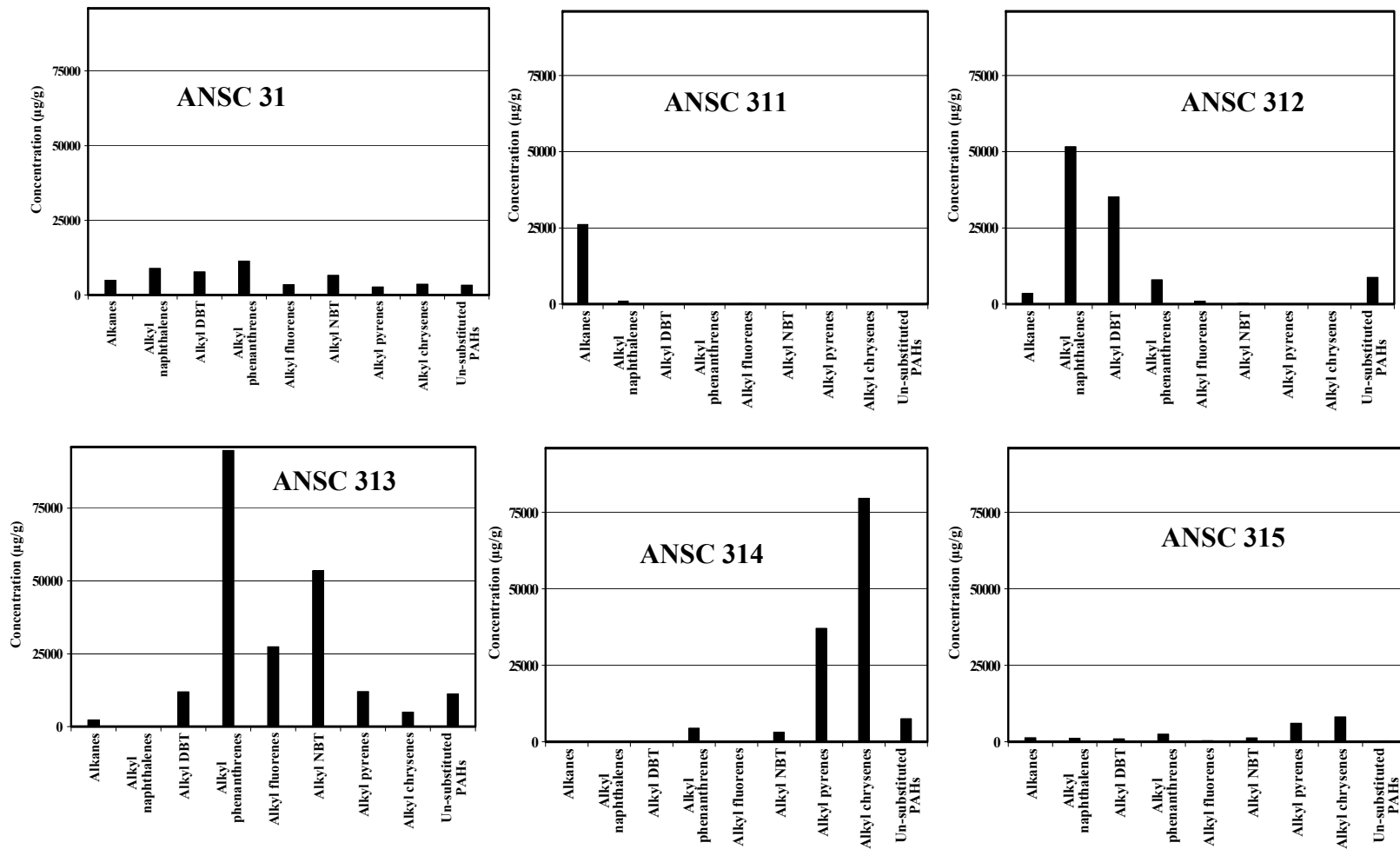
Figure 3.4: The total concentrations of different PAH classes and alkanes present in ANSC 31 normal phase sub-fractions.
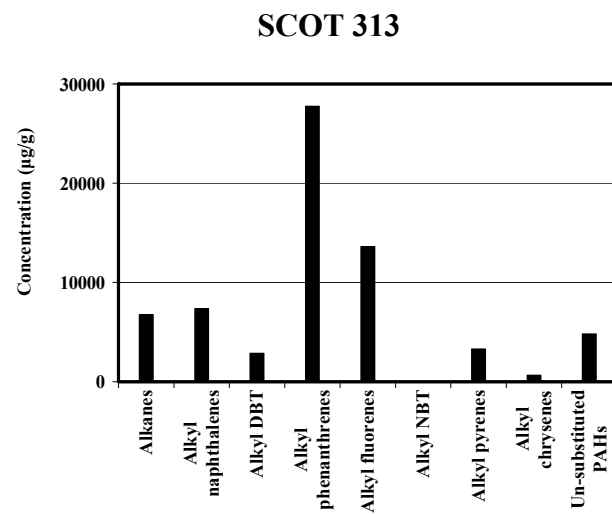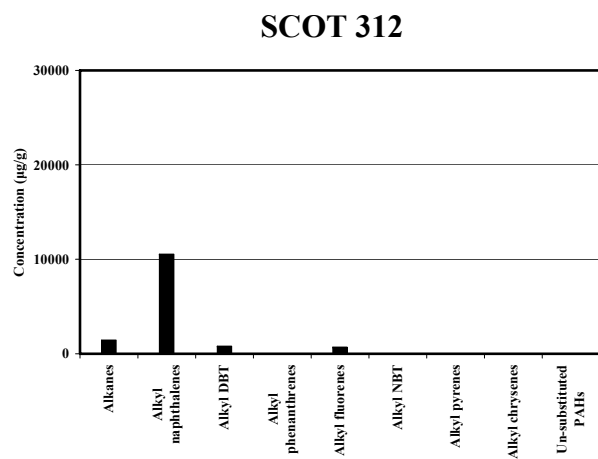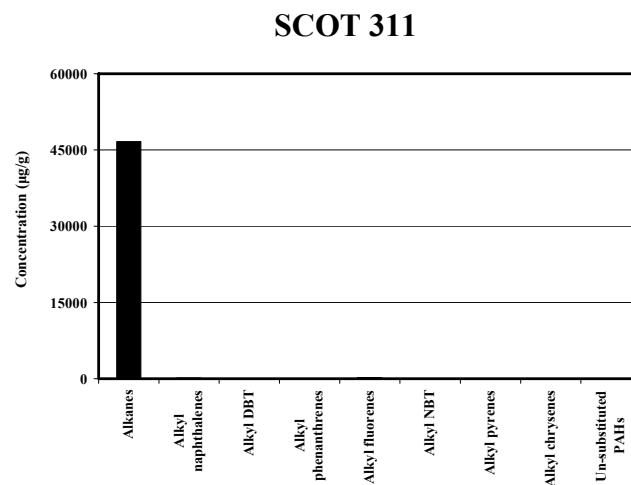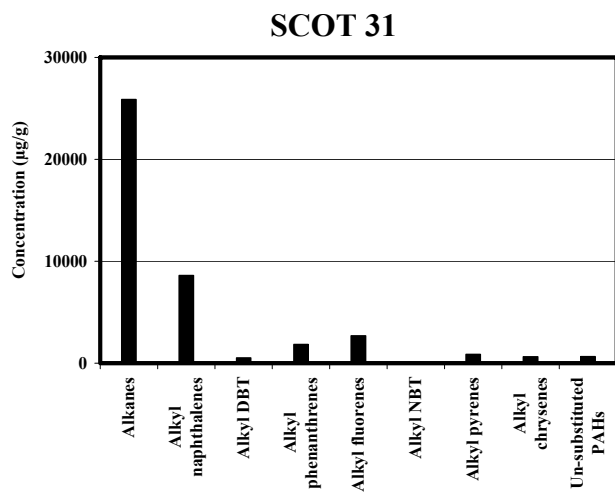
Figure 3.5: The total concentrations of different PAH classes and alkanes present in SCOT 31 normal phase sub-fractions. The concentration of target compounds was below detection limit in SCOT 314 and SCOT 315 fractions.

Table 3.8: Median effective concentration (EC50) of normal phase sub-fractions of ANSC 31 and SCOT 31 fractions. EC50 values are calculated using the data presented in Figures 3.2 and 3.3. NI = no induction observed in the concentration range tested.

Name of the oil	Fraction name	EC50 (mg/L)
ANSC	ANSC 31	0.05
	ANSC 32	NI
	ANSC 311	NI
	ANSC 312	NI
	ANSC 313	0.02
	ANSC 314	0.004
	ANSC 315	0.001
SCOT	SCOT 31	4.17
	SCOT 32	NI
	SCOT 311	NI
	SCOT 312	NI
	SCOT 313	0.23
	SCOT 314	0.16
	SCOT 315	0.06

EROD induction assay: The normal phase PAH sub-fractions of ANSC and SCOT crude oil were subjected to CYP1A assay to identify which classes of PAHs contain CYP1A inducers. Figures 3.2 and 3.3 show the relative EROD induction in fish exposed to different nominal concentrations of PAH sub-fractions of ANSC and SCOT crude oils respectively. Relative induction was calculated by normalizing the absolute induction with respect to the water control. For both the oils, the normal phase fractions 313, 314 and 315 showed a dose-dependent EROD activity in the concentration range tested in this study. It can be noted from Table 3.8 that the EC50 values for the CYP1A induction in fish for the sub-fractions ANSC 313 – ANSC 315 and SCOT 313 – SCOT 315 are lower

compared to ANSC 31 and SCOT 31 fractions, respectively. Moreover, the CYP1A inducing normal phase sub-fractions constitute only 32% for ANSC 31 fraction and 22% for SCOT 31 fraction. This indicates that the normal phase sub-fractionation of ANSC 31 and SCOT 31 has successfully isolated major CYP1A inducing components of these crude oils.

Normal phase sub-fraction 311, containing predominantly alkanes, did not induce CYP1A enzymes. This is consistent with our previous experiments in which the wax residue did not induce CYP1A in fish (Chapter 2). In addition to alkanes, as indicated in Tables 3.5 and 3.6, the normal phase sub-fraction 312 is dominated by two ring alkyl PAHs such as naphthalenes and dibenzothiophenes. Although these PAHs are present in high concentrations in 312 fraction, very low CYP1A activities observed in fish exposed to 312 fractions (Figures 3.2 and 3.3) suggest that alkyl naphthalenes and alkyl dibenzothiophenes do not contribute significantly for the CYP1A inducing activity of ANSC and SCOT crude oils. High CYP1A activity observed in fish exposed to fraction 313 can be attributed to the presence of higher concentrations of alkyl isomers of phenanthrene, fluorene and naphthobenzothiophene (Table 3.5 and Table 3.6). Alkyl chrysenes are only present in low concentrations in this fraction. The analysis of bioassay solutions indicated that the fish were exposed to higher concentrations of three-ring PAHs compared to alkyl chrysenes for this fraction. Therefore, although the relative CYP1A potency of alkyl chrysenes is higher than alkyl phenanthrenes [17], one would expect that their contribution to the overall CYP1A activity observed on exposure to this fraction to be marginal. In Previous studies, exposure of fish to

alkyl phenanthrenes caused higher CYP1A activity and toxicity [7, 8, 31]. Barron *et al.* have evaluated four different mechanistic model to correlate the early-life stage toxicity in fish [32] . Among the models tested, they found that the predictive power of the alkyl phenanthrene model was the highest. This suggests the importance of less potent but more abundant alkyl PAHs such as alkyl phenanthrenes in CYP1A assessment. On the other hand, higher concentrations of alkyl chrysenes and alkyl pyrenes present in fraction 314 are associated with high CYP1A activity produced by this fraction. For both the oils, fraction 315 caused high EROD induction. Although several known alkyl PAHs are present in this fraction, they were present in a much lower concentration compared to fractions 313 and 314 (Figure 3.4). Alkyl PAHs with more than three rings can exist in several isomeric forms with different biological activity. Therefore, high induction seen from this fraction could be either due to the presence of different alkyl PAH isomers that are more potent than the ones present in the previous fractions, or due to the presence of other unknown CYP1A inducers.

1.

Comparing the EC50 values of the PAH sub-fractions from ANSC and SCOT crude oils (Table 3.8), it is clear that the ANSC sub-fractions are about 10 to 100 times more potent than SCOT sub-fractions.

In this study we have included an extensive list of PAH classes and alkanes that are analyzed during oil spill investigation. In spite of this, the total mass of the analytes measured accounted only for about 2% to 20% of the mass of the normal phase sub-fractions (Tables 3.5 and 3.6). This implies that the

sub-fractions contain a large amount of compounds that are not analyzed in this work but might play a role in CYP1A induction. Nevertheless, it appears that the presence of relatively higher concentrations of PAHs in ANSC sub-fractions compared to SCOT sub-fractions correlates with the high CYP1A potency observed in ANSC sub-fractions. In Figures 3.4 and 3.5 the relative concentrations of PAH classes are compared among different normal phase sub-fractions of ANSC 31and SCOT 31 oil samples. The concentration of alkyl phenanthrenes, alkyl fluorenes, alkyl napthobenzothiophenes and alkyl chrysenes are 10 to 50 times higher in ANSC sub-fractions compared to SCOT sub-fractions. Thus, our results strongly suggest that the alkyl PAHs with more than two aromatic rings present in crude oil can induce CYP1A activity in rainbow trout. Sundberg *.et al.* [19] have used the EDFA approach to isolate and identify CYP1A inducing components present in contaminated sediments. The fraction containing higher amounts of polycyclic aromatic compounds (PAC) was found to cause high CYP1A activity. Further fractionation of the PACs using HPLC, with CYP1A testing of the sub-fractions, showed that sub-fractions containing higher levels of alkylated three and four ring PAHs induced CYP1A activity. Similarly, Brack *.et al.* [33], following an EDFA approach that used multi-step chromatographic fractionation, associated the presence of alkyl chrysenes and alkyl benz[a]anthracenes with the high CYP1A activity observed from high molecular weight PAC fractions. Alkyl PAHs are relatively resistant to weathering and hence dominate in weathered crude oils [34]. Field studies

conducted at oil contaminated sites many years after the Exxon Valdez Oil Spill in Prince William Sound, Alaska, identified several alkyl PAHs in the CYP1A inducing fractions [35]. This indicates that the alkyl PAHs present in crude oils could contribute to the overall CYP1A induction and toxicity observed in field trials.

Conclusion

In this work, we have used the EDFA approach to fractionate the PAH fraction of ANSC and SCOT crude oils. We have shown that alkyl PAHs belonging to phenanthrene, fluorene, naphthobenzothiophene, pyrene and chrysene induce CYP1A activity in fish. On the other hand, alkyl PAHs of naphthalene and dibenzothiophene do not contribute significantly to the overall CYP1A induction. These results suggest that in addition to the PAHs in the priority pollutant list, regular monitoring of alkyl PAHs would provide better knowledge of overall toxicity profile of oil-contaminated sites.

References

1.   Short, J.W., *Long-Term Effects of Crude Oil on Developing Fish: Lessons from the Exxon Valdez Oil Spill.* Energy Sources, Part A: Recovery, Utilization, and Environmental Effects, 2003. **25**(6): p. 509-517.

2.   Rice, S.D., R.E. Thomas, M.G. Carls, R.A. Heintz, A.C. Wertheimer, M.L. Murphy, J.W. Short and A. Moles, *Impacts to Pink Salmon Following the Exxon Valdez Oil Spill: Persistence, Toxicity, Sensitivity, and Controversy.* Reviews in Fisheries Science, 2001. **9**(3): p. 165 - 211.

3.   Carls, M.G., J.E. Hose, R.E. Thomas and S.D. Rice, *Exposure of Pacific herring to weathered crude oil: assessing effects on ova.* Environmental Toxicology and Chemistry, 2000. **19**(6): p. 1649-1659.

4.   Ramachandran, S.D., P.V. Hodson, C.W. Khan and K. Lee, *Oil dispersant increases PAH uptake by fish exposed to crude oil.* Ecotoxicology and Environmental Safety, 2004. **59**(3): p. 300-308.

5.   Heintz, R.A., J.W. Short and S.D. Rice, *Sensitivity of fish embryos to weathered crude oil: Part II. Increased mortality of pink salmon (Oncorhynchus Gorbuscha) embryos incubating downstream from weathered Exxon Valdez crude oil.* Environmental Toxicology and Chemistry, 1999. **18**(3): p. 494-503.

6.   Carls, M.G., R.A. Heintz, G.D. Marty and S.D. Rice, *Cytochrome P4501A induction in oil-exposed pink salmon Oncorhynchus gorbuscha embryos predicts reduced survival potential.* Marine Ecology: Progress Series, 2005. **301**: p. 253-265.

7.   Brinkworth, L.C., P.V. Hodson, S. Tabash and P. Lee, *CYP1A induction and blue sac disease in early developmental stages of rainbow trout (Oncorhynchus mykiss) exposed to retene.* Toxicology and environmental health, 2003. **66**(7): p. 526-546.

8.   Hawkins, S.A., S.M. Billiard, S.P. Tabash, R.S. Brown and P.V. Hodson, *Altering cytochrome P4501A activity affects polycyclic aromatic hydrocarbon metabolism and toxicity in rainbow trout (Oncorhynchus mykiss).* Environmental Toxicology and Chemistry, 2002. **21**(9): p. 1845-1853.

9.   Stegeman, J.J. and J.J. Lech, *Cytochrome P-450 Monooxogenase Systems in Aquatic Species: Carinogen Metabolism and Biomarkers for Carcinogen and Pollutant Exposure.* Environmental Health Perspectives, 1991. **90**: p. 101-109.

10.   Whyte, J.J., R.E. Jung, C.J. Schmitt and D.E. Tillitt, *Ethoxyresorufin-O-deethylase (EROD) Activity in Fish as a Biomarker of Chemical Exposure.* Critical Reviews in Toxicology, 2000. **30**(4): p. 347 - 570.

11.   Arinc, E., A. Sen and A. Bozcaarmutlu, *Cytochrome P4501A and associated mixedfunction oxidase induction in fish as a biomarker for toxic carcinogenic pollutants in the aquatic environment.* Pure and Applied Chemistry, 2000. **72**(6): p. 985-994.

12.   Bucheli, T.D. and K. Fent, *Induction of cytochrome P450 as a biomarker for environmental contamination in aquatic ecosystems.* Critical Reviews in Environmental Science and Technology, 1995. **25**(3): p. 201-68.

13.   Payne, J.F., *Field Evaluation of Benzopyrene Hydroxylase Induction as a Monitor for Marine Petroleum Pollution.* Science, 1976. **191**(4230): p. 945-946.

14.   Kafafi, S.A., H.Y. Afeefy, H.K. Said and A.G. Kafafi, *Relationship between aryl hydrocarbon receptor binding, induction of aryl hydrocarbon hydroxylase and 7-ethoxyresorufin O-deethylase enzymes, and toxic activities of aromatic xenobiotics in animals. A new model.* Chem. Res. Toxicol., 1993. **6**(3): p. 328-334.

15.   Trejo, F., G. Centeno and J. Ancheyta, *Precipitation, fractionation and characterization of asphaltenes from heavy and light crude oils.* Fuel, 2004. **83**(16): p. 2169-2175.

16.   Waller, C.L. and J.D. McKinney, *Three-Dimensional Quantitative Structure-Activity Relationships of Dioxins and Dioxin-like Compounds: Model Validation and Ah Receptor Characterization.* Chem. Res. Toxicol., 1995. **8**(6): p. 847-858.

17.   Barron, M.G., R. Heintz and S.D. Rice, *Relative potency of PAHs and heterocycles as aryl hydrocarbon receptor agonists in fish.* Marine Environmental Research, 2004. **58**(2-5): p. 95-100.

18.   Billiard, S.M., N.C. Bols and P.V. Hodson, *In vitro and in vivo comparisons of fish-specific CYP1A induction relative potency factors for selected polycyclic aromatic hydrocarbons.* Ecotoxicology and Environmental Safety, 2004. **59**(3): p. 292-299.

19.   Sundberg, H., R. Ishaq, G. Akerman, U. Tjarnlund, Y. Zebuhr, M. Linderoth, D. Broman and L. Balk, *A Bio-Effect Directed Fractionation Study for Toxicological and Chemical Characterization of Organic Compounds in Bottom Sediment.* Toxicological Sciences, 2005. **84**(1): p. 63-72.

20. Hollert, H., M. Durr, H. Olsman, K. Halldin, B. van Bavel, W. Brack, M. Tysklind, M. Engwall and T. Braunbeck, *Biological and Chemical Determination of Dioxin-like Compounds in Sediments by Means of a Sediment Triad Approach in the Catchment Area of the River Neckar.* Ecotoxicology, 2002. **11**(5): p. 323-336.

21. Wang, Z., B.P. Hollebone, M. Fingas, B. Fieldhouse, L. Sigouin, M. Landriault, P. Smith, J. Noonan and G. Thouin, *Development of a composition database for selected multicomponent oil.* 2002, Environment Canada: Ottawa.

22. Brack, W., *Effect-directed analysis: a promising tool for the identification of organic toxicants in complex mixtures?* Analytical and Bioanalytical Chemistry, 2003. **377**(3): p. 397-407.

23. Sundberg, H., U. Tjarnlund, G. Akerman, M. Blomberg, R. Ishaq, K. Grunder, T. Hammar, D. Broman and L. Balk, *The distribution and relative toxic potential of organic chemicals in a PCB contaminated bay.* Marine Pollution Bulletin, 2005. **50**(2): p. 195-207.

24. Hilscherova, K., K. Kannan, Y.-S. Kang, I. Holoubek, M. Machala, S. Masunaga, J. Nakanishi and J.P. Giesy, *Characterization of dioxin-like activity of sediments from a Czech river basin.* Environmental Toxicology and Chemistry, 2001. **20**(12): p. 2768-2777.

25. Martel, P.H., T.G. Kovacs, B.I. Connor and R.H. Voss, *Source and identity of compounds in a thermomechanical pulp mill effluent inducing hepatic mixed-function oxygenase activity in fish.* Environmental Toxicology and Chemistry, 1997. **16**(11): p. 2375-2383.

26. Khan, C.W., S.D. Ramachandran, L.M.J. Clarke and P.V. Hodson. *EROD activity (CYP1A) inducing compounds in fractionated crude oil.* in *Proceedings of the twenty-seventh Artic and Marine Oilspill Program (AMOP) technical seminar.* 2004. Edmonton, Alberta: Emergencies Science and Technology division, Environment Canada.

27. King, T.L. and K. Lee. *Assessment of sediment quality based on toxic equivalent benzo[a]pyrene concentrations.* in *Artic and Marine Oilspill Program (AMOP).* 2004. Edmonton, Alberta, Canada: Environmental science and technology division, Environment Canada, Ottawa, ON, Canada.

28. King, T.L., J.F. Uthe and C.J. Musial, *Polycyclic aromatic hydrocarbons in the digestive glands of the American lobster, Homarus americanus, captured in the proximity of a coal-coking plant.* Bulletin of Environmental Contamination and Toxicology, 1993. **50**(6): p. 907-914.

29. Hodson, P.V., S. Efler, J.Y. Wilson, A. El-Shaarawi, M. Maj and T.G. Williams, *Measuring the potency of pulp mill effluents for induction of hepatic mixed-function oxygenase activity in fish.* Journal of toxicology and environmental health: Part A, 1996. **49**: p. 101-128.

30. Basu, N., S. Billiard, N. Fragoso, A. Omoike, S. Tabash, S. Brown and P. Hodson, *Ethoxyresorufin O-deethylase induction in trout exposed to mixtures of polycyclic aromatic hydrocarbons.* Environmental Toxicology and Chemistry, 2001. **20**(6): p. 1244-1251.

31. Billiard, S.M., K. Querbach and P.V. Hodson, *Toxicity of retene to early life stages of two freshwater fish species.* Environmental Toxicology and Chemistry, 1999. **18**: p. 2070-2077.

32. Barron, M.G., M.G. Carls, R. Heintz and S.D. Rice, *Evaluation of Fish Early Life-Stage Toxicity Models of Chronic Embryonic Exposures to Complex Polycyclic Aromatic Hydrocarbon Mixtures.* Toxicol. Sci., 2004. **78**(1): p. 60-67.

33. Brack, W. and K. Schirmer, *Effect-Directed Identification of Oxygen and Sulfur Heterocycles as Major Polycyclic Aromatic Cytochrome P4501A-Inducers in a Contaminated Sediment.* Environmental Science & Technology, 2003. **37**(14): p. 3062-3070.

34. Wang, Z., M. Fingas and D.S. Page, *Oil spill identification.* Journal of Chromatography A, 1999. **843**(1-2): p. 369-411.

35. Carls, M.G., L.G. Holland, J.W. Short, R.A. Heintz and S.D. Rice, *Monitoring polycyclic aromatic hydrocarbons in aqueous environments with passive low-density polyethylene membrane devices.* Environmental Toxicology and Chemistry, 2004. **23**(6): p. 1416-1424.

CHAPTER 4

A multi-dimensional high performance liquid chromatographic method for fingerprinting polycyclic aromatic hydrocarbons and their alkyl-homologs in the Heavy Gas Oil fraction of Alaskan North Slope Crude

Gurusankar Saravanabhavan[1], Anjali Helferty[1], Peter V. Hodson[2] and R. Stephen Brown[1]*

[1] Department of Chemistry and School of Environmental Studies, Queens University, Kingston, ON, Canada.
[2] Department of Biology and School of Environmental Studies, Queens University, Kingston, ON, Canada.   K7L 3N6

* Corresponding Author

Abstract

We report an offline multi-dimensional high performance liquid chromatography (HPLC) technique for the group separation and analysis of PAHs in a heavy gas oil fraction (boiling range 287°C-481°C). Waxes present in the heavy gas oil fraction were precipitated using cold acetone at –20°C. Recovery studies showed that the extract contained 93% (+/- 1%; n=3) of the PAHs that were originally present while the wax residue contained only 6% (+/- 0.5%; n=3). PAHs present in the extract were fractionated, based on number of rings, into 5 fractions using a semi-preparative silica column (normal-phase HPLC). These fractions were analyzed using reverse-phase HPLC (RP-HPLC) coupled to a diode array detector (DAD). The method separated alkyl and unsubstituted PAHs on two reverse-phase columns series using an acetonitrile/water mobile phase. UV spectra of the chromatographic peaks were used to differentiate among PAH groups. Further characterization of PAHs within a given group to determine the substituent alkyl carbon number was done by retention time matching with a suite of alkyl-PAH standards. Naphthalene, dibenzothiophene, phenanthrene and fluorene and their C1-C4 alkyl isomers were quantified. The concentrations of these compounds obtained using the current method were compared with that of a GC-MS analysis obtained from an independent oil chemistry laboratory.

Key words: Unsubstituted and alkyl-substituted PAH analysis, HPLC, crude oil, DAD detection

Introduction

Determining the chemical constituents of crude oils is of paramount importance for both the oil industry as well as regulatory agencies. Crude oil is a complex mixture of chemical compounds with a wide range of polarities and volatilities, which makes its chemical characterization a challenging task. Generally, analysis of crude oil is done at two different levels of sophistication. The "group-type" analysis involves the separation of compounds into groups, mainly based on polarity, where the groups are classified as Saturates, Aromatics, Resins and Asphaltenes (SARA). For this separation, several liquid chromatographic methods using column liquid chromatography (LC) or high performance liquid chromatography (HPLC) have been developed using polar stationary phases such as silica or alumina [1-8]. Recently, Islas-Flores *et al*. [1] showed that group-type separation of oil samples using HPLC is simple and effective and yields comparable results to traditional open column liquid chromatography.

SARA analysis of crude oil is relatively quick and finds several applications in the oil industry. Precise knowledge of the group-type composition of crude oil is useful in solving problems during oil drilling and transportation processes [9]. It is also used extensively to guide the process control operations in refineries. Chromatographic procedures that have been developed and validated for SARA analysis have been recently reviewed [10, 11]. SARA fractions have been further separated and/or analyzed using chromatographic techniques to characterize the molecular composition of crude oil [12]. Among other compound classes, polycyclic aromatic hydrocarbons (PAHs), which are abundant in the aromatic

fraction of crude oil, have been analyzed extensively [13, 14]. The type and amount of PAHs present vary widely among different crude oils. PAH profiling finds several applications in oil exploration and also in monitoring environmental pollution. The PAH profile of a given crude oil gives information on its thermal maturity, and several maturity indices have been developed for this purpose [15]. PAHs are also environmental pollutants and PAH profiling of crude oils is useful when assessing the relative toxicity of crude oils. Standard PAH analysis normally targets unsubstituted PAHs, such as the sixteen compounds on the United States Environmental Protection Agency (US-EPA) "priority PAH" list. Recent toxicity studies from our group, as well as others, suggest that alkyl-substituted PAH compounds may be more important in characterizing PAH toxicity to early life stages of fish [16-21]. Notably, alkyl-substituted PAHs are significantly more abundant than unsubstituted PAHs in crude oil, typically comprising 80% to 90% of total PAH [22].

For oil spills, the PAH profile of the spilled oil together with the analysis of saturated hydrocarbons and other biomarker compounds has been used successfully to identify the nature and type of oil that was spilled and its weathering status [23, 24]. PAH profiling in these studies involved analysis of naphthalene, phenanthrene, fluorene, dibenzothiophene, and chrysene, plus their alkyl-homologs with one to four additional carbon atoms as substituents (C1- to C4-PAHs). The 16 US-EPA priority PAHs were also analyzed [14]. The relative concentrations of these PAHs can give several important clues during an oil spill investigation:

1. PAH distribution can be used to differentiate the contribution of petrogenic and pyrogenic sources. In general, unsubstituted PAHs dominate the pyrogenic sources whereas alkyl-PAHs are found in abundance in a petrogenic source;

2. PAH distribution patterns of crude oils differ substantially. Therefore, comparing the PAH distribution pattern at a spill site to a crude oil database can identify potential crude oil candidates for further investigation; and

3. The concentration pattern of the C0-C4 PAH can be used as a diagnostic tool to determine the weathering status of the crude oil, as more highly substituted alkyl-PAHs tend to dominate after the oil is weathered (C0 < C1 < C2 < C3 < C4). Hence, there is a need to develop analytical methods for the analysis of alkyl-substituted PAHs as well as unsubstituted PAHs. Several chromatographic methods have been developed for the separation and analysis of PAHs and other petroleum hydrocarbons in crude oil and petroleum products [10]. Among them, gas chromatographic (GC) techniques utilizing a flame ionization detector (FID) or a mass spectrometric detector (MS) have been developed and used routinely in oil chemistry laboratories [14, 25-27]. However, extensive sample cleanup, including prior group-type fractionation using a liquid chromatographic (LC) method, is often required before the final GC analysis. Recently, Wang and Fingas [26] reviewed the gas chromatographic methods used in oil spill identification.

LC methods have also been used for group-type separation as well as individual PAH analysis in crude oil or oil fractions. LC techniques have a unique advantage of fractionating complex samples into simpler mixture and producing
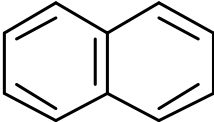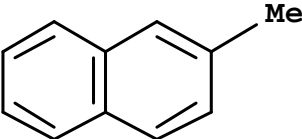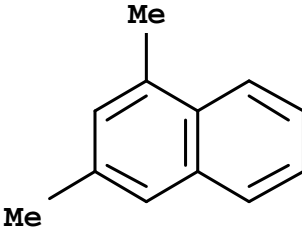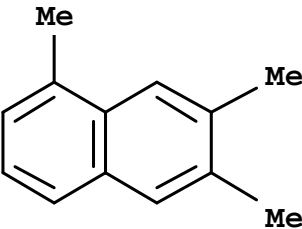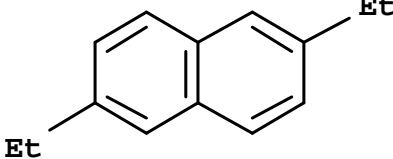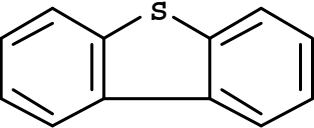
quantities which can be further analyzed using other techniques. Secondly, PAH classes such as alkyl-phenanthrenes, alkyl-anthracenes, alkyl-chrysenes and alkyl-benz[a]anthracenes and even non-substituted isomers of benzofluoranthenes are difficult to distinguish in GC-MS in the absence of authentic standards. These sets of compounds are easily distinguished in HPLC methods with diode-array detection. Moreover, high molecular weight PAHs (> 6 aromatic rings) and more polar residues can be easily analyzed, whereas analysis of these compounds could be difficult using GC-MS techniques [28]. Analysis of PAHs using only liquid chromatography can be done with a combination of LC methods. In this approach, PAHs are fractionated based on the number of rings using a normal-phase column, which is followed by separation using a reverse-phase column [29]. Fluorescence detection is a very sensitive method and has been routinely used for quantification of PAHs in standard reference materials [29]. The results obtained using HPLC with fluorescence detection have been found to be in close agreement with GC-MS [30].
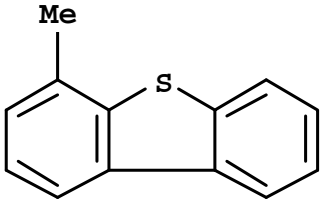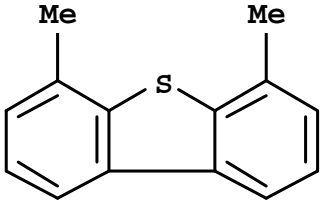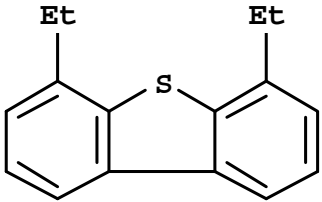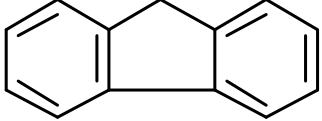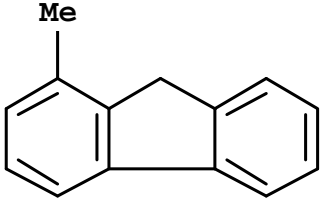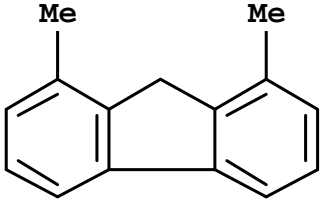
McKinney et al. [31] have attempted to analyze PAHs and alkyl-PAHs in five coal liquification process streams using normal-phase HPLC with a diode array detector. The two and three-ring PAHs that have very similar spectra could not be resolved and appeared as an un-resolved hump. Sufficient resolution to separate the unsubstituted PAHs from their alkyl-homologs was also not obtained. Therefore, it was necessary to collect individual fractions for further analysis using mass spectrometry (MS) to confirm the alkyl-PAHs.
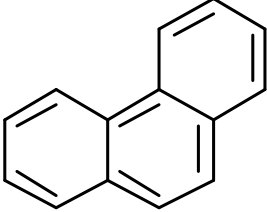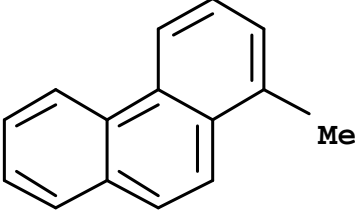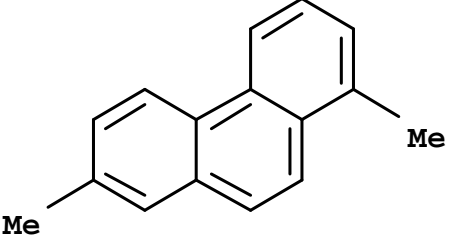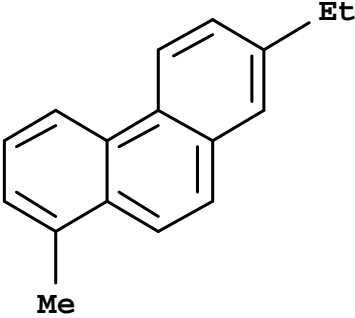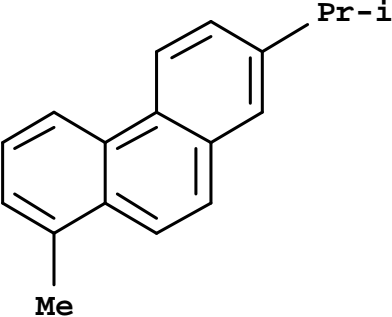
On the other hand, Akhlaq and Gotze used a tiered approach for the characterization of crude oil samples [32]. They used a single-wavelength UV detector for RP-HPLC analysis, and peak assignments were based solely on the retention time of available standards. Although their method can discriminate between different crude oils and diesel fuel, they could not achieve the quantification of PAHs. It should also be noted that the direct determination of PAHs, whether using normal-phase HPLC with diode array detection or the tiered approach with single wavelength UV detection, did not produce detailed PAH fingerprints of crude oil or oil fractions comparable to GC-MS analysis. Based on these observations, we proposed a tiered approach with diode array detection to characterize the PAHs present in the crude oil samples.

Here we report a method for the analysis of unsubstituted and alkyl-substituted PAHs in the heavy gas oil fraction (boiling range 287 to 481°C) of Alaskan North Slope crude oil using high performance liquid chromatography. The wax materials present in the heavy gas oil fraction were precipitated prior to HPLC fractionation. The PAHs were separated into 5 fractions based on the number of rings using normal-phase HPLC. These fractions were then analyzed using two reverse-phase columns connected in series and coupled to a diode array detector. The PAH analysis results obtained using this method were compared to GC-MS results obtained from an independent oil chemistry laboratory.

Table 4.1: Structure of PAH standards used in this study

Name of the PAH (abbrivated name)	Structure	Calculated logP value
Naphthalene (C_0 Naph)		3.45
2-Methyl naphthalene (C_1 Naph)		3.91
1,3 dimethyl naphthalene (C_2 Naph)		4.37
2,3,5-trimethyl naphthalene (C_3 Naph)		4.83
2,6- diethyl naphthalene (C_4 Naph)		5.43
Dibenzothiophene (C_0 Dibenzo)		4.38

4-methyl dibenzothiophene (C$_1$ Dibenzo)		4.84
4,6-dimethyl dibenzothiophene (C$_2$ Dibenzo)		5.30
4,6-diethyl dibenzothiophene (C$_4$ Dibenzo)		6.37
Fluorene (C$_0$ Fluorene)		4.16
1-methyl fluorene (C$_1$ Fluorene)		4.62
1,8-dimethyl fluorene (C$_2$ Fluorene)		5.08

Phenanthrene (C$_0$ Phen)		4.68
1-methyl phenanthrene (C$_1$ Phen)		5.14
1,7-dimethyl phenanthrene (C$_2$ Phen)		5.60
7-ethyl-1-methyl phenanthrene (C$_3$ Phen)		6.13
7-isopropyl-1-methyl phenanthrene (C$_4$ Phen)		6.48

Materials and method

Alaskan North Slope crude (ANSC) oil was fractionated into four fractions using low temperature fractional distillation at Dr. Zhendi Wang's lab at Environment Canada (Ottawa, ON). The details of this procedure were reported elsewhere [22]. GC-MS analysis of the third fraction (ANSC3, "heavy gas oil", boiling range 287 - 481$°$C) was done using a method reported elsewhere [14]. The GC-MS results showed the presence of a wide variety of 2-5 ring PAHs and their alkyl-homologs. SARA analysis of this fraction showed that it did not contain asphaltenes (unpublished results).

HPLC grade hexanes, methylene chloride and acetonitrile were procured from Fisher Scientific (Ottawa, ON). ACS-certified grade acetone (Fisher) was used for wax precipitation. Doubly-distilled water from an in-house still was used for HPLC. All unsubstituted and alkyl-substituted PAH standards used in this study were purchased from Sigma Aldrich (Milwaukee, WI). They are >98% pure and were used without further purification. Table 4.1 shows the structure of the PAH standards and their log P values obtained from *Scifinder* (Chemical Abstract Service, Columbus, OH).

Precipitation of waxes: The waxes in the heavy gas oil fraction were isolated using Burger's method with a few modifications [33]. Briefly, the oil fraction was heated to 70$°$C for 30 minutes in a water bath to completely dissolve the waxes. About 5 g of ANSC3 was transferred to a 100 mL Erlenmeyer flask. To this, 50 mL of acetone was added and stirred well. The mixture was placed in a freezer at

–20°C for 5 hr to allow waxes to precipitate, then passed through a 0.22 μm nylon filter and the extract collected (ANSC3-1). The precipitated residue was washed with an aliquot of cold acetone (maintained at –20°C) and the wash added to the extract. The residue (ANSC3-2) was dissolved and quantitatively transferred to a pre-weighed vial from the filter paper using 5 mL of hexane followed by 5 mL of dichloromethane. Both the residue and extract were evaporated under nitrogen and weighed on an analytical balance. Loss of volatile compounds such as naphthalene was not a concern as these compounds are not found in the heavy gas oil fraction [17]. Finally, both the residue and the extract were dissolved in 10 mL hexane and analyzed using normal-phase HPLC.

Recovery studies: The relative proportions of PAHs in the extract and the wax residue were determined. For this, two ANSC3 samples of equal weight (+/-5 mg) were compared. One was subjected to cold acetone extraction. The cold acetone extract, residue, and the untreated ANSC3 sample were dissolved separately in 10 mL of hexane and analyzed using normal-phase HPLC.

Normal-phase HPLC system: PAH fractionation and analysis were carried out using a Varian HPLC system (Varian, Mississauga, ON), consisting of two pump modules (Prostar 215) and a UV absorbance detector (Prostar 330) operating at 254 nm. The fractionation was done on a semi-preparative silica column (Zorbax sil, 9.4 mm i.d. x 25 cm length; 5 μm silica particle packing) (Agilent, Mississauga, ON). In PAH analysis, typically 650 μg of the sample (in 20 μL hexane) was injected onto the column. The PAHs were eluted using the mobile

phase conditions given in Table 4.2. The column was regenerated by backflushing with 100% methylene chloride to remove resins and other polar materials as indicated in Table 4.2. Column regeneration was checked by injecting the PAH standard mixture and verifying that retention times were within 1 min of expected values.

Table 4.2: Optimized mobile phase condition for the fractionation and analysis of PAHs on normal phase HPLC

Time (min)	Operation mode	Mobile phase composition	Flow rate (mL/min)
0	Normal	98% hexane/2% methylene chloride	1.5
80	Normal	98% hexane/2% methylene chloride	1.5
Column regeneration			
85	Backflush mode	100% methylene chloride	7
125	Backflush mode	100% methylene chloride	7
130	Backflush mode	98% hexane/2% methylene chloride	7
160	Backflush mode	98% hexane/2% methylene chloride	7
165	Equlibrate	98% hexane/2% methylene chloride	1.5

For fractionation, 200 µL of hexane containing 6.0 mg of cold acetone extract was injected onto the column and five fractions were collected with a fraction collector (Dynamax model FC-4, Varian). The fractionation time windows were determined by analyzing a suite of unsubstituted and alkylated PAH standards, and are given in Table 4.3. The expected fraction composition based on the

elution times of the standards is also indicated in the table. The fractionation was repeated five times and the corresponding fractions from each repeat pooled together. The composite fractions were reduced to 2 mL using a rotary evaporator and solvent exchanged to 2 mL of 25% dichloromethane in acetonitrile (for ANSC3-1-1) or 10% dichloromethane in acetonitrile (for ANSC3-1-2 to ANSC3-1-5). All five normal-phase fractions were analyzed using RP-HPLC.

Table 4.3: Time-windows for the PAH fraction collection on normal phase HPLC

Fraction no	Expected composition	Time window
ANSC3-1-1	Saturated aliphatic hydrocarbons	0-23 minute
ANSC3-1-2	2 ring PAHs and dibenzothiophenes	23 – 37 minutes
ANSC3-1-3	3 ring PAHs	37 – 67 minutes
ANSC3-1-4	4 and 5 ring PAHs	67 – 80 minutes
ANSC3-1-5	>5 ring PAHs, and resins	80 – 165 minutes

Reverse-phase HPLC analysis: RP-HPLC analyses used a Varian HPLC system equipped with an autosampler (Prostar 430), a single piston pump (Prostar 240) with three-way dynamic mixer, and a DAD (Prostar 330). The PAHs were separated on two columns connected in series, a Zorbax ODS 4.6 mm X 25 cm column (Agilent) followed by a Supelcosil LC-PAH 4.6mm X 25 cm (Supelco, Mississauga, ON), using an acetonitrile/water mobile phase gradient as in Table 4.4. ANSC3-1-1, 3-1-2, 3-1-3 and 3-1-5 fractions were analyzed using Program 1

(Table 4.4) while the ANSC3-1-4 fraction, which contained predominantly chrysenes and other high molecular weight PAHs, was analyzed using Program 2 (Table 4.4). The peak "purity" of the chromatographic peaks was assessed by the visual comparison of DAD signals obtained at five different points across the chromatographic peak using *PolyView 2000* software (Varian).

Table 4.4. Optimized elution program for the analysis of PAHs on reverse phase HPLC. The PAHs were separated on a Zorbax ODS column (4.6 mm X 25 cm) followed by a Supelcosil LC-PAH column (4.6mm X 25 cm) using the following acetonitrile/water mobile phase gradient. Flow rate was maintained at 2 ml/min.

Time (minutes)	% Acetonitrile	% Water
Program 1		
0	70	30
20	70	30
60	80	20
90	100	0
110	100	0
Program 2		
0	80	20
60	80	20
70	100	0
110	100	0

PAH quantification: PAHs and their alkyl-homologs were quantified using an external calibration method. A five-point calibration curve was obtained by analyzing a mixture of PAHs and alkyl-PAH standards. Table 4.5 shows the linear regression equations for the analyzed PAHs. The slope of the linear regression reflects the relative molar extinction coefficient of alkyl-PAHs. The limit of quantitation (LOQ) for the PAH standards was estimated as the amount injected which would give a signal-to-noise ratio of ten.

Table 4.5. Linear regression equation used for the quantification of PAHs in crude oil fractions. Regression equations used injection of PAH amounts in the range of 0.2–5.0 µg. Limit of quantification (LOQ) was determined by repeated injection (50 µL, n = 3) of an amount close to the LOQ and estimating the amount to give S/N = 10.

PAH identity	Quantification wavelength	Linear regression parameters		LOQ (ng injected)
		Slope (peak area/ng)	r^2	
C_0 Naphthalene	215 nm	1.72×10^8	0.996	9.6
C_1 Naphthalene	215 nm	1.35×10^8	0.999	12.5
C_2 Naphthalene	215 nm	1.02×10^8	> 0.999	6.7
C_3 Naphthalene	215 nm	9.97×10^7	> 0.999	8.6
C_4 Naphthalene	215 nm	9.93×10^7	> 0.999	7.6
C_0 Dibenzothiophene	320 nm	5.76×10^6	0.995	72
C_1 Dibenzothiophene	320 nm	5.49×10^6	> 0.999	79
C_2 Dibenzothiophene	320 nm	5.44×10^6	> 0.999	106
C_4 Dibenzothiophene	320 nm	4.40×10^6	0.999	190
C_0 Fluorene	254 nm	4.99×10^7	0.999	3.4
C_1 Fluorene	254 nm	4.03×10^7	> 0.999	7.8
C_2 Fluorene	254 nm	1.86×10^7	> 0.999	15.4
C_0 Phenanthrene	254 nm	1.01×10^8	0.999	1.4
C_1 Phenanthrene	254 nm	1.23×10^8	> 0.999	N.A
C_2 Phenanthrene	254 nm	1.12×10^8	0.999	2.2
C_3 Phenanthrene	254 nm	1.02×10^8	> 0.999	N.A
C_4 Phenanthrene	254 nm	6.69×10^7	0.999	2.9

Results and Discussion

Wax precipitation: In addition to being rich in PAHs, the heavy gas oil fraction contains wax materials and resins. During fractional distillation, the wax materials accumulate in the heavy gas oil fraction due to the boiling range similarity. Removing the waxes prior to HPLC analysis increased the column loading capacity during the PAH fractionation step. About 46% (± 6%; n=6) of the total material was precipitated at -20°C. The use of acetone as the solvent instead of a mixture of acetone and petroleum ether as in the Burger method [28] increased the total amount of wax residue precipitated. Recovery studies were conducted to measure the relative PAH content of the extract and the residue samples. As shown in Figure 4.1, 2 to 5 ring PAH standards eluted between 20 and 80 minutes under the mobile phase conditions given in Table 4.2.
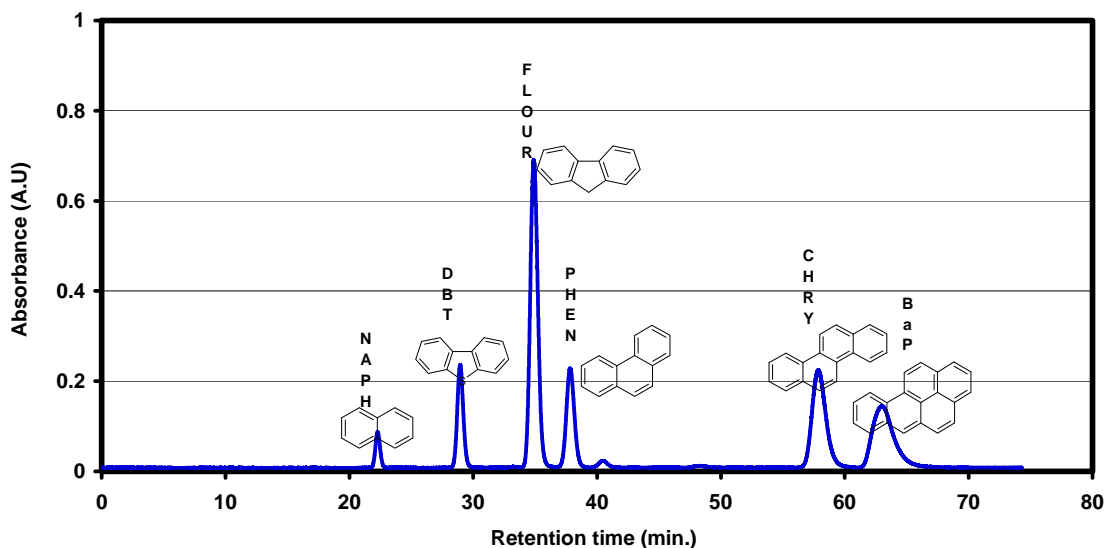
Figure 4.1: Analysis of PAH standards with varying number of aromatic rings on normal phase HPLC. PAHs are detected at 254 nm. The separation used the semi-prep silica column with mobile phase conditions given in Table 4.1.

154

As the alkyl-homolog of these PAHs elute very close to the unsubstituted PAHs on a silica column, one can assume that the area under the chromatogram between 20 and 80 minutes gives an estimation of total PAHs present in a given sample.
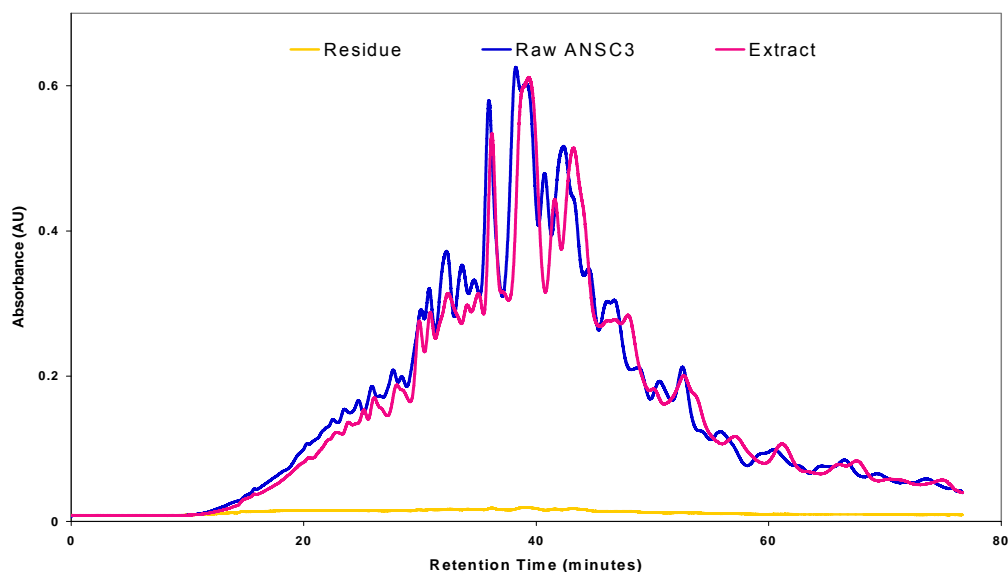
Figure 4.2: Recovery studies on cold acetone extraction technique. 650 μg of each sample was separated on the semi-preparative silica column with mobile phase conditions given in Table 4.1. PAHs are detected at 254 nm.

Table 4.6: Percentage distributions of PAHs in extract and wax residue after cold acetone extraction. Uncertainties are standard deviation

Trail No.	Total recovery by mass			PAH content (measured using HPLC)	
	Mass of Oil used	Mass % of extract	Mass % of residue	% total PAH in extract	% total PAH in residue
Trial 1	1.9998g	69	31	94	6
Trial 2	2.0010g	58	42	94	7
Trial 3	4.5009g	61	38	92	6

Figure 4.2 shows that the PAH profile of the extract and the un-treated ANSC3 sample overlap each other, indicating that most of the PAHs in the ANSC3 were extracted into the cold acetone. Moreover, the total PAH content of the residue was much lower than that of the extract. Quantitative estimates of relative PAH content using the total chromatogram area (see Table 4.6) indicated that the extract contained about 93% (+/- 1%; n=3) of total PAHs, while the residue contained only 6% (+/- 0.6%; n=3).
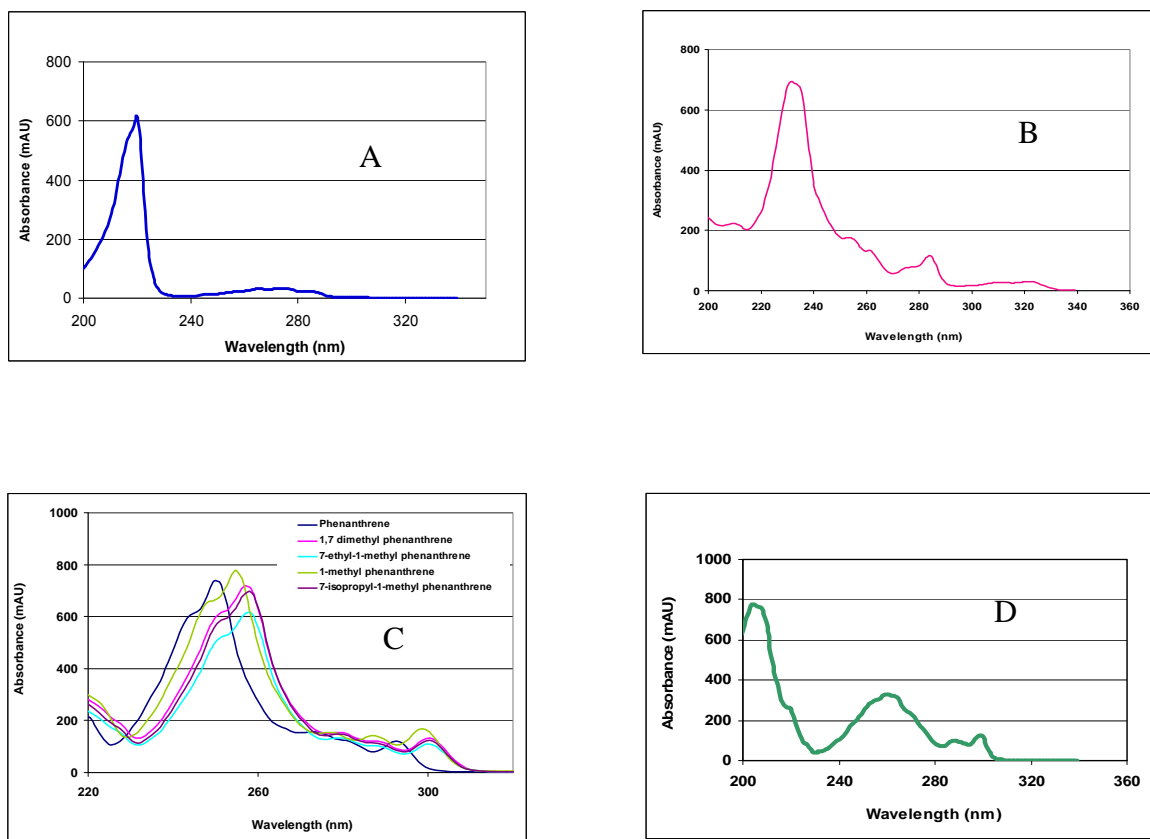
Figure 4.3: The diode array spectra of PAH standards. A = Naphthalene; B = Dibenzothiophene; C = Phenanthrene and alkyl phenanthrenes; D= Fluorene
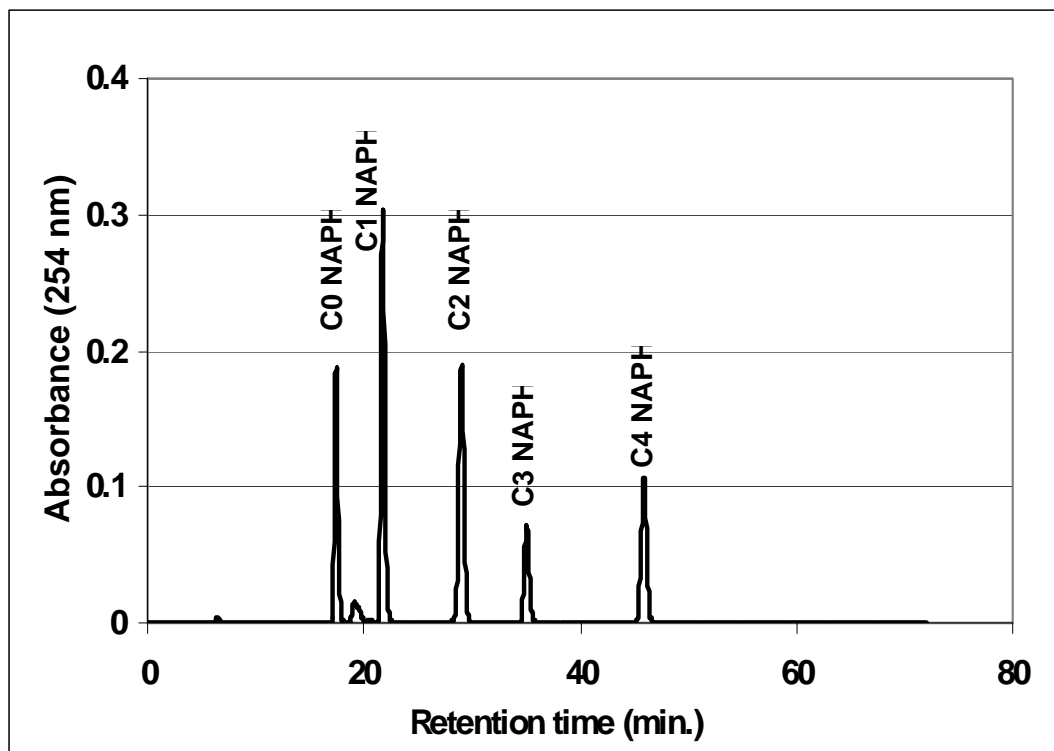
Figure 4.4: Chromatograph of naphthalene and alkyl naphthalene standards. Separation used two C18 columns connected in series with the mobile phase conditions given in Table 4.3 (Program 1). PAHs are monitored at 254 nm.

PAH analysis: The normal-phase fractions (ANSC3-1-1 to ANSC3-1-5) were analyzed for their PAH content using RP-HPLC coupled to a DAD. Several authors have recommended the tiered approach for the analysis of PAHs using HPLC [29, 32, 34, 35]. In this work, orthogonal separation was achieved by separating the PAH (based on number of rings) using the normal-phase column in the first dimension followed by the analysis of these fractions using a reverse-phase method. The reverse-phase analysis was performed using two columns in series. Preliminary chromatograms showed that resolution with the two columns

in series was better than with either used separately. It is likely that the LC-PAH improves separation based on PAH type, whereas the C18 phase provides further separation of compounds with different numbers of alkyl carbons. The general methodology used for peak assignment is as follows:

1. The chromatographic peaks were classified into different PAH classes based on their absorption spectra. The UV-Visible absorption spectra of PAHs vary significantly based on the number of aromatic rings they contain. As illustrated in Figure 4.3, the absorption spectra of chromatogram peaks can be used to easily distinguish between the major PAH types, even for peaks where a corresponding standard compound is not available. The 3-ring PAH phenanthrene has a major absorption band at 258 nm and minor bands at 215 nm and 300 nm. As shown in Figure 4.3D, the addition of alkyl-substituents to phenanthrene shifts the absorption peak maxima to slightly longer wavelengths, but the overall absorption profile is not changed. A similar result was seen for all alkyl-PAH standard groups.

2. The chromatographic peaks that belongs to a given PAH class (such as naphthalene) were assigned appropriate alkyl carbon numbers based on their retention factor. In general, retention of PAHs on a reverse-phase column is based on their hydrophobicity (log P). The hydrophobicity of alkyl-PAHs increases with an increase in alkyl substitution, resulting in elution patterns as shown for alkyl-substituted naphthalene standards in Figure 4.4. Therefore, alkyl carbon numbers were assigned by comparing

the retention factors for the PAH peaks in the sample to those of the available alkyl standards.

3. Figure 4.5 shows a plot of log P vs. retention factor obtained by analyzing PAHs and alkyl-PAH standards with a wide range of log P values on a reverse-phase column. Experimental log P values for only a very limited number of PAHs are available in the literature. Therefore, theoretical log P values for all PAH standards used in this study were obtained from the *Scifinder* database. A linear regression equation {*log P = 3.1065 X log (retention factor) + 3.737,* } was found to fit the experimental data (r^2 = 0.9479). This plot was used to assign alkyl carbon numbers for the PAH peaks for which alkyl standards were not commercially available.
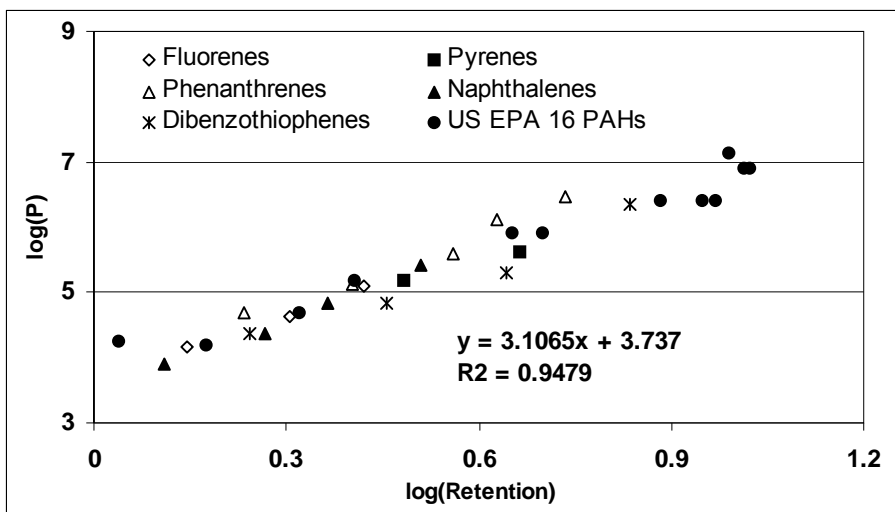
Figure 4.5: Relationship between log P and log(retention factor) for a suite of unsubstituted and alkyl substituted PAHs. Retention factor was calculated as [(retention time – void time)/void time] using retention data such as from Figure 4.4.

The main objective of this study was to analyze unsubstituted and alkyl-substituted (C0-C4) PAHs present in the heavy gas oil fraction. After normal-phase fractionation, most of the PAHs of interest were found in ANSC3-1-2, 3-1-3 and 3-1-4 sub-fractions. The ANSC3-1-1 fraction was expected to consist of mainly saturated hydrocarbons which do not absorb light, and significant chromatographic peaks were not seen with the DAD. ANSC3-1-5 was expected to consist of resinous substances and other polar molecules, and PAH peaks were not seen in the chromatogram.

The UV spectral analysis of the chromatogram showed that the ANSC3-1-2 fraction contained only naphthalenes and dibenzothiophenes. However, there was significant overlap of some of the alkyl-naphthalenes and dibenzothiophene peaks due to co-elution. To quantify these compounds, separate detection was achieved by plotting the chromatograms at wavelengths selective to naphthalenes and dibenzothiophenes. Naphthalene has a strong absorbance band at 215 nm while the dibenzothiophenes absorb very little. On the other hand, at 320 nm dibenzothiophenes absorb strongly compared to naphthalenes. Figures 4.6a and 4.6b show the chromatograms of the ANSC3-1-2 fraction plotted at 215 nm and 320 nm, respectively. It should be noted that the concentrations of naphthalenes and dibenzothiophenes in the co-eluting peaks were unknown and hence, merely using the retention time of the standard mixture could not have revealed the identity of the co-eluting peaks. This methodology clearly demonstrates the usefulness of DAD for the analysis of

alkyl-PAHs present in complex samples. The usefulness of the DAD for the identification of PAHs has been noted by other authors as well [28, 31].
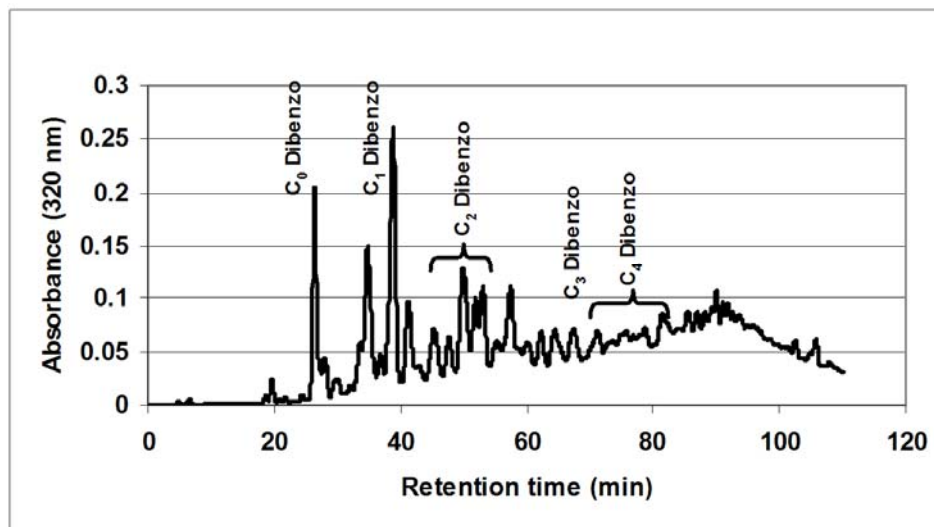
Figure 4.6a: Analysis of alkyl dibenzothiophenes present in ANSC3-1-2 fraction. The separation used two C18 columns connected in series with the mobile phase conditions given in Table 4.3 (Program 1). Dibenzothiophenes are quantified at 320 nm.
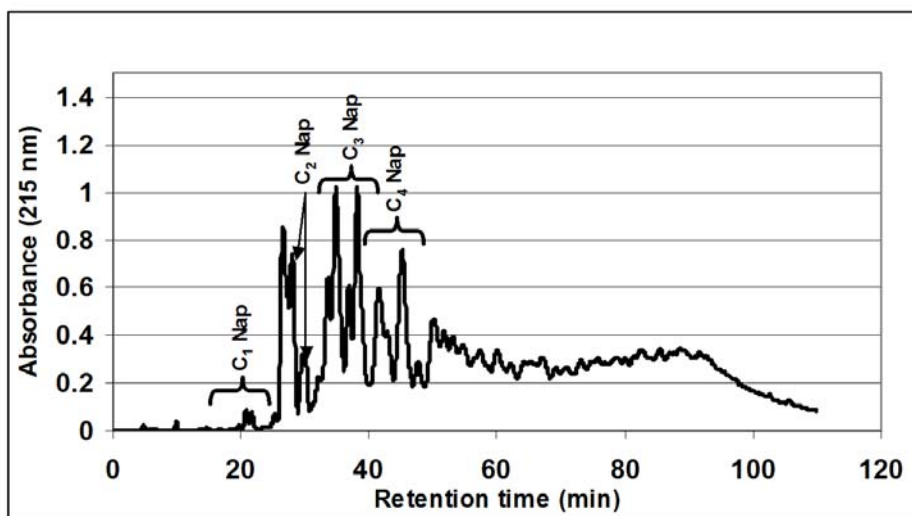
Figure 4.6b: Analysis of alkyl naphthalenes present in ANSC3-1-2 fraction. The separation used two C18 columns connected in series with the mobile phase conditions given in Table 4.3 (Program 1). Naphthalenes are quantified at 215 nm.
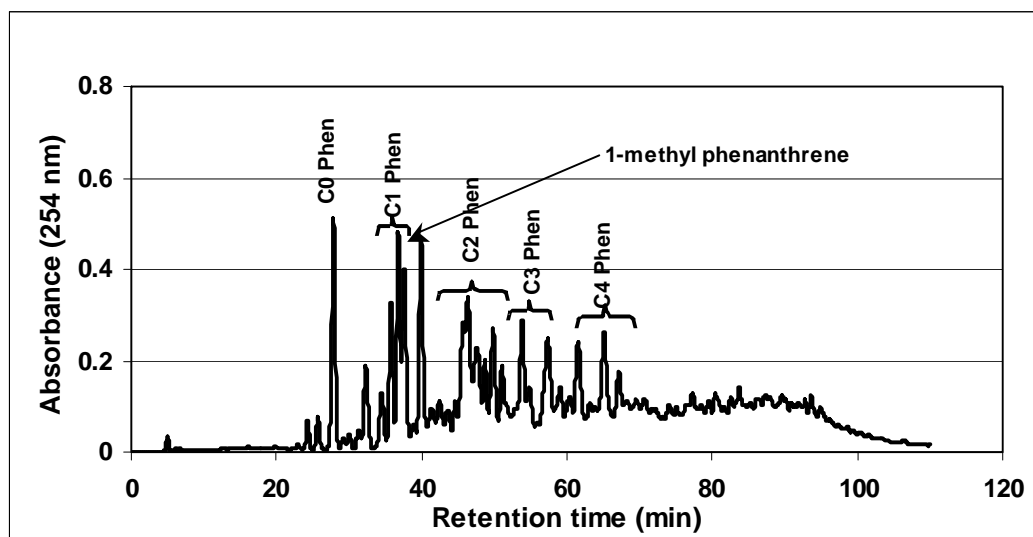
Figure 4.7a: Analysis of alkyl phenanthrenes and alkyl fluorenes present in ANSC3-1-3 fraction. The separation used two C18 columns connected in series with the mobile phase conditions given in Table 4.3 (Program 1). Detection at 254 nm
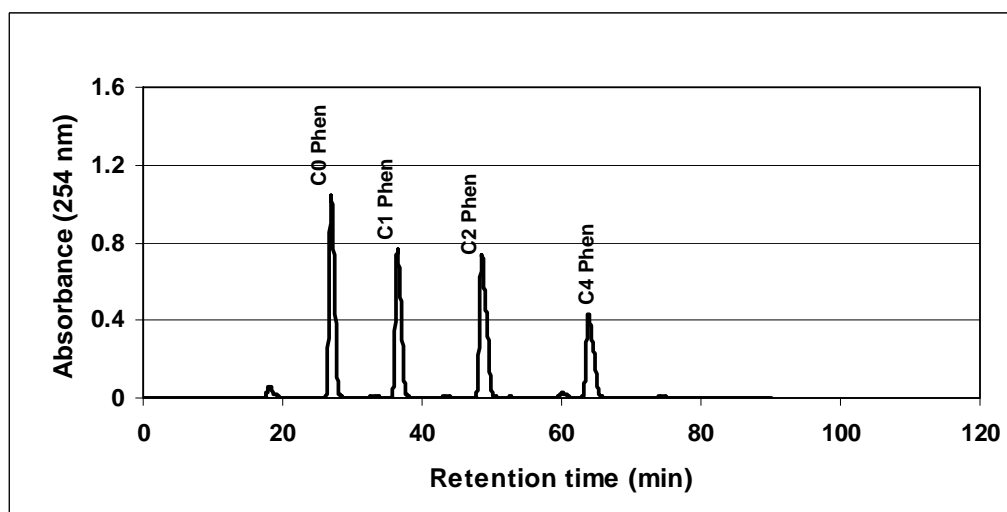
Figure 4.7b: Chromatograph of alkyl phenanthrene standards. The separation used two C18 columns connected in series with the mobile phase conditions given in Table 4.3 (Program 1). Detection at 254 nm

Figure 4.7a shows the chromatographic trace of the ANSC3-1-3 fraction. For comparison, the chromatogram of an alkyl-phenathrene standard mixture is shown in Figure 4.7b. The spectral analysis of this fraction indicated that it contains mostly alkyl phenanthrenes and alkyl fluorenes. Pyrene was found only in trace levels and there were no chrysenes. The PAH peak assignment and quantification was done using the general methodology described above. It is interesting to note that in Figure 4.7a there are four chromatographic peaks which are very close to each other at the retention time of the 1-methylphenanthrene standard. All these peaks have similar UV spectra that closely resemble that of phenanthrene. The 1-methylphenanthrene peak was positively identified by matching its retention time with that of the 1-methylphenanthrene standard. We believe that the other three peaks are three other methylphenanthrene isomers. Due to molecular symmetry, only 5 different methyl isomers of phenanthrenes are possible in nature. As these isomers differ only slightly in their log P values, they appear as a cluster in the chromatogram.

Figure 4.8 shows the RP-HPLC chromatogram of the ANSC3-1-4 fraction. Based on the DAD spectra and the retention time, we could positively identify triphenylene, chrysene and methylchrysene peaks. Small amounts of C3 fluorene and C3 phenanthrene were also identified. However, the identity of smaller peaks could not be determined due to the complex DAD spectra.
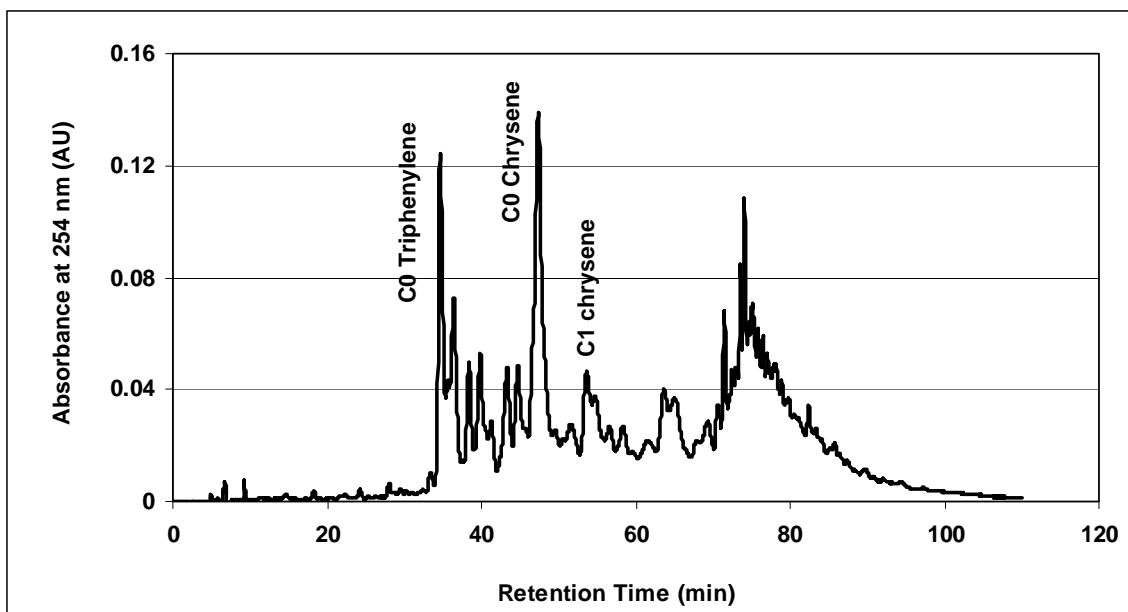
Figure 4.8: Analysis of ANSC3-1-4 fraction. The separation used two C18 columns connected in series with the mobile phase conditions given in Table 4.3 (Program 2). PAHs are detected at 254 nm.
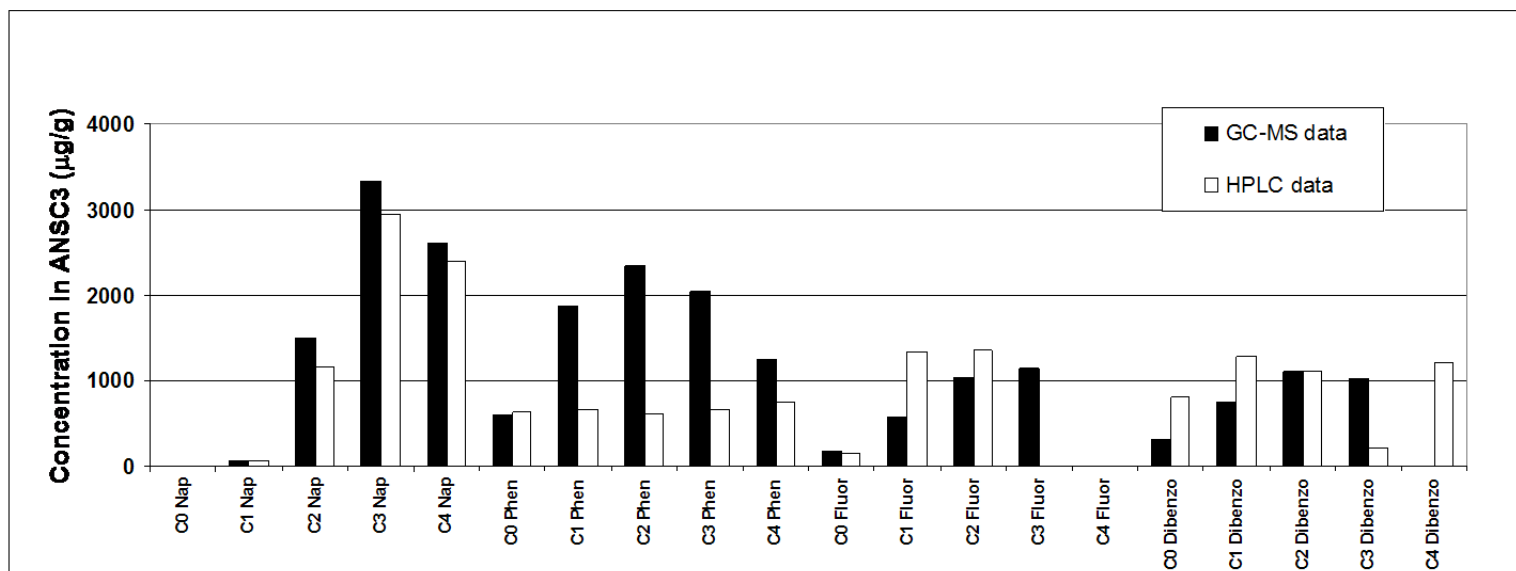
**Figure 4.9:** Comparison of the concentrations of PAHs and alkyl PAHs present in the heavy gas oil sample using HPLC-DAD and GC-MS techniques.

Quantitative comparison with GC-MS: In Figure 4.9, the relative concentrations of PAHs and their alkyl-homologs in ANSC3 measured using the current HPLC method is shown. For comparison, the concentrations of the same analytes, measured using GC-MS and reported in the literature, are shown [22]. In general, the PAH profile obtained using the current HPLC method shows good agreement with the published GC-MS data. The quantification profiles of naphthalene, dibenzothiophene, fluorene and their alkyl-homologs match well with that of GC-MS data. Compared to the GC-MS method, our method gives a lower concentration for alkyl-phenanthrenes. Some variation in the concentrations of individual PAHs between HPLC-DAD and GC-MS is not surprising. Generally, quantification of PAHs in complex matrices depends on several factors including sample handling, clean-up steps used, instrument sensitivity, and the calibration procedures employed [36]. The variation in the individual concentrations of PAHs between HPLC-DAD and GC-MS results may be attributed to such variation in the methodology. In an earlier study, an inter-laboratory exercise among nine laboratories was reported [37]. In this study, all nine laboratories analyzed a PAH extract prepared from a soil sample using identical sample extraction and clean-up procedures. The laboratories used GC-MS, GC-FID or HPLC with fluorescence or UV detection for the quantification of PAHs. In spite of analyzing identical samples, a large variation in individual PAH concentrations was reported. This clearly demonstrates the variability in quantifying PAHs, which is primarily due to a change in the instrumental analysis [37].

Conclusion

In this study a combined HPLC–DAD method was developed for PAHs and their alkyl-homologs present in a crude oil fraction, which could be adapted for whole oils as well. This method cannot substitute for the existing GC-MS methods as the resolution is not as high, and several classes of petroleum hydrocarbons such as saturated hydrocarbons cannot be analyzed by the HPLC method with DAD detection. On the other hand, this method can distinguish some of the alkyl-PAHs (e.g. alkyl-phenanthrenes and alkyl-anthracenes) that are very difficult to differentiate in GC-MS. The usefulness of the new method was demonstrated by analyzing PAHs present in the heavy gas oil fraction of Alaska North Slope crude. We used cold acetone precipitation to remove wax material prior to PAH analysis. Recovery studies demonstrated that the PAHs were not lost in the wax precipitation step.

Overall, quantitative comparison of the PAH profile obtained using this HPLC-DAD method with that from GC-MS analysis shows very promising results, illustrating the suitability of the current method for PAH profiling in crude oil or oil fractions. As discussed above, PAH profiling of crude oil has several applications including estimating the maturity of the oil and in oil spill investigations. This method can also be extended to analyze PAHs in other environmental matrices with appropriate sample clean-up steps. We believe that this method can be improved further so that it can be used as a complimentary technique to GC-MS for analysis of alkyl-PAHs in crude oil and their oil fractions.

References

1.   Islas-Flores, C.A., E. Buenrostro-Gonzalez and C. Lira-Galeana, *Comparison between open column chromatography and HPLC SARA fractionations in Petroleum.* Energy & Fuels, 2005. **19**: p. 2080-2088.

2.   Ali, M.A., *Resolution and Quantification of Ring Type Aromatics by HPLC Method Using n-Hexane Elution.* Petroleum Science and Technology, 2003. **21**(5): p. 963 - 970.

3.   Kaminski, M., R. Kartanowicz and A. Przyjazny, *Application of high-performance liquid chromatography with ultraviolet diode array detection and refractive index detection to the determination of class composition and to the analysis of gasoline.* Journal of Chromatography A, 2004. **1029**(1-2): p. 77-85.

4.   Kaminski, M. and R. Kartanowicz, *Selectivity of hydrocarbon group-type separation of petroleum vacuum distillates and base oils by HPLC.* Chemia Analityczna (Warsaw, Poland), 2003. **48**(3): p. 531-542.

5.   Sarowha, S.L.S., D.C. Madhwal, S. Singh, B.M.L. Bhatia, S. Ram and S.D. Bhagat, *High performance liquid chromatographic analysis of petroleum fractions.* Indian Journal of Technology, 1993. **31**(9): p. 645-648.

6.   Trisciani, A. and F. Munari, *Characterization of fuel samples by online LC-GC with automatic group-type separation of hydrocarbons.* Journal of High Resolution Chromatography, 1994. **17**(6): p. 452-456.

7.   Ali, M.A. and A. Hassan, *Hydrocarbon group types analysis of petroleum products: A comparative evaluation of HPLC and TLC analytical performance.* Petroleum Science and Technology, 2002. **20**(7&8): p. 751-762.

8.   Jorikova, L., J. Ruman and M. Davidova, *The application of HPLC techniques to the analysis of fuels and oils.* Petroleum and Coal, 2000. **42**(3-4): p. 185-187.

9.   Andersen, S.I., T. Hofsäss , W. Kleinitz and I. Rahimian, *Organic precipitates in oil production of a Venezuelan oil field.* Petroleum science and technology, 2001. **19**(1-2): p. 55-74.

10.   Barman, B.N., V.L. Cebolla and L. Membrado, *Chromatographic techniques for petroleum and related products.* Critical Reviews in Analytical Chemistry, 2000. **30**(2-3): p. 75-120.

11.   Kaminski, M., R. Kartanowicz, E. Gilgenast and J. Namiesnik, *High-Performance Liquid Chromatography in Group-Type Separation and*

Technical or Process Analytics of Petroleum Products. Critical Reviews in Analytical Chemistry, 2005. **35**(3): p. 193-216.

12. Wise, S.A., S.N. Chesler, H.S. Hertz, L.R. Hilpert and W.E. May, *Chemically bonded aminosilane stationary phas for the high-performance liquid chromatographic separation of polyneuclear aromatic compounds.* Analytical Chemistry, 1977. **49**(14): p. 2306-2309.

13. Grizzle, P.L. and D.M. Sablotny, *Automated liquid chromatographic compound class group type separation of crude oils and bituments using chemically bonded aminosilane.* Analytical Chemistry, 1986. **58**(12): p. 2389-2396.

14. Wang, Z., M. Fingas and K. Li, *Fractionation of a light crude oil and identification and quantitation of aliphatic, aromatic and biomarker compounds by GC-FID and GC-MS, Part I.* Journal of Chromatographic Science, 1994. **32**: p. 361-366.

15. Requejo, A.G., R. Sassen, T. McDonald, G. Denoux, M.C. Kennicutt II and J.M. Brooks, *Polynuclear aromatic hydrocarbons (PAH) as indicators of the source and maturity of marine crude oils.* Organic Geochemistry, 1996. **24**: p. 1017-1033.

16. Basu, N., S. Billiard, N. Fragoso, A. Omoike, S. Tabash, S. Brown and P. Hodson, *Ethoxyresorufin O-deethylase induction in trout exposed to mixtures of polycyclic aromatic hydrocarbons.* Environmental Toxicology and Chemistry, 2001. **20**(6): p. 1244-1251.

17. Billiard, S.M., K. Querbach and P.V. Hodson, *Toxicity of retene to early life stages of two freshwater fish species.* Environmental Toxicology and Chemistry, 1999. **18**: p. 2070-2077.

18. Billiard, S.M., N.C. Bols and P.V. Hodson, *In vitro and in vivo comparisons of fish-specific CYP1A induction relative potency factors for selected polycyclic aromatic hydrocarbons.* Ecotoxicology and Environmental Safety, 2004. **59**(3): p. 292-299.

19. Carls, M.G., R.A. Heintz, G.D. Marty and S.D. Rice, *Cytochrome P4501A induction in oil-exposed pink salmon Oncorhynchus gorbuscha embryos predicts reduced survival potential.* Marine Ecology: Progress Series, 2005. **301**: p. 253-265.

20. Kiparissis, Y., P. Akhtar, P.V. Hodson and R.S. Brown, *Partition Controlled Delivery (PCD) of Toxicants: A Novel In Vivo Approach for Embryotoxicity Testing, Environmental Science and Technology.* Environmental Science & Technology, 2003. **37**: p. 2262-2266.

21.   Tysklind, M., P. Andersson, P. Haglund, B. vanBavel and C. Rappe, *Selection of Polychlorinated Biphenyls for use in Quantitative Structure-Activity Modelling.* SAR and QSAR in Environmental Research, 1995. **4**(1): p. 11 - 19.

22.   Wang, Z., B.P. Hollebone, M. Fingas, B. Fieldhouse, L. Sigouin, M. Landriault, P. Smith, J. Noonan and G. Thouin, *Development of a composition database for selected multicomponent oil.* 2002, Environment Canada: Ottawa.

23.   Wang, Z., M. Fingas and L. Sigouin, *Characterization and identification of a "mystery" oil spill from Quebec (1999).* Journal of Chromatography A, 2001. **909**(2): p. 155-169.

24.   Wang, Z. and M. Fingas, *Study of the effects of weathering on the chemical composition of a light crude oil using GC/MS GC/FID.* Journal of Microcolumn Separations, 1995. **7**(6): p. 617-639.

25.   Wise, S.A., *Standard reference materials (SRMs) for the determination of polycyclic aromatic compounds - twenty years of progress.* Polycyclic Aromatic Compounds, 2002. **22**(3-4): p. 197-230.

26.   Wang, Z. and M. Fingas, *Oil and petroleum product fingerprinting analysis by gas chromatographic techniques.* 3 ed. Chromatographic analysis of the environment, ed. L.N.L. Nollet. 2006, Boca Raton, Florida: Taylor & Francis Group.

27.   Radke, M., H. Willsch and D.H. Welte, *Class separation of aromatic compounds in rock extracts and fossil fuels by liquid chromatography.* Analytical Chemistry, 1984. **56**(13): p. 2538-2546.

28.   Fetzer, J.C., W.R. Biggs and K. Jinno, *HPLC analysis of the large polycyclic aromatic hydrocarbons in a diesel particulate.* Chromatographia, 1986. **21**(8): p. 439-42.

29.   Wise, S.A., L.C. Sander and W.E. May, *Determination of polycyclic aromatic hydrocarbonss using liquid chromatography.* Journal of Chromatography, 1993. **642**: p. 329-349.

30.   Wise, S.A., L.R. Hilpert, G.D. Byrd and W.E. May, *Comparison of liquid chromatography with fluorescence detection and gas chromatography/mass spectrometry for the determination of polycyclic aromatic hydrocarbons in environmental samples.* Polycyclic Aromatic Compounds, 1990. **1**(1-2): p. 81-98.

31.   McKinney, D.E., D.J. Clifford, L. Hou, M.R. Bogdan and P.G. Hatcher, *High performance liquid chromatography (HPLC) of coal liquefaction*

process streams using normal-phase separation with diode array detection. Energy & Fuels, 1995. **9**(1): p. 90-96.

32. Akhlaq, M.S. and P. Gotze, *Detailed analysis of crude oil group types using reversed-phase high-performance liquid chromatography.* Journal of Chromatography A, 1994. **677**(2): p. 265-272.

33. Burger, E.D., T.K. Perkins and J.H. Striegler, Journal of Petroleum Technology, 1981: p. 1075.

34. Packham, A.J. and P.R. Fielden, *Column switching for the high-performance liquid chromatographic analysis of polynuclear aromatic hydrocarbons in petroleum products.* Journal of Chromatography A, 1991. **552**: p. 575-582.

35. Palmentier, J.-P.F., A.J. Britten, G.M. Charbonneau and F.W. Karasek, *Determination of polycyclic aromatic hydrocarbons in lubricating oil base stocks using high-performance liquid chromatography and gas chromatography--mass spectrometry.* Journal of Chromatography A, 1989. **469**: p. 241-251.

36. Gratz, L.D., S.T. Bagley, D.G. Leddy, J.H. Johnson, C. Chiu and P. Stommel, *Interlaboratory comparison of HPLC-fluorescence detection and GC/MS: analysis of PAH compounds present in diesel exhaust.* Journal of Hazardous Materials, 2000. **74**(1-2): p. 37-46.

37. Blankenhorn, I., D. Meijer and R.J. Delft, *Inter-laboratory comparison of methods used for analysing polycyclic aromatic hydrocarbons (PAHs) in soil samples.* Fresenius' Journal of Analytical Chemistry, 1992. **343**(6): p. 497-504.

CHAPTER 5

An off-line two-dimensional high performance liquid chromatographic method for the analysis of un-substituted and alkyl substituted polycyclic aromatic hydrocarbons (PAHs) present in Alaskan North Slope Crude oil

Gurusankar Saravanabhavan and R. Stephen Brown*

Department of Chemistry, Queen's University, Kingston, ON, Canada.

*Corresponding author

Abstract

We report the development of an off-line multidimensional chromatographic method for the analysis of alkyl PAHs present in the crude oil samples. The alkyl PAHs were first fractionated on a semi-preparative silica column into 91 fractions. These fractions were then analyzed using reverse phase high performance liquid chromatography coupled to a diode array detector (RP-HPLC-DAD). A data analysis protocol was developed to analyze the DAD data. These data were used for the detailed analysis of alkyl PAHs in different PAH classes. Our method clearly distinguished PAHs which cannot be distinguished in gas chromatography with mass spectrometric detection (GC-MS), such as alkyl chrysenes and alkyl triphenylenes. Good agreement between the concentrations of alkyl PAHs obtained by the current method and the standard GC-MS method was observed. Finally, contour plots were developed using the chromatographic data and their use in the analysis of alkyl PAHs is described.

Introduction

Crude oil is a complex mixture of organic compounds including a suite of aliphatic and aromatic hydrocarbons. The chemical composition of the crude oils is predominantly determined by the geological conditions that prevailed during its formation and hence varies widely between the sources. Broadly, crude oil components can be classified into saturates, aromatics, resins and asphaltenes (SARA). The precipitation of saturates and asphaltene compounds at low temperatures poses serious problems during the extraction and transportation of the crude oil [1, 2]. Hence SARA analysis of crude oils is the most common characterization of crude oil, and is used to guide the optimal extraction and transportation conditions. Several methods have been developed for SARA analysis including open column liquid chromatography (LC), supercritical liquid chromatography (SFC), and thin layer chromatography (TLC) [3-6]. High performance liquid chromatographic (HPLC) methods are the preferred LC methods due to their simplicity and reproducibility [7, 8].

SARA analysis gives very limited information about the individual chemical compounds present in crude oils. More detailed chemical analysis of crude oil and its sub-fractions is often needed by the oil industry as well as regulatory agencies. The concentration of individual aliphatic and aromatic hydrocarbons constitutes a "chemical fingerprint" of the crude oil and has been used for several purposes. Firstly, thermal maturity indices based on the concentrations of aliphatic and polycyclic aromatic hydrocarbons (PAHs) have been widely used in petroleum exploration [9, 10]. Secondly, many PAHs are known environmental

pollutants capable of producing toxic effects in organisms [11]. However, the toxicity of PAHs varies widely and hence detailed analysis is of great importance to isolate and identify toxic PAH components. Thirdly, chemical fingerprinting techniques have been widely used during oil spill investigations. PAH concentrations in the sites affected by an oil spill can give definitive information about the type and the weathering stage of the spilled oil and can hold the key for the successful source identification [12].

Usually a tiered approach is followed for analysis of PAHs in crude oil samples [13, 14]. In the first step, asphaltenes are removed by precipitation with 1:40 (w/v) pentane. The resulting maltene fraction is subjected to column chromatographic fractionation employing polar stationary phases such as silica to separate saturates from the aromatic hydrocarbons. These fractions are then separately analyzed using chromatographic methods.

Due to their volatility and thermal stability, petroleum hydrocarbons are amenable to gas chromatographic methods. Several methods using gas chromatography-mass spectrometry (GC-MS) and gas chromatography-flame ionization detector (GC-FID) have been developed and routinely used in the oil chemistry laboratory. The high resolving power of the GC-MS technique is very useful for the precise identification of some alkyl PAH isomers. However, as a large number of different alkyl PAH isomers are present in the crude oils, many are either not well resolved or co-elute in GC-MS. Moreover, alkyl PAHs belonging to different PAH classes such as (chrysene and triphenylene) have identical molecular masses and similar fragmentation patterns, and hence cannot be distinguished using MS detection in

the absence of standards. Hence, multi-dimensional chromatographic approaches such as GC-GC, LC-LC, LC-GC have been proposed to improve the resolving power of the overall chromatographic method [15].

A typical on-line two-dimensional (2D) chromatographic system consists of two chromatographic columns with different stationary phase chemistry connected by an appropriate interface. The second column is then coupled to the detector system to analyze the eluting components. The main purpose of the interface is to collect, concentrate and re-focus the eluent from the first column onto the second column. A rapid analysis method is usually employed in the second dimension so that each chromatographic peak eluting from the first column is sampled multiple times. This results in the improved sensitivity, resolution and the overall peak capacity of the chromatographic method [16].

Several 2D methods have been specifically developed for the analysis of hydrocarbons present in crude oils. Frysinger and Gaines [15]developed a GC-GC-MS method for the analysis of hydrocarbons present in diesel fuel. Their method could resolve over 750 peaks and helped in identification of several new compounds that were present in low concentrations. In a further development, these researchers used this technique to identify the source of a marine diesel spill by comparing the 2D contour plots of the oil spill sample with two suspected diesel samples [17].

Quantification of BTEX chemicals using GC-MS techniques often requires their prior fractionation from polyaromatic compounds. Recently, a GC-GC-FID method was reported for the quantification of BTEX and aromatic compounds in

gasoline samples [18]. In this approach, the hydrocarbons were separated based on their volatility in the first dimension using a dimethylpolysiloxane column. The eluent from the first column was separated using a more polar cyanopropyl methylsiloxane column in the second dimension. This resulted in the clear separation of the volatile BTEX compounds from the polyaromatic species. A similar GC-GC-FID based system was also reported to be useful for the analysis of PAHs, alkyl PAHs and biomarker compounds present in Alaskan north slope crude oil [19]. The 2D chromatographic plot was compared with a standard GC-MS chromatogram of the same oil sample to assign peaks corresponding to several individual isomers of dimethyl naphthalene, trimethyl naphthalenes, methyl dibenzothiophene, dimethyl dibenzothiophenes and methyl phenanthrene. Currently for fuel analysis, GC-GC methods are predominantly employed. Hybrid chromatographic separation methods (such as LC-GC) have been employed only with limited success. An online method in which a normal phase HPLC column was coupled to a GC-time of flight (ToF) MS system was reported for the analysis of hydrocarbons in a diesel sample [20]. Although this method was found to be suitable to identify major compound classes present in the diesel, individual compound analysis could not be achieved.

Recently Dugo et al. reviewed the theory and application of comphrehensive multidimensional liquid chromatographic techniques [21]. On-line two-dimensional HPLC techniques (LC-LC) find wide applications in the analysis of proteins, peptides, pharmaceuticals, polymers and some environmental contaminants [22, 23]. Most of the 2D HPLC methods developed for peptide

analysis involve the coupling of either size exclusion chromatography or ion-exchange chromatography in the first dimension with reverse phase chromatography in the second dimension. To get maximum benefit from 2D HPLC separation for environmental analysis, it is desirable to combine normal phase and reverse phase modes (NPLC-RPLC) in an on-line 2D system. A major problem for constructing such a 2D HPLC system is the incompatibility of solvents that are used in normal phase and reverse phase chromatography. Secondly, the commonly used normal phase solvents have strong elution strength in the reverse phase mode. Hence, injecting a large volume of eluent from the normal phase onto the reverse phase column would result in significant band broadening. Sonnerfeld et al. attempted to overcome these difficulties by coupling a semi-preparative aminosilane column to a C18 column via a diamine concentrator column [24]. The oil sample was initially applied onto the aminosilane column. The PAH fraction was isolated and trapped on the diamine column. The normal phase solvents were evaporated by purging the diamine column with nitrogen gas. The PAH analytes were desorbed using reverse phase mobile phase and subsequently injected onto the C18 column. Tian et al. recently developed a new solvent exchange interface for 2D HPLC [25]. In this system, the eluent from the first column was transferred into a sample loop that is mounted on a six-port valve. The other end of the sample loop was connected to vacuum. During operation, the sample loop was heated to 90°C with a heating tape pasted on the external surface. The combination of heat and vacuum helped in the quick evaporation of the normal phase solvent, resulting in the deposition

of the analytes on the inner walls of the sample loop. Finally the sample loop was flushed with the reverse phase solvent to desorb the analytes and to refocus them onto the reverse phase column. When the performance of this system was tested using 16 US EPA PAHs, very low recovery rates were observed for low boiling and thermally labile PAHs. It should be noted that both the techniques discussed above could be of limited use for comprehensive separation as the solvent evaporation requires a significant amount of time.

Dugo et al. [26] have developed a comprehensive 2D HPLC system by coupling a microbore supelcosil LC-SI column (normal phase mode; first dimension) to a C18 monolith column (reverse phase mode; second dimension) via a 10-port-2-position switching valve. The normal phase eluent was stored into two sample loops (20 μL capacity) connected to the switching valve and transferred alternatively onto the reverse phase column. The normal phase column was run in an isocratic mode with hexane/acetonitrile (75/25) at a flow rate of 20 μL/min while the reverse phase was operated in gradient mode with acetonitrile/water at a flow rate of 4 mL/min. Due to the use of acetonitrile, a common mobile phase in both dimensions, the solvent incompatibility issue was somewhat mitigated. Moreover, as only 20 μL of the normal phase eluent was transferred to the reverse phase mode in every cycle, band dispersion was not very significant. The technique was used to demonstrate the separation of oxygen heterocyclic components present in cold-pressed lemon oil samples. In an another method, Murahashi [27] first extracted the PAHs from gasoline using acetonitrile. The PAH extract was then analyzed using an online comprehensive LC-LC system

employing a pentabromobenzyl column in the first dimension and two C18 columns in the second dimension. Similar methods were also developed by other researchers for the analysis of brominated biphenyls, dioxins, alkyl benzenes, PAHs, and alkyl phenyl ketones from environmental samples [28].

In previous work, we have demonstrated that the analysis of alkyl PAHs using a liquid chromatographic technique can provide complimentary information to that obtained by standard GC-MS analysis [29]. The aim of the present work is to develop an off-line 2D HPLC method to achieve better quantification of the un-substituted and alkyl substituted PAHs present in the crude oil fractions. An oil fraction was subjected to normal phase fractionation using a semi-preparative silica column. Ninety-one normal phase fractions were collected using an automated fraction collector. After solvent exchange, all these fractions were then analyzed using the reverse phase HPLC – DAD technique. A method for the quantification of the PAHs was also developed. Finally, a comparison of the PAH concentrations obtained by this method with the GC-MS method was reported.

Materials and Methods

Alaskan North Slope Crude (ANSC) crude oil was fractionated into four fractions using low temperature fractional distillation at Dr. Zhendi Wang's lab at Environment Canada, Ottawa. The details of this fractionation procedure are reported elsewhere [30]. GC-MS analysis of the third fraction ("heavy gas oil"; boiling point range 287°C- 481°C) was done using a method reported earlier [14]. The GC-MS results showed the presence of a wide variety of 2-5 ring PAHs and

their alkyl homologues. Therefore, this fraction was subjected to 2D HPLC analysis in this work.

Table 5.1: List of PAH standards, their code names and log P values used in this study. To maintain uniformity, all calculated log P values were obtained from Scifinder Scholar program (Chemical Abstract Services, Columbus, OH)

Name of PAH	Code	Log P value
Naphthalene	C0 NAPH	3.45
2-methyl naphthalene	C1 NAPH	3.91
1,3-dimethyl naphthalene	C2 NAPH	4.37
2,3,5-trimethyl naphthalene	C3 NAPH	4.83
2,6-diethyl naphthalene	C4 NAPH	5.43
Dibenzothiophene	C0 DBT	4.38
4-methyl dibenzothiophene	C1 DBT	4.84
4,6-dimethyl dibenzothiophene	C2 DBT	5.30
4,6-diethyl dibenzothiophene	C4 DBT	6.37
Fluorene	C0 FLUOR	4.16
1-methyl fluorene	C1 FLUOR	4.62
1,8-dimethyl fluorene	C2 FLUOR	5.08
Phenanthrene	C0 PHEN	4.68
1-methyl phenanthrene	C1 PHEN	5.14
1,7-dimethyl phenanthrene	C2 PHEN	5.60
7-ethyl-1-methyl phenanthrene	C3 PHEN	6.13
7-isopropyl-1-methyl phenanthrene	C4 PHEN	6.48
Pyrene	C0 PYR	5.17
Triphenylene	C0 TRIPH	5.91
Chrysene	C0 CHRY	5.91
Acenaphthylene	Acl	4.26
Acenaphthene	Ace	4.18
Anthracene	An	4.68
Fluoranthene	Fl	5.17
Benzo[a]anthracene	BaA	5.91
Benzo[b]fluoranthene	BbF	6.40
Benzo[k]fluoranthene	BkF	6.40
Benzo[a]pyrene	BaP	6.40
Dibenzo[a,h]anthracene	DA	7.14
Benzo[g,h,i]perylene	BP	6.89
Indeno[1.2.3-cd]pyrene	IP	6.89

HPLC grade hexanes, methylene chloride and acetonitrile were procured from Fisher Scientific (Ottawa, ON). ACS certified grade acetone (Fisher) was used for wax precipitation. Doubly distilled water from an in-house distillation setup was used for HPLC. All un-substituted and alkyl substituted PAHs used in this study were purchased from Sigma Aldrich (Milwaukee, WI). They were >98% pure and used without further purification. Table 5.1 shows the list of the PAH standards and their log P values obtained from *Scifinder* (Chemical Abstract Service, Columbus, OH) software.

Normal Phase HPLC system: The waxes present in the heavy gas oil fraction were precipitated using a method described previously [29]. The cold acetone extract that contained most of the PAHs was then subjected to normal phase fractionation. PAH fractionation and analysis were carried out using a Varian HPLC system (Varian, Mississauga, ON), consisting of two pump modules (Prostar 215) and a UV absorbance detector (Prostar 330) operating at 254 nm. The fractionation was done on a semi-preparative silica column (Zorbax sil, 9.4 mm i.d. x 25 cm length; packed with silica particles of diameter 5 μm; Agilent, Mississauga, ON). For fractionation experiments, 200 μL of hexane solution containing 100 mg of cold acetone extract was injected onto the column. The PAHs were eluted using the mobile phase conditions given in Table 5.2. The column was regenerated by back-flushing with 100% methylene chloride to remove resins and other polar materials as indicated in Table 5.2. The eluent from the column was collected every minute using an automated fraction collector (Dynamax model FC-4, Varian). In total, 91 normal phase fractions were

collected. Column regeneration was ascertained by analyzing a PAH standard mixture immediately after every sample run and flushing further if retention times were not within a designated range.

Reverse phase HPLC analysis: All the fractions were transferred to pre-weighed vials and 5 mL of acetonitrile was added, concentrated to 1.00 mL and analyzed using reverse phase HPLC. Reverse phase HPLC analyses were performed using a Waters HPLC system consisting of Waters 2695 separation module, autosampler, and a Waters 2996 photodiode array detector (Waters Corporation, USA). The PAHs were separated on an Eclipse PAH column (4.6 mm X 25 cm; 5 micron particles; Agilent) using an acetonitrile/water mobile phase gradient shown in Table 5.3. The reverse phase column was kindly donated by Dr. Faizy Ahamed, Agilent Technologies, Wilmington, DE.

Table 5.2: Optimized mobile phase conditions for the fractionation of PAHs present in the ANS crude oil fraction. The fractionation was done using a semi-preparative normal phase HPLC column (Zorbax sil, 9.4 mm i.d. x 25 cm length; packed with silica particles of diameter 5 micron)

| Time (min)	Operation mode	Mobile phase composition	Flow rate (mL/min)
0	Normal	98% hexane/2% methylene chloride	1.5
80	Normal	98% hexane/2% methylene chloride	1.5
Column regeneration			
85	Backflush	100% methylene chloride	7
125	Backflush	100% methylene chloride	7
130	Backflush	98% hexane/2% methylene chloride	7
160	Backflush	98% hexane/2% methylene chloride	7
165	Equlibrate	98% hexane/2% methylene chloride	1.5
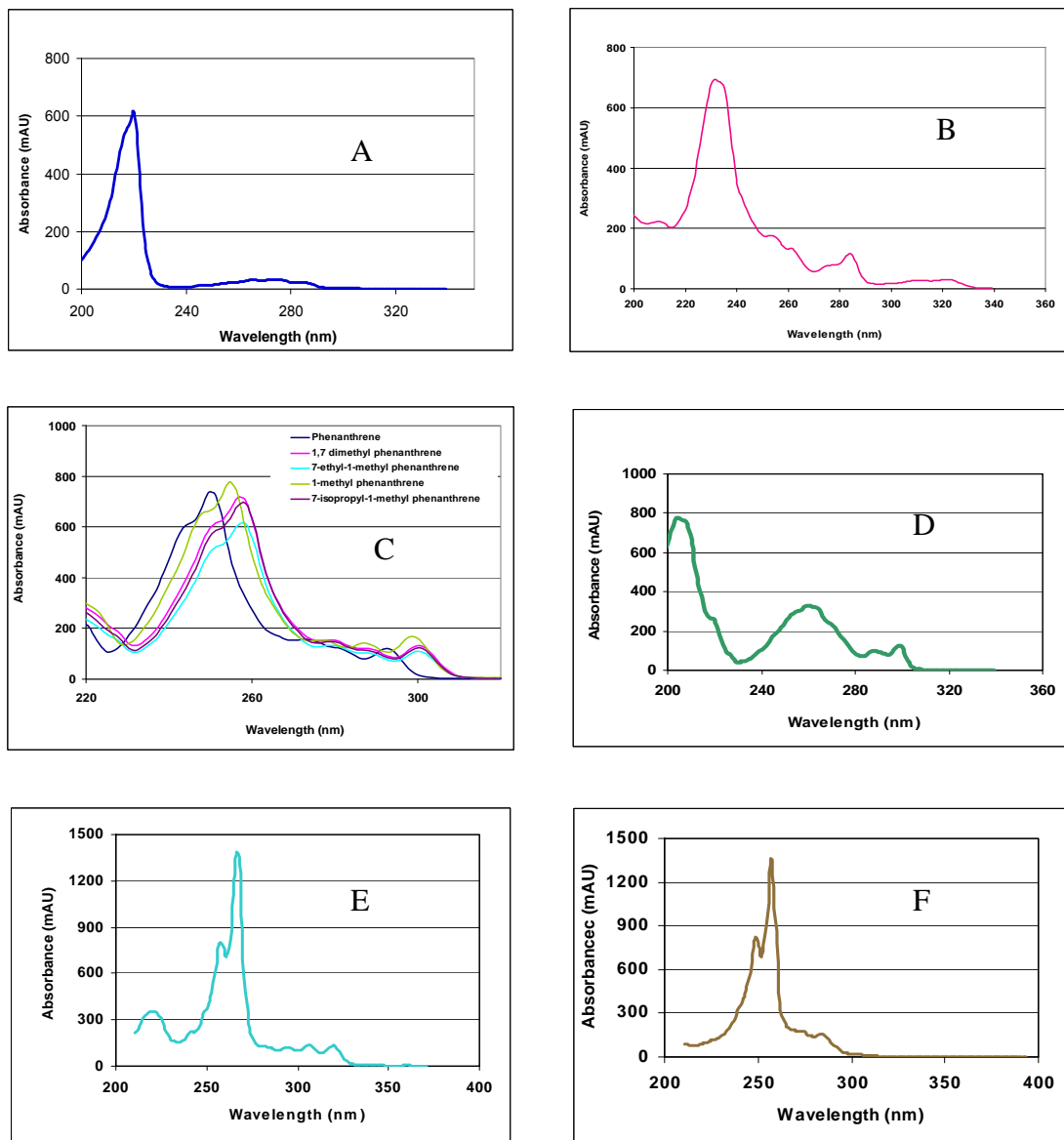
Figure 5.1: UV absorbance spectra of PAHs studied in this work. A: Naphthalene; B: Dibenzothiophene; C: Phenanthrene; D: Fluorene; E: Chrysene; F: Triphenylene. Alkyl substitutions on the ring do not significantly alter the spectral profile as illustrated for a number of alkyl phenanthrenes (C).

Table 5.3: Optimized reverse phase mobile phase condition for the analysis of alkyl PAHs. PAHs were separated on a Eclipse PAH column (4.6 mm X 25 cm; 5 micron particles). The mobile phase flow rate was maintained at 0.7 mL/min.

Time	% Acetonitrile	% Water
0.00	60	40
20.00	60	40
40.00	80	20
50.00	100	0
70.00	100	0

Table 5.4: Linear regression equation used for the quantification of PAHs in crude oil fractions. Regression equations used injection of PAH amounts in the range of 20 – 5000 ng. Limit of quantification (LOQ) was determined by repeated injection (50 µL, n = 3) of an amount close to the LOQ and estimating the amount to give S/N = 10.

PAH identity	Quantification wavelength	Linear regression parameters			LOQ (ng)
		Slope (peak area/ng)	Intercept (peak area)	r^2	
C_0 Naphthalene	215 nm	39589	151720	>0.999	<12
C_1 Naphthalene	215 nm	26118	206940	>0.999	<12
C_2 Naphthalene	215 nm	16842	190067	>0.999	<12
C_3 Naphthalene	215 nm	14655	191571	>0.999	<12
C_4 Naphthalene	215 nm	17821	56125	>0.999	<12
C_0 Dibenzothiophene	320 nm	1013	-4095	>0.999	<50
C_1 Dibenzothiophene	320 nm	1093	-7486	>0.999	<50
C_2 Dibenzothiophene	320 nm	1066	-4222	>0.999	<50
C_4 Dibenzothiophene	320 nm	922	-3749	>0.999	<50
C_0 Fluorene	254 nm	8118	-33708	>0.999	<12
C_1 Fluorene	254 nm	7268	-24301	>0.999	<12
C_2 Fluorene	254 nm	3676	-11953	>0.999	<12
C_0 Phenanthrene	254 nm	21531	40671	>0.999	<12
C_1 Phenanthrene	254 nm	17584	42221	>0.999	<12
C_2 Phenanthrene	254 nm	28108	475195	>0.999	<12
C_3 Phenanthrene	254 nm	11210	125344	>0.999	<12
C_4 Phenanthrene	254 nm	14206	310106	>0.999	<12
C0 Chrysene	254 nm	29830	37447	>0.999	<2
C0 Triphenylene	254 nm	16098	64944	>0.999	<2

PAH quantification: PAHs and their alkyl homologues were quantified using an external calibration method. An eight-point calibration curve was developed for each un-substituted and alkyl PAH standard in the range of 5000 ng to 2 ng. Table 5.4 shows the linear regression equations for the analyzed PAHs. The limit of quantification (LOQ) estimate was calculated at ten times the signal-to-noise ratio for the lowest concentration standards.

Results and discussion

Precise identification and quantification of alkyl PAHs in crude oil finds wide applications both in oil exploration as well as in oil spill investigations. However, several alkyl PAHs are not well resolved in standard chromatographic techniques and hence methods based on multi-dimensional chromatography are developed for their analysis in crude oils. Also, only a very limited number of alkyl PAH standards are commercially available. Therefore, identification of alkyl PAHs in a complex mixture solely based on their chromatographic retention time is problematic. Many alkyl PAHs belonging to different PAH classes have identical molecular weight and fragmentation patterns (e.g. methyl chrysenes and methyl triphenylenes) and hence are difficult to distinguish based on MS detection in the absence of a standard. HPLC-DAD techniques were developed in our group is found to mitigate some of these problems [29]. As shown in Figure 5.1 different classes of PAHs exhibit unique spectral futures in the UV region. Moreover the alkyl substitution on the ring does not affect the UV spectral characteristic of the PAH significantly. Thus the DAD spectrum of alkyl PAHs can be used to differentiate PAH classes in crude oil. On a reverse phase column, the

chromatographic retention of alkyl PAHs increases with an increase in the number of alkyl carbons (explained below). Hence the reverse phase retention indices can be used to assign the alkyl carbon numbers. Therefore, ring-type fractionation on a normal phase column followed by a detailed alkyl PAH analysis of these sub-fractions using HPLC-DAD technique can be a powerful tool for the identification and quantification of different classes of alkyl PAHs present in crude oil.
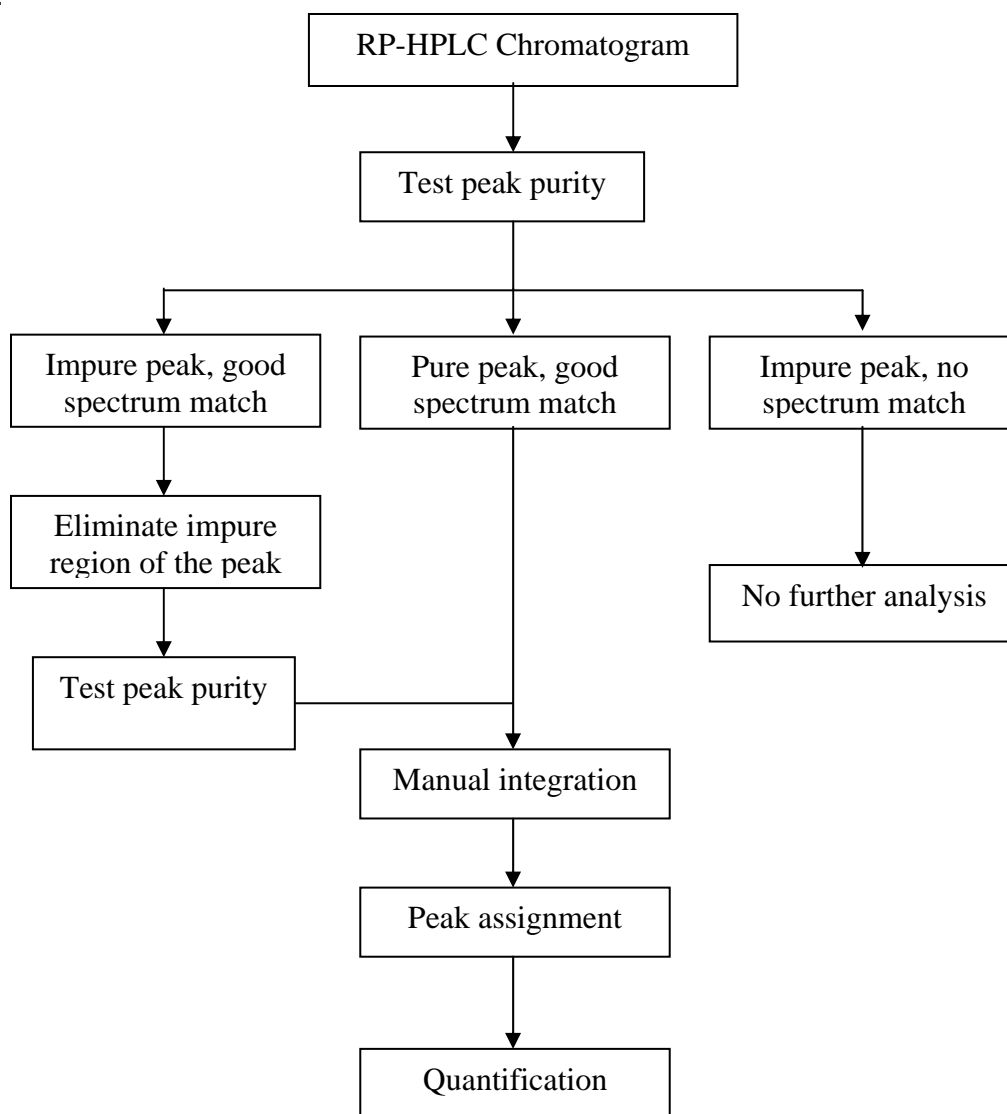
```
                    ┌─────────────────────────┐
                    │   RP-HPLC Chromatogram  │
                    └───────────┬─────────────┘
                                │
                    ┌───────────┴─────────────┐
                    │    Test peak purity     │
                    └───────────┬─────────────┘
            ┌───────────────────┼───────────────────┐
            │                   │                   │
    ┌───────┴────────┐  ┌───────┴───────┐  ┌────────┴───────┐
    │ Impure peak,   │  │  Pure peak,   │  │ Impure peak,   │
    │ good spectrum  │  │ good spectrum │  │ no spectrum    │
    │    match       │  │    match      │  │    match       │
    └───────┬────────┘  └───────┬───────┘  └────────┬───────┘
            │                   │                   │
    ┌───────┴────────┐          │          ┌────────┴───────┐
    │ Eliminate      │          │          │ No further     │
    │ impure region  │          │          │ analysis       │
    │ of the peak    │          │          └────────────────┘
    └───────┬────────┘          │
            │                   │
    ┌───────┴────────┐          │
    │ Test peak      ├──────────┤
    │ purity         │          │
    └────────────────┘          │
                        ┌───────┴───────┐
                        │ Manual        │
                        │ integration   │
                        └───────┬───────┘
                        ┌───────┴───────┐
                        │ Peak          │
                        │ assignment    │
                        └───────┬───────┘
                        ┌───────┴───────┐
                        │ Quantification│
                        └───────────────┘
```

Figure 5.2: Protocol for the analysis of alkyl PAH chromatographic peaks present in the oil samples based on their diode array spectral data

Diode array data analysis: The HPLC-DAD data analysis was done using Empower Professional PDA software (Waters Corporation). Figure 5.2 shows the schematic of the data analysis protocol used in this work.

- First, the peak purity of the given chromatographic peak was ascertained by comparing at least 5 DAD spectra obtained at different locations across the chromatographic peak. An built-in function in Empower Pro Software (Waters Corporation) determined the peak purity. This method compares each DAD spectrum against the apex spectrum of the chromatographic peak. Based on this, the purity angle is calculated. These purity angle values are compared to the purity threshold values obtained based on the background noise in the chromatogram. If the purity angle is less than the purity threshold, the peak is considered to be homogeneous.

- Second, the chromatographic peaks present in the given chromatogram were classified into (a). pure peaks with good spectral match; (b). impure peaks with good spectral match; (c). impure peaks with no spectral match. It was found that more than 70% of the total peak area of all chromatograms fell within the first two categories.

- Third, the peaks that fall under category (b) were further analyzed to ascertain the impure region. After eliminating the impure region of the peak, the peak purity test was repeated. The peaks that cleared the peak purity testing were carried on to the next stage of processing.

- Fourth, the peaks were classified into different PAH classes based on their DAD spectra.

- Finally, the alkyl carbon numbers were assigned based on the retention time of the chromatographic peak. The octanol/water partition coefficient of alkyl PAHs increases with an increase of number of alkyl carbons and retention of the solute increases with an increase in its log P value. Hence we have measured the retention time of several alkyl PAH standards in the RP-HPLC-DAD method. Then by using the calculated log P values of these standards a plot of log P vs log retention factor was developed. The log retention factor of alkyl PAHs were found to increase linearly with log P value with a regression formula *logP = 6.0263 X log (retention factor) – 1.5688* with an *r^2* value of *0.9765* (Figure 5.3). Based on this, retention time windows were generated for the assignment of alkyl PAH carbon numbers for different PAH classes and depicted in Table 5.5.
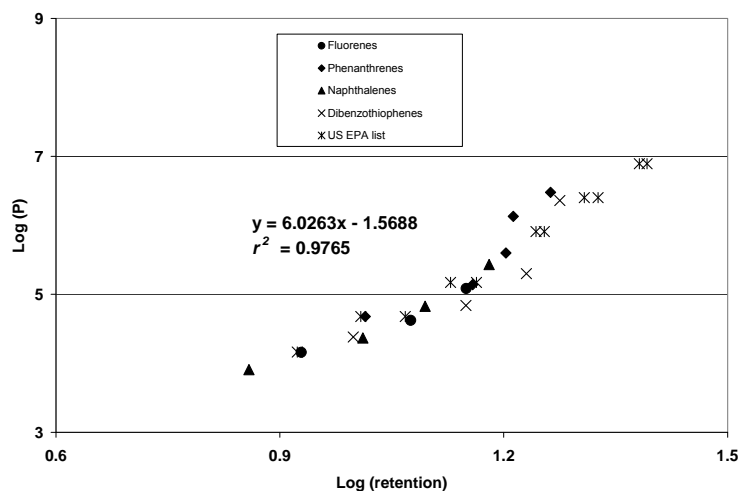

Figure 5.3: Correlation between the chromatographic retention and the log P values of the alkyl PAH standards used in this study. The alkyl PAHs were analyzed using Eclipse PAH column using an acetonitrile/water mobile phase gradient shown in Table 5.3.

189

Table 5.5: Retention time windows used for the assignment of alkyl carbon number for chromatographic peaks in different PAH classes. Retention time windows are based on the elution of the alkyl PAH standards as well as the log P relationship shown in Figure 5.3. Please refer to Table 5.1 for PAH class nomenclature.

| PAH class	Retention time window (min.)
CO NAP	13.9 – 14.6
C1 NAP	14.7 – 22.0
C2 NAP	22.1 – 30.0
C3 NAP	30.1 – 37.1
C4 NAP	37.2 – 44.6
C0 DBT	29.6 – 30.0
C1 DBT	30.1 – 35.0
C2 DBT	35.1 – 42.0
C3 DBT	42.1 – 50.0
C4 DBT	50.1 – 60.0
C0 FLUOR	25.6 – 26.0
C1 FLUOR	26.1 – 35.0
C2 FLUOR	35.1 – 44.5
C3 FLUOR	44.6 – 51.0
C0 PHEN	30.3 – 30.8
C1 PHEN	30.9 – 38.0
C2 PHEN	38.1 – 48.5
C3 PHEN	48.6 – 51.8
C4 PHEN	51.9 – 57.1
C0 TRIPH	45.4 – 45.9
C0 CHRY	50.3 – 50.9
C1 CHRY/C1 TRIPH	51.0 – 58.0
C2 CHRY/C2 TRIPH	58.1 – 71.0
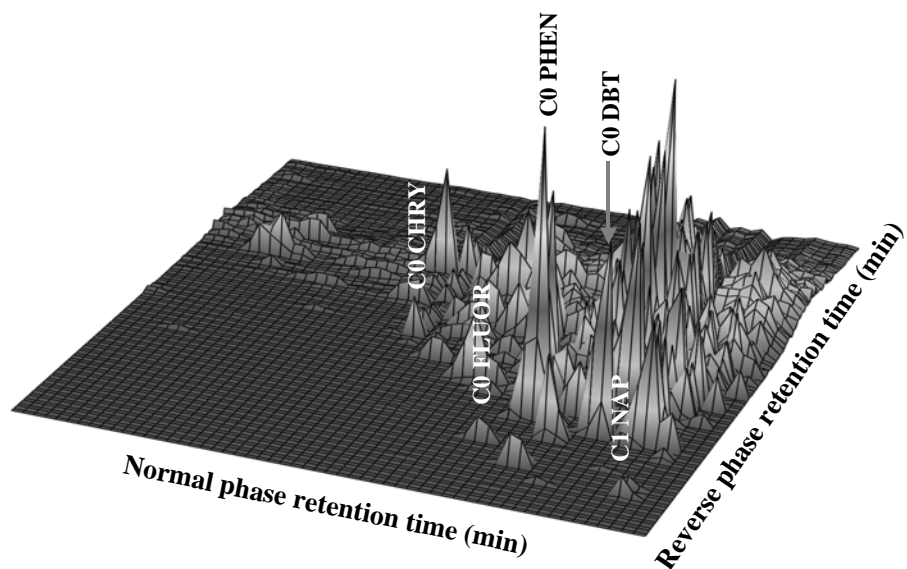
Figure 5.4: 3D chromatogram of the alkyl PAHs present in the heavy gas oil fraction. The graph displays the analysis of normal phase fractions eluted between 20 and 75 minutes. The reverse phase axis extends from 20 to 70 min. The reverse phase elution parameters are shown in Table 5.3. The retention time markers used for the normal phase fractionation are indicated.

Development of 3D surface: The main objective of this work is to characterize un-substituted and alkyl substituted PAHs present in the crude oil fractions. The crude oil fraction was first fractionated into 91 fractions using normal phase HPLC (first dimension) followed by the analysis of these fractions in RP-HPLC coupled to DAD detection (second dimension). All these data were used to construct a 3D surface (Figure 5.4 using Sigma Plot software) in which the reverse phase and normal phase retention times are plotted on the *x* and *y*- axis respectively, and the total UV absorbance (integrated over 200 nm to 400 nm) is plotted on the z-axis. The plot also highlights the retention time markers that were used during the normal phase fractionation. Orthogonal separation achieved in this work resulted in a higher peak capacity of the 3D surface. Thus, using the current method about 450 PAH peaks were resolved and quantified.

The residual saturates present in the fractions eluted before 1-methyl naphthalene standard. As saturates do not absorb in the UV region (200 – 400 nm), fractions 1-20 were not further analyzed using the reverse phase method. Analysis of back-flush fractions (fraction 85-91) in the RP-HPLC-DAD method showed a large unresolved hump. The hump was characterized by several small peaks with complex DAD spectra that did not match with any of the known PAHs in our library. Therefore, in this work we focused our attention on the analysis of fraction from 21 to 84.

To extract information about the alkyl PAH distribution among various normal phase fractions, a contour plot of the 3D surface was constructed (Figure 5.5). To

improve clarity, the contour plot used absorbance values at 254 nm. The contour

plot represents the aerial view of the 3D surface, and hence each peak in the 3D

surface is represented by a contour maximum. As the alkyl PAH isomers have

very close retention times, the PAH peaks appear in clusters throughout the

contour plot. PAHs are separated based on the number of rings in the normal

phase and in the reverse phase they are separated based on their alkyl

substitution. Hence, in the contour plot, the PAHs are arranged both based on

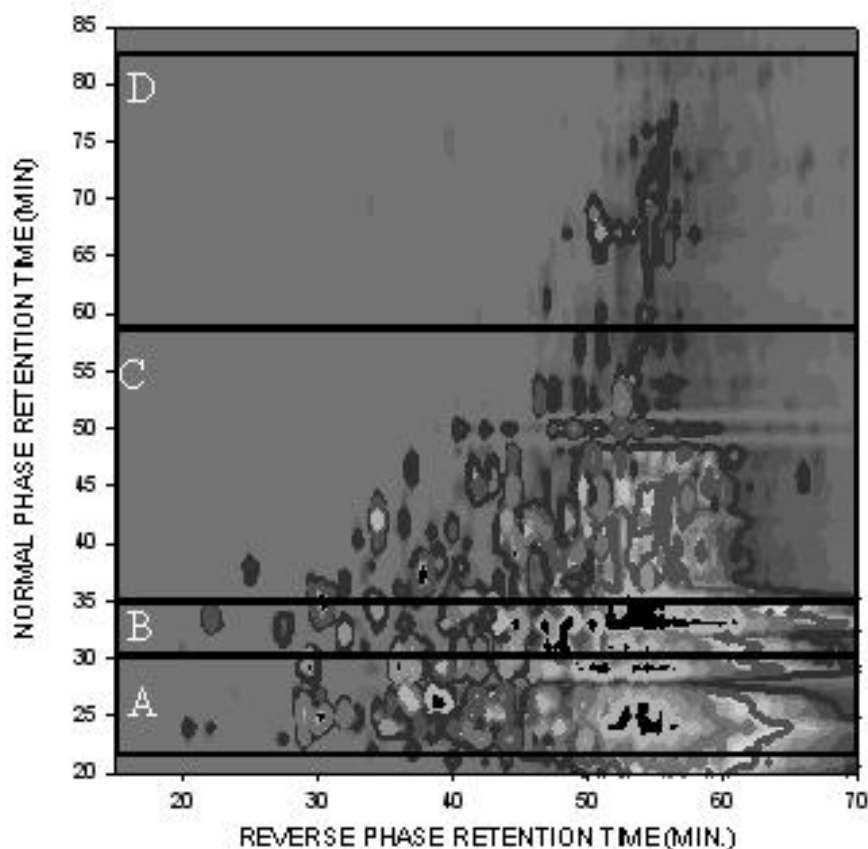the number of rings as well as their alkyl substitution.

Figure 5.5: Contour plot of the 3D data shown in Figure 5.3. Alkyl PAHs belonging to different PAH classes are marked as follows: A: Naphthalenes; B:

Dibenzothiophenes; C: Phenanthrenes and fluorenes; D: Chrysenes and triphenylenes.
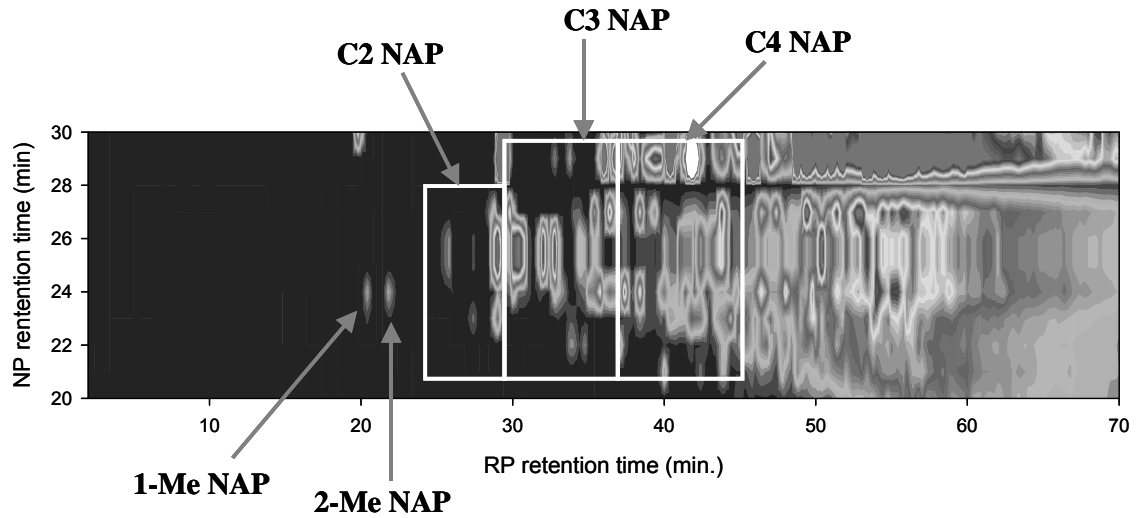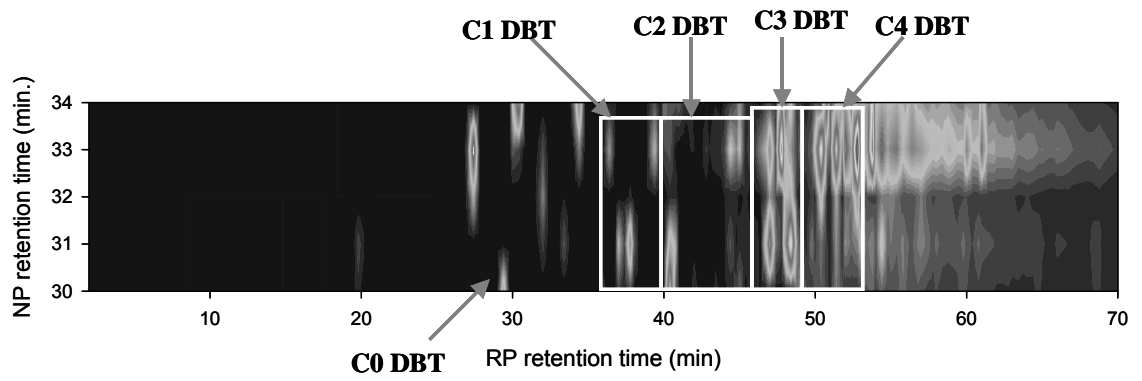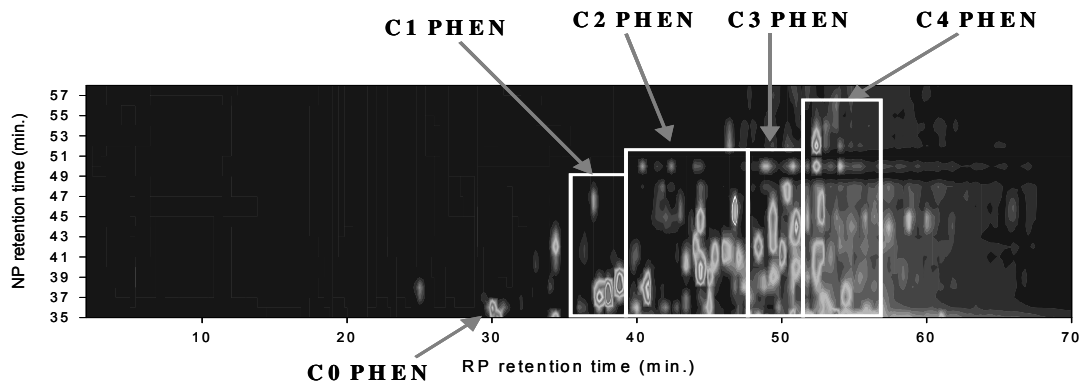

Figure 5.6a
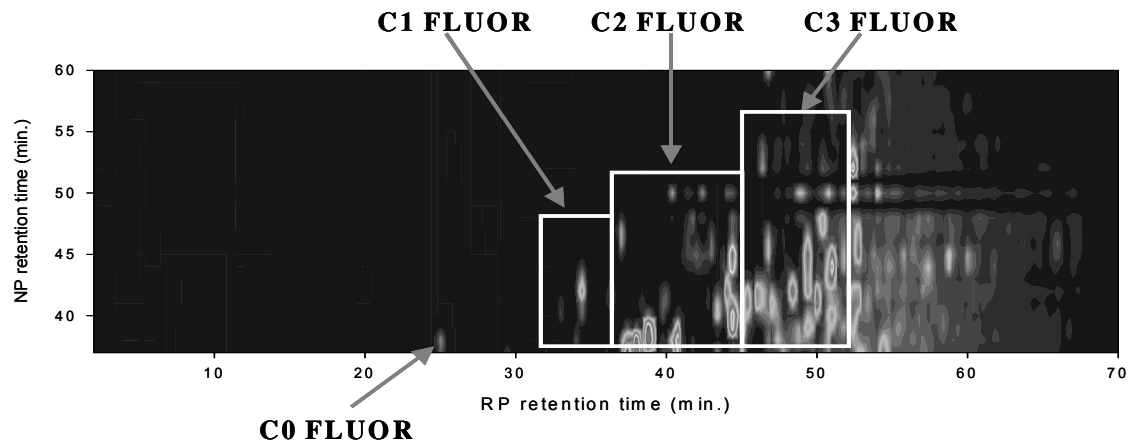

Figure 5.6b
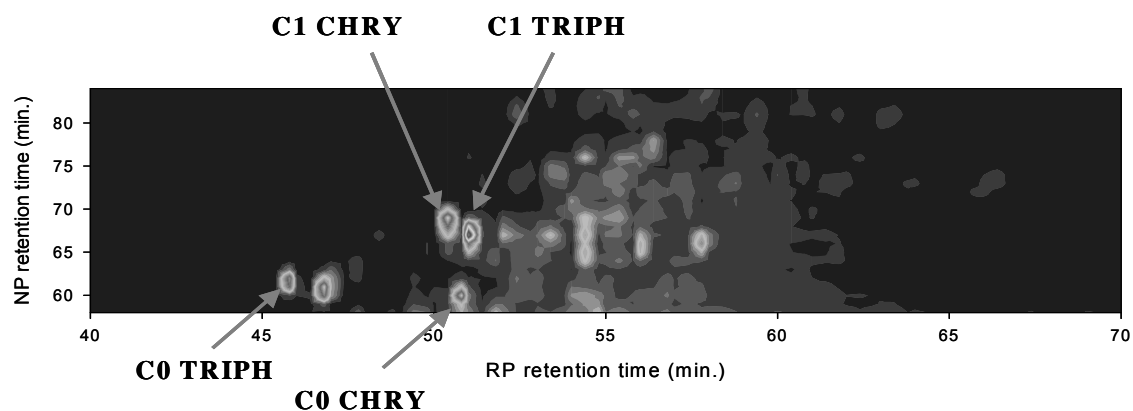

Figure 5.6c

Figure 5.6d

Figure 5.6e

Figure 5.6: Analysis of contour plot. The contour plot was divided into five segments for the detailed analysis of alkyl PAHs present in the following PAH classes: (a). Naphthalenes; (b). Dibenzothiophenes; (C). Phenanthrenes; (D). Fluorenes; (E). Chrysenes and triphenylenes

To clarify contour analysis, the entire contour plot was divided into five segments such that each segment represents the elution of alkyl PAHs with a specific number of benzene rings. In Figure 5.6a-e, each segment is expanded to reveal the elution of different alkyl PAH isomers within a PAH class. The figure also indicates the elution of different alkyl PAH isomers (C1 to C4).

Table 5.6: Analysis of methyl isomers found in the crude oil fraction using RP-HPLC-DAD technique

PAH Class	Methyl standard used	No. of possible isomers	No. of peaks detected	Detection of methyl standard used
Naphthalenes	2-Me Naph	2	2	Yes
phenanthrenes	1-Me Phen	5	5	No
dibenzothiophenes	4-Me DBT	4	3	Yes
Fluorenes	1-Me Fluor	5	3	Yes

For PAHs, the total number of theoretically possible alkyl isomers increases both with the number of benzene rings as well as with the number of alkyl carbon. For example, progressive alkyl substitution in naphthalene can give 2 C1 naphthalenes (methyl naphthalenes), 12 C2 naphthalenes (10 dimethyl naphthalenes + 2 ethyl naphthalenes), 32 C3 naphthalenes (18 trimethyl naphthalenes + 10 ethyl- methyl naphthalenes + 2 propyl naphthalenes + 2 isopropyl naphthalenes), and > 100 C4 naphthalenes. Table 5.6 shows the number of possible methyl isomers of different PAHs, together with the number of methyl PAH peaks observed in the current study. In the case of naphthalenes

both methyl isomers were identified positively based on the retention time of the authentic standard. There were four peaks observed in the C1 DBT time window out of which 4-methyl DBT was identified positively based on the retention time of the pure standard. Similarly, among the 3 observed methyl fluorene peaks, 1-methyl fluorene was positively identified. In the case of methyl phenanthrenes, there were five peak observed in the C1 retention window. However, none of these peaks eluted at the retention time of 1-methyl phenanthrene. Previously we had observed the presence of 1-methyl phenanthrene in ANSC 31 using the chromatographic method discussed in Chapter 4. Therefore, we believe that the matrix effects and the chromatographic conditions applied in this work might be responsible for the observed retention time differences between the standard and the sample chromatographic runs. Alternatively, This might indicate that one of the C1 phenanthrene peaks could possibly be a C2 phenanthrene isomer. One way to evaluate matrix effects would be to use the standard addition method. However, in the current work we did not explore this possibility.

Analysis of chrysenes and triphenylenes: Both triphenylene and chrysene are four ring PAHs that are abundant in crude oils. However, due to their identical molecular weight, alkyl isomers of these two classes could not be differentiated using GC-MS methods. The UV spectra of these compounds are very different (Figure 5.1) and hence it is possible to differentiate these using the DAD detector. The UV spectrum of chrysene shows a sharp absorption band at 267 nm with a shoulder around 258 nm. It also contains smaller absorption bands at 220 nm, 307 nm and 320 nm. The triphenlyene UV spectrum shows only one

strong band at 257 nm with a shoulder at 249 nm. Moreover, like other PAH classes, the UV spectra of alkyl substituted triphenylenes and chrysenes are expected to be resemble the un-substituted compounds. Therefore, with the current method we could differentiate the alkyl triphenylene isomers from alkyl chrysenes easily. Figure 5.6e shows the expanded view of the chrysene region of the contour plot. It should be noted that both triphenylene and chrysene eluted in the same fraction during the normal phase fractionation. However, as the triphenylene molecule is non-planar, it eluted before chrysene on the reverse phase column. As no alkyl triphenylene standards were commercially available, the alkyl triphenylene peak cluster at 51.00 min. was assigned as methyl triphenylene isomers based on the calculated log P value.

Chrysenes offers a unique case among the analyzed PAH classes as some of the methyl chrysene isomers have been shown to elute earlier than chrysene [31]. Under the reverse phase condition used in this study, C0 chrysene eluted at 50.72 minutes. However as shown in Figure 5.6e, two peak clusters at 50.74 minutes and 50.35 minutes were observed in the contour plot that exhibit DAD spectral characteristic of chrysenes. As these two clusters eluted in different normal phase time windows, these peaks are different chrysene isomers. C0 chrysene elutes in fractions 58 to 60, so the peak cluster at 50.74 minute is assigned as C0 chrysene. Wise et al. have analyzed the chromatographic retention behavior of methyl isomers of several PAHs in detail [31]. The retention of methyl PAHs on reverse phase column depends on several factors including their shape and planarity. As the some of the methyl isomers of chrysene (such

as 5-methyl chrysene and 6-methyl chrysene) are non-planar, these compounds were found to elute before C0 chrysene in polymeric C18 columns [31]. Hence the peak cluster at 50.35 minute eluting in fractions 66 - 70 is probably one or more C1 chrysene isomers. It should be noted that if the C0 chrysene and methyl chrysene isomers were in a single fraction, these compounds could co-elute on the reverse phase column leading to false identification and quantification. Moreover, unlike other PAH classes, the normal phase HPLC gave a better separation between un-substituted and alkyl substituted chrysene isomers than the reverse phase HPLC.
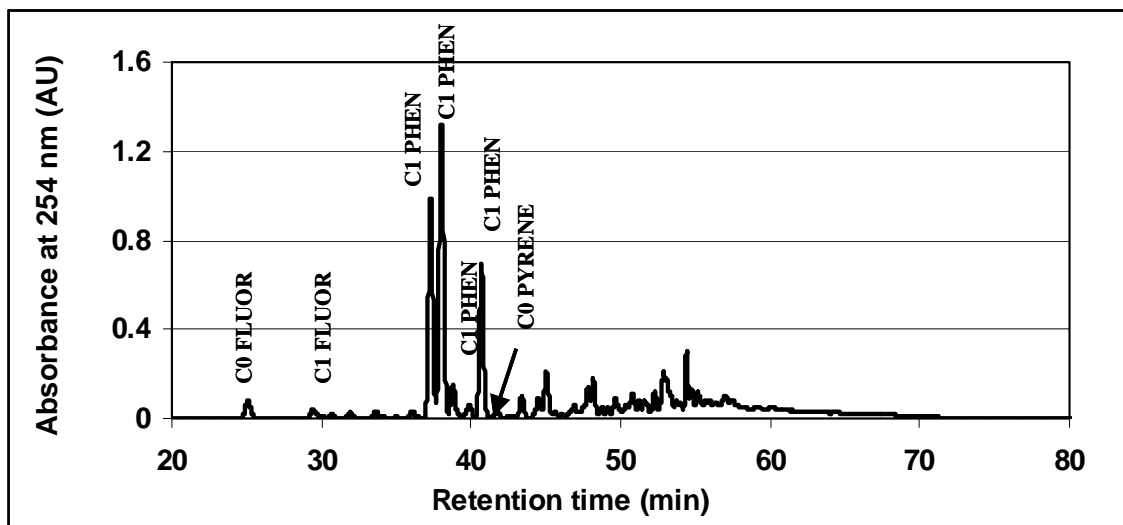

Figure 5.6a: Analysis of C0 pyrene in the normal phase fraction 37 using RP-HPLC-DAD technique. The sample was analyzed on a Eclipse PAH column using mobile phase gradient shown in Table 5.3.
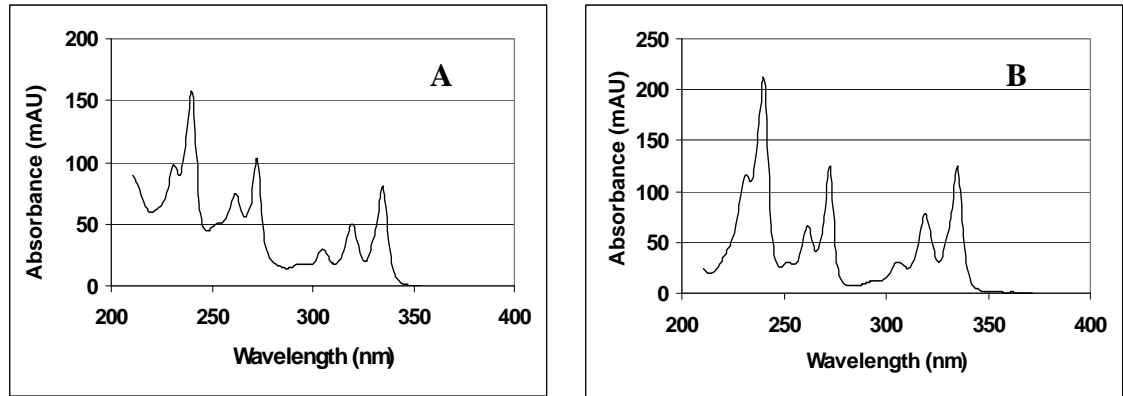
199

Figure 5.6b: (A). DAD spectrum observed in the C0 pyrene peak in fraction 37 chromatogram (Figure 5.6a); (B). The DAD spectra of the pure C0 pyrene standard.
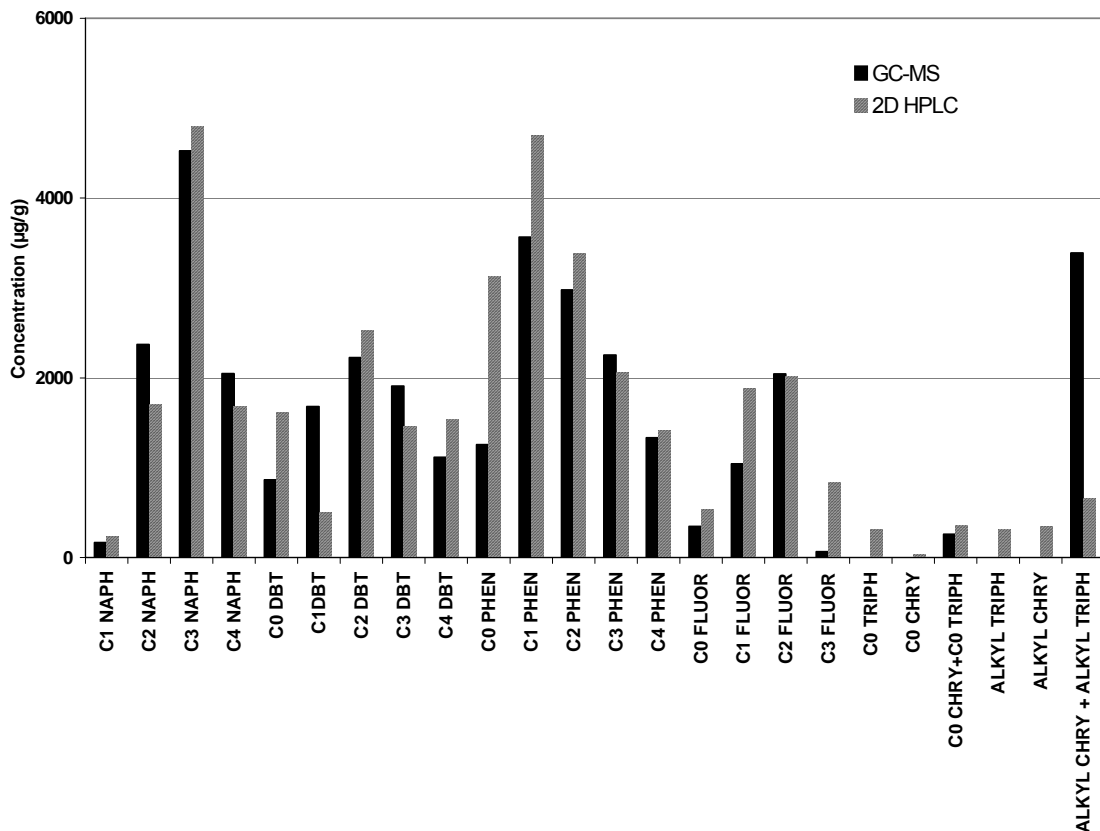

Figure 5.7: Comparison of the concentrations of alkyl PAHs present in the heavy gas oil fraction using 2D HPLC and GC-MS methods.

Table 5.7: Concentration of alkyl PAHs present in various normal phase fractions measured by RP-HPLC-DAD technique. The quantification was done using the calibration equations shown in Table 5.4.

PAH class	Concentration in ANSC 31 (μg/g)
C1 NAPH	230
C2 NAPH	1706
C3 NAPH	4801
C4 NAPH	1680
C0 DBT	1612
C1DBT	501
C2 DBT	2523
C3 DBT	1458
C4 DBT	1539
C0 PHEN	3126
C1 PHEN	4700
C2 PHEN	3384
C3 PHEN	2056
C4 PHEN	1413
C0 FLUOR	538
C1 FLUOR	1879
C2 FLUOR	2014
C3 FLUOR	831
C0 TRIPH	314
C0 CHRY	40
ALKYL TRIPH	354
ALKYL CHRY	313

Detection of trace components: Pyrene and alkyl pyrene isomers are present only in trace levels in ANSC and hence their detection using the DAD is very difficult. They would be better identified and quantified using a mass spectrometric or fluorescence detector. However, the multi-dimensional chromatographic approach allowed us to isolate and concentrate pyrene and alkyl pyrenes and helped to identify these using the DAD detector. Figure 5.6a shows the analysis of fraction 37 using the method developed in this work. For simplicity, only major peaks were labeled in the chromatogram. Figure 5.6b shows the DAD spectrum of the peak at 41.60 minutes and the C0 pyrene library spectrum. Due to the near perfect matching, this peak was assigned as C0 pyrene. Similarly, C1 and C2 pyrene isomers were identified in fractions 38-40 and 40-43 respectively. However, these compounds are not quantified in this work. As the alkyl pyrene peaks are very small relative to phenanthrenes, their signal might have been lost in the background if normal phase fractionation was not done.

PAH quantification: Table 5.7 shows the concentration of PAHs present in the ANSC 31 fraction measured using the current method. Peak areas were converted to the amounts of PAH by using corresponding alkyl PAH calibration curves (Table 5.4). As C3 fluorene and C3 DBT standards were not available, the calibration curves of respective C2 isomers were used for their quantification. For the quantification of alkyl triphenylene and alkyl chrysenes, C0 triphenylene and C0 chrysene calibration curves were used respectively. Interestingly we found that the total concentration of C0 triphenylene was much higher than that of C0

chrysene. Finally, we compared the concentrations of alkyl PAHs found in this study with that of the GC-MS results (Figure 5.7). In general, we found good agreement between the methods for all the target analytes. However, our method has over estimated the concentrations of C0 PHEN and C0 DBT and underestimated the concentration of total alkyl chrysenes relative to the GC-MS results. Such variations in the observed concentrations are expected owing to the differences in the chromatographic and analysis conditions employed in these two methods.

Conclusion

The multi-dimensional chromatographic approach developed in this work was found to be very useful for the identification and quantification of PAHs present in crude oil samples. As most oil spill investigation work relies on the comparison of a PAH profile from the spilled site to that of a source oil, PAH contour plot such as those developed in this work could find useful application in oil spill investigation.

References

1.   Ajienka, J.A. and C.U. Ikoku, *Waxy Crude Oil Handling in Nigeria: Practices, Problems, and Prospects.* Energy Sources, Part A: Recovery, Utilization, and Environmental Effects, 1990. **12**(4): p. 463 - 478.

2.   Agrawal, K.M., H.U. Khan, M. Surianarayanan and G.C. Joshi, *Wax deposition of Bombay high crude oil under flowing conditions.* Fuel, 1990. **69**(6): p. 794-796.

3.   Fan, T. and J.S. Buckley, *Rapid and Accurate SARA Analysis of Medium Gravity Crude Oils.* Energy Fuels, 2002. **16**(6): p. 1571-1575.

4.   Sharma, B.K., S.L.S. Sarowha, S.D. Bhagat, R.K. Tiwari, S.K. Gupta and P.S. Venkataramani, *Hydrocarbon group type analysis of petroleum heavy fractions using the TLC-FID technique.* Fresenius' Journal of Analytical Chemistry, 1998. **360**(5): p. 539-544.

5.   Rudzinski, W.E., T.M. Aminabhavi, S. Sassman and L.M. Watkins, *Isolation and Characterization of the Saturate and Aromatic Fractions of a Maya Crude Oil.* Energy Fuels, 2000. **14**(4): p. 839-844.

6.   Barman, B.N., V.L. Cebolla and L. Membrado, *Chromatographic techniques for petroleum and related products.* Critical Reviews in Analytical Chemistry, 2000. **30**(2-3): p. 75-120.

7.   Islas-Flores, C.A., E. Buenrostro-Gonzalez and C. Lira-Galeana, *Comparison between open column chromatography and HPLC SARA fractionations in Petroleum.* Energy & Fuels, 2005. **19**: p. 2080-2088.

8.   Kaminski, M., R. Kartanowicz, E. Gilgenast and J. Namiesnik, *High-Performance Liquid Chromatography in Group-Type Separation and Technical or Process Analytics of Petroleum Products.* Critical Reviews in Analytical Chemistry, 2005. **35**(3): p. 193-216.

9.   Radke, M., P. Garrigues and H. Willsch, *Methylated dicyclic and tricyclic aromatic hydrocarbons in crude oils from the Handil field, Indonesia.* Organic Geochemistry, 1990. **15**(1): p. 17-34.

10.   Radke, M., S.P. Vriend and R.G. Schaefer, *Geochemical characterization of Lower Toarcian source rocks from NW Germany: Interpretation of aromatic and saturated hydrocarbons in relation to depositional environment and maturation effects.* Journal of Petroleum Geology, 2001. **24**(3): p. 287-307.

11.   Barron, M.G., M.G. Carls, R. Heintz and S.D. Rice, *Evaluation of Fish Early Life-Stage Toxicity Models of Chronic Embryonic Exposures to*

Complex Polycyclic Aromatic Hydrocarbon Mixtures. Toxicol. Sci., 2004. **78**(1): p. 60-67.

12.   Wang, Z., M. Fingas and D.S. Page, *Oil spill identification.* Journal of Chromatography A, 1999. **843**(1-2): p. 369-411.

13.   Wang, Z., M. Fingas and K. Li, *Fractionation of a light crude oil and identification and quantitation of aliphatic, aromatic, and biomarker compounds by GC-FID and GC-MS, Part II.* Journal of Chromatographic Science, 1994. **32**(9): p. 367-382.

14.   Wang, Z., M. Fingas and K. Li, *Fractionation of a light crude oil and identification and quantitation of aliphatic, aromatic and biomarker compounds by GC-FID and GC-MS, Part I.* Journal of Chromatographic Science, 1994. **32**: p. 361-366.

15.   Frysinger, G.S. and R.B. Gaines, *Comprehensive Two-Dimensional Gas Chromatography with Mass Spectrometric Detection (GC × GC/MS) Applied to the Analysis of Petroleum.* Journal of High Resolution Chromatography, 1999. **22**(5): p. 251-255.

16.   Beens, J. and U.A.T. Brinkman, *Comprehensive two-dimensional gas chromatography-a powerful and versatile technique.* The Analyst, 2005. **130**(2): p. 123-127.

17.   Gaines, R.B., G.S. Frysinger, M.S. Hendrick-Smith and J.D. Stuart, *Oil Spill Source Identification by Comprehensive Two-Dimensional Gas Chromatography.* Environmental Science & Technology, 1999. **33**(12): p. 2106-2112.

18.   Frysinger, G.S., R.B. Gaines and E. B. Ledford Jr., *Quantitative Determination of BTEX and Total Aromatic Compounds in Gasoline by Comprehensive Two-Dimensional Gas Chromatography (GC×GC).* Journal of High Resolution Chromatography, 1999. **22**(4): p. 195-200.

19.   Frysinger, G.S. and R.B. Gaines, *Separation and identification of petroleum biomarkers by comprehensive two-dimensional gas chromatography.* Journal of Separation Science, 2001. **24**(2): p. 87-96.

20.   de Koning, S., H.-G. Janssen and U.A.T. Brinkman, *Group-type characterisation of mineral oil samples by two-dimensional comprehensive normal-phase liquid chromatography-gas chromatography with time-of-flight mass spectrometric detection.* Journal of Chromatography A, 2004. **1058**(1-2): p. 217-221.

21.   Dugo, P., F. Cacciola, T. Kumm, G. Dugo and L. Mondello, *Comprehensive multidimensional liquid chromatography: Theory and applications.* Journal of Chromatography A, 2007: p. In press.

22. Kimura, H., T. Tanigawa, H. Morisaka, T. Ikegami, K. Hosoya, N. Ishizuka, H. Minakuchi, K. Nakanishi, M. Ueda, K. Cabrera, and N. Tanaka, *Simple 2D-HPLC using a monolithic silica column for peptide separation.* Journal of Separation Science, 2004. **27**(10-11): p. 897-904.

23. Stroink, T., M.C. Ortiz, A. Bult, H. Lingeman, G.J. de Jong and W.J.M. Underberg, *On-line multidimensional liquid chromatography and capillary electrophoresis systems for peptides and proteins.* Journal of Chromatography B, 2005. **817**(1): p. 49-66.

24. Sonnefeld, W.J., W.H. Zoller, W.E. May and S.A. Wise, *On-line multidimensional liquid chromatographic determination of polynuclear aromatic hydrocarbons in complex samples.* Anal. Chem., 1982. **54**(4): p. 723-727.

25. Tian, H., J. Xu, Y. Xu and Y. Guan, *Multidimensional liquid chromatography system with an innovative solvent evaporation interface.* Journal of Chromatography A, 2006. **1137**(1): p. 42-48.

26. Dugo, P., O. Favoino, R. Luppino, G. Dugo and L. Mondello, *Comprehensive Two-Dimensional Normal-Phase (Adsorption)-Reversed-Phase Liquid Chromatography.* Anal. Chem., 2004. **76**(9): p. 2525-2530.

27. Murahashi, T., *Comprehensive two-dimensional high-performance liquid chromatography for the separation of polycyclic aromatic hydrocarbons.* Analyst (Cambridge, United Kingdom), 2003. **128**(6): p. 611-615.

28. Tanaka, N., H. Kimura, D. Tokuda, K. Hosoya, T. Ikegami, N. Ishizuka, H. Minakuchi, K. Nakanishi, Y. Shintani, M. Furuno, and K. Cabrera, *Simple and Comprehensive Two-Dimensional Reversed-Phase HPLC Using Monolithic Silica Columns.* Anal. Chem., 2004. **76**(5): p. 1273-1281.

29. Saravanabhavan, G., A. Helferty, P.V. Hodson and R.S. Brown, *A multi-dimensional high performance liquid chromatographic method for fingerprinting polycyclic aromatic hydrocarbons and their alkyl-homologs in the heavy gas oil fraction of Alaskan North Slope crude.* Journal of Chromatography A, 2007. **1156**(1-2): p. 124-133.

30. Wang, Z., B.P. Hollebone, M. Fingas, B. Fieldhouse, L. Sigouin, M. Landriault, P. Smith, J. Noonan and G. Thouin, *Development of a composition database for selected multicomponent oil.* 2002, Environment Canada: Ottawa.

31. Wise, S.A., L.C. Sander, R. Lapouyade and P. Garrigues, *Anomalous behavior of selected methyl-substituted polycyclic aromatic hydrocarbons in reversed-phase liquid chromatography.* Journal of Chromatography, 1990. **514**(2): p. 111-22.

CHAPTER 6

Discussion and conclusion

Overall Project Objectives

This thesis examined the effect-driven fractionation and analysis (EDFA) approach to screen for the toxic components present in crude oils. The goals of this research project were (i) to develop fractionation methods for the EDFA scheme to examine the impact of specific oil components on fish; (ii). to examine the toxicity of specific fractions on fish to better understand the relationship between oil composition and effects, and (iii). to develop new multi-dimensional HPLC techniques for characterizing the aromatic compounds in oil fractions and related samples.

Fractionation methods: Earlier studies found that the heavy gas oil fraction of the ANSC and SCOT crude oils, obtained using low temperature vacuum distillation, contained a majority of toxic components from these crude oils [1]. Hence, in this work, the heavy gas oil was subjected to further fractionation to isolate potential toxicants including the alkyl PAHs. The heavy gas oil fraction contained a large amount of the saturated hydrocarbons in addition to PAHs. Therefore, a low temperature wax precipitation method was developed to isolate the PAHs from waxes. Precipitation parameters such as the nature of the solvent and temperature were optimized (Chapter 2). HPLC and GC-MS analysis showed that the extract contained a variety of PAHs and alkyl PAHs belonging to different PAH classes while only trace levels of PAHs were found in the residue.

In the next stage, the alkyl PAHs present in the cold acetone extract were fractionated. A fractionation method using semi-preparative normal phase HPLC separation of PAHs based on the number of aromatic rings was developed (Chapter 3). Using appropriate retention time markers, the extract components were separated into saturates, a naphthalene fraction, a phenanthrene fraction, a chrysene fraction and a high molecular weight PAH fraction. This enabled the bulk fractionation of the cold acetone extract for further CYP1A induction and toxicity testing.

CYP1A induction of sub-fractions: The CYP1A induction assay conducted on the cold acetone extract and wax residue revealed that the extract contained the toxic components. The wax residue was found to be inactive in the toxicity testing. Among the normal phase sub-fractions of the cold acetone extract, fractions containing phenanthrene, chrysene and high molecular weight PAHs showed high toxicity. Saturate and naphthalene fractions neither induced CYP1A nor showed any chronic toxicity [2]. Detailed GC-MS analysis of toxic normal phase sub-fractions showed the presence of alkyl PAHs belonging to the classes of phenathrene, fluorene, naphthobenzothiophenes, and chrysenes. Table 6.1 shows the total concentration of un-substituted and alkyl substituted PAHs measured in the toxic normal phase fractions. In each case, we found that the total concentration of alkyl PAHs was much higher than the un-substituted PAHs. Previous laboratory studies have shown that some of the alkyl phenanthrenes induced CYP1A enzymes and cause chronic toxicity to fish [3-5]. Recent field studies at Exxon Valdez Oil spill sites in Prince William Sound,

Alaska showed the presence of several alkyl PAHs analyzed in this work [6]. This suggests that the alkyl PAHs play an important role in determining the toxicity of crude oils. Although the high molecular weight PAH fraction showed high toxicity, the concentrations of the analyzed PAHs were relatively lower in this fraction. This might indicate either the presence of highly toxic alkyl PAH isomers or the presence of other PAHs that were not studied in this work.

Table 6.1: Total concentration of unsubstituted and alkyl substituted PAHs in different toxic normal phase sub-fractions.

Fraction name	Fluorenes (FLUOR)		Phenanthrenes (PHEN)		Naphthobenzo thiophenes (NBT)		Chrysenes (CHRY)	
	C0 FLUOR	C1-C4 FLUOR	C0 PHEN	C1-C4 PHEN	C0 NBT	C1-C4 NBT	C0 CHRY	C1-C4 CHRY
ANSC 313 (μg/g)	3037	27421	3043	94787	2207	53495	1623	4977
ANSC 314 (μg/g)				4461		3142	4013	79598
ANSC 315 (μg/g)		316	143	2473		1268		8149
SCOT 313 (μg/g)	766	14393	2967	30718				654

The success of the EDFA methodology relies on the progressive enrichment of toxicants from the complex mixtures. Fractional composition and the associated toxicity of different sub-fractions were used to examine the toxicity enrichment

during different stages of the EDFA approach. In the first fractionation stage, the heavy gas oil fraction (ANSC 3) which constitutes 33% by weight of ANSC was found to contain the majority of PAHs that induce CYP1A enzymes and cause chronic toxicity in fish. This indicates a three-fold enrichment of toxicity. When ANSC 3 was subjected to the wax precipitation technique, the extract (ANSC 31) constituted ~ 35% of the heavy gas oil by weight and contained most of the toxicants, corresponding to another three-fold toxicity enrichment. In the next stage, among the five normal phase sub-fractions of ANSC 31, only fractions ANSC 313, 314 and 315 induced CYP1A activity. All these fractions together constituted 32% by weight of the ANSC 31 resulting in another three-fold enrichment. Therefore, each fractionation stage in the EDFA approach enriched the toxicants by a factor of 3, resulting in an overall enrichment factor of 27.

Multi-dimensional HPLC methods: Developing robust analytical methods for the analysis of the alkyl PAHs during different stages of the EDFA protocol was required for both compound identification and also to aid further fractionation. Currently, GC-MS based analytical methods are predominantly used for analysis of alkyl PAHs in the oil chemistry laboratories [7]. However, alkyl PAHs with identical molecular weights but belonging to different PAH classes (such as methyl triphenylenes and methyl chrysenes) are difficult to differentiate in GC-MS without authentic analytical standards. To overcome this problem, we have developed HPLC –DAD based analytical methods for the analysis of alkyl PAHs (Chapter 4). Different PAH classes exhibit unique DAD spectra; moreover, alkyl substitution does not alter their UV spectra significantly. Therefore, we found that

210

the HPLC-DAD based method developed in this work is more reliable for PAH class identification.

The reverse phase chromatogram of alkyl PAH fractions are often too complex due to the presence of a number of alkyl PAH isomers. Hence, an off-line multi-dimensional HPLC separation and analysis method was developed to characterize alkyl isomers in the crude oil sub-fractions (Chapter 5). Orthogonal separation was achieved by first fractionating the extract (ANSC 31) on a normal phase column followed by the analysis using reverse phase HPLC coupled to DAD detector. These data were then used to develop a 2D contour plot in which the alkyl PAHs from different PAH classes were distributed in an structured way based on the number of aromatic rings as well as log P values.

Major research findings

The EDFA approach was found to be very useful for isolating and identifying toxic alkyl PAHs in crude oil samples. Based on the results obtained in this work the following general conclusions are drawn regarding the nature of the alkyl PAHs:

1. Throughout this study, the ANSC sub-fractions were found to be relatively more toxic than the SCOT sub-fractions. This was consistent with the fact that the concentration of PAHs in ANSC oil is much higher than that in SCOT oil.

2. Fractions containing alkyl PAHs with three and higher numbers of benzene rings were found to be chronically toxic to fish; specifically, fractions containing alkylated phenanthrenes, fluorenes,

naphthobenzothiophenes and chrysenes were found to be induce CYP1A enzymes and cause chronic toxicity in fish.

3. Although alkylated naphthalenes and dibenzothiophenes were found in abundance in crude oils, they neither induced CYP1A enzymes nor caused chronic toxicity to fish.

4. The reverse phase HPLC-DAD method developed in this work was found to be very useful for PAH class identification and quantification.

5. Comparison of the concentration of PAHs obtained using the HPLC-DAD with GC-MS data showed good agreement. The HPLC-DAD method can be used as a complementary technique for chemical fingerprinting.

General application

The EDFA protocol developed in this work could be used as a general method for the isolation and identification of toxic alkyl PAHs from crude oil samples. *In vivo* toxicity testing often demands a large amount of crude oil sub-fraction. Hence, the wax precipitation protocol could be useful for the preliminary separation of PAHs from saturates before detailed HPLC fractionation. The HPLC-DAD method demonstrated in this work could be used as a general identification and quantification method of these compounds in other environmental matrices such as soil and sediment extracts. The two-dimensional contour plot of the alkyl PAHs in crude oil could be used to compare the alkyl PAH distribution from an oil spill site with that of suspected sources of crude oils.

This can be a valuable tool for the positive identification of the crude oil source during an oil spill investigation.

Future work

Even after three stages of fractionation, the toxic crude oil sub-fractions obtained in this work are too complex to conclusively identify any individual compound as toxic. Hence further fractionation of the normal phase sub-fractions is necessary. In this respect, the results obtained during the two-dimensional chromatographic separation could be useful to aid further normal phase fractionation. Figure 6.1 shows the retention time windows of different alkyl PAHs present in the ANSC 31 using the chromatographic conditions presented in Chapter 3 and Chapter 5. It can be noted that the silica column gave a good separation of alkyl naphthalenes and alkyl dibenzothiophenes. However, clear separation of alkyl phenanthrenes from alkyl fluorenes present in fraction ANSC 313 as well as alkyl chrysenes from alkyl triphenylenes in fraction ANSC 314 was not achieved using the silica column. Therefore, other normal phase columns with slightly different selectivity (e.g. an aminopropyl phase) should be explored.

On the other hand, further fractionation of normal phase sub-fractions could be achieved using reverse phase columns. As shown in Chapter 4 and Chapter 5, the alkyl PAHs are separated in the C18 reverse phase mode based on their log P value. Therefore, alkyl PAH fractionation in the reverse phase mode can help to collect PAHs within a desired log P range. Moreover, as most of the alkyl

PAHs are separated well in the reverse phase mode (compared to the normal phase), this method could be useful to identify predominant alkyl PAHs in a given fraction for further fractionation and analysis.
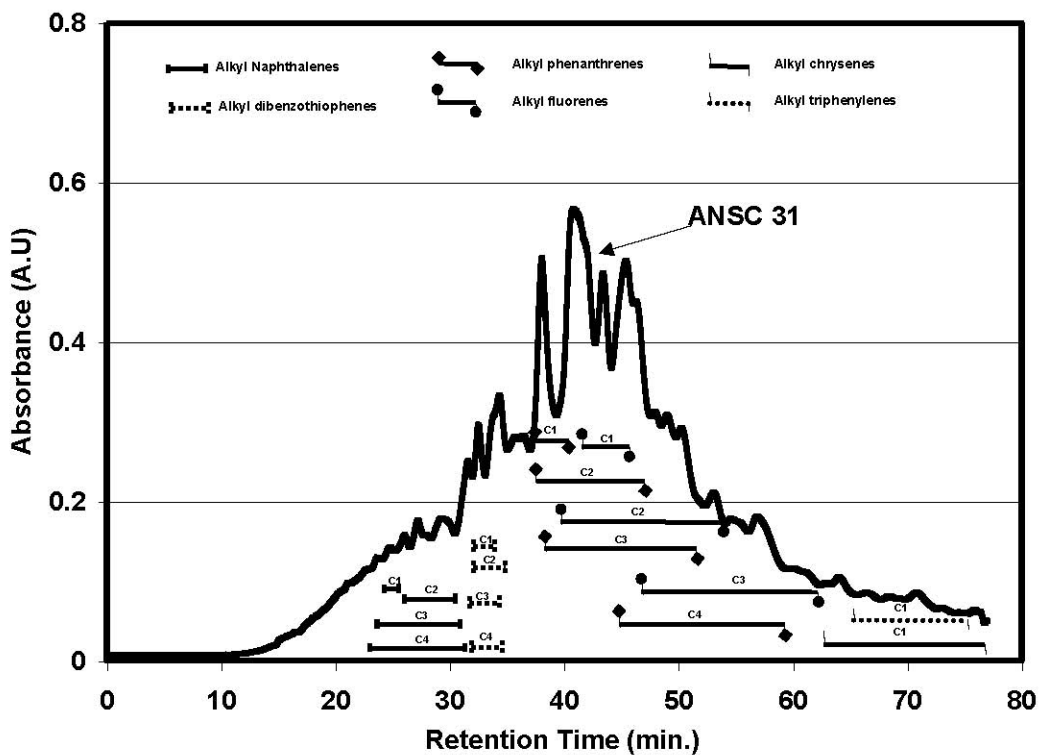

Figure 6.1: Distribution of alkyl PAHs of different PAH classes in the cold acetone extract during the normal phase fractionation.

Alkyl PAH analysis using the multi-dimensional liquid chromatographic approach developed in this work correlated well with the GC-MS results. However, as there are no standardized HPLC methods available, the assignment of alkyl carbons to the PAH peaks are still problematic. Previous studies have shown that the elution

of alkyl PAHs on reverse phase HPLC depends on several factors including size, shape and hydrophobicity. Therefore, incorporation of size and shape parameters (e.g. length/breath ratio) in addition to the log P parameter might improve the quantitative results.

References

1.   Khan, C.W., S.D. Ramachandran, L.M.J. Clarke and P.V. Hodson. *EROD activity (CYP1A) inducing compounds in fractionated crude oil.* in *Proceedings of the twenty-seventh Artic and Marine Oilspill Program (AMOP) technical seminar.* 2004. Edmonton, Alberta: Emergencies Science and Technology division, Environment Canada.

2.   Hodson, P.V., C.W. Khan, G. Saravanabhavan, L.M.J. Clarke and R.S. Brown. *Alkyl PAH in crude oil cause chronic toxicity to early life stages of fish.* in *Proceedings of the thirtieth Artic and Marine Oilspill Program (AMOP) technical seminar.* 2007. Edmonton, Alberta: Emergencies Science and Technology division, Environment Canada.

3.   Billiard, S.M., K. Querbach and P.V. Hodson, *Toxicity of retene to early life stages of two freshwater fish species.* Environmental Toxicology and Chemistry, 1999. **18**: p. 2070-2077.

4.   Brinkworth, L.C., P.V. Hodson, S. Tabash and P. Lee, *CYP1A induction and blue sac disease in early developmental stages of rainbow trout (Oncorhynchus mykiss) exposed to retene.* Toxicology and environmental health, 2003. **66**(7): p. 526-546.

5.   Carls, M.G., R.A. Heintz, G.D. Marty and S.D. Rice, *Cytochrome P4501A induction in oil-exposed pink salmon Oncorhynchus gorbuscha embryos predicts reduced survival potential.* Marine Ecology: Progress Series, 2005. **301**: p. 253-265.

6.   Short, J.W., M.R. Lindeberg, P.M. Harris, J.M. Maselko, J.J. Pella and S.D. Rice, *Estimate of Oil Persisting on the Beaches of Prince William Sound 12 Years after the Exxon Valdez Oil Spill.* Environmental Science & Technology, 2004. **38**(1): p. 19-25.

7.   Wang, Z. and M.F. Fingas, *Development of oil hydrocarbon fingerprinting and identification techniques.* Marine Pollution Bulletin, 2003. **47**(9-12): p. 423-452.